OFFICE OF CIVILIAN RADIOACTIVE WASTE MANAGEMENT

ANALYSIS/MODEL COVER SHEET

Complete Only Applicable Items

1. QA: QA

Page: 1 of: 89

2. ☒ Analysis — Check all that apply

Type of Analysis:
- ☐ Engineering
- ☐ Performance Assessment
- ☒ Scientific

Intended Use of Analysis:
- ☒ Input to Calculation
- ☒ Input to another Analysis or Model
- ☐ Input to Technical Document
- ☐ Input to other Technical Products

Describe use:

Determine geometry of both lithophysae and fracture porosity to obtain upper bound of actinide accumulation volume.

3. ☐ Model — Check all that apply

Type of Model:
- ☐ Conceptual Model
- ☐ Abstraction Model
- ☐ Mathematical Model
- ☐ System Model
- ☐ Process Model

Intended Use of Model:
- ☐ Input to Calculation
- ☐ Input to another Model or Analysis
- ☐ Input to Technical Document
- ☐ Input to other Technical Products

Describe use:

4. Title:

Description of Fracture Systems for External Criticality Reports

5. Document Identifier (including Rev. No. and Change No., if applicable):

ANL-NBS-GS-000010 REV 00

6. Total Attachments:

Four

7. Attachment Numbers - No. of Pages in Each:

I(1), II(1), III(3), IV(CD-ROM)

	Printed Name	Signature	Date
8. Originator	Jean-Philippe Nicot	Susan LeStrange for	9/19/01
9. Checker	James T. Kam	James Kam	9/20/01
10. Lead/Supervisor	Susan L. LeStrange	Susan L LeStrange	9/21/01
11. Responsible Manager	Daniel A. Thomas	D A Thomas	09/21/2001

12. Remarks:

OFFICE OF CIVILIAN RADIOACTIVE WASTE MANAGEMENT

ANALYSIS/MODEL REVISION RECORD

Complete Only Applicable Items

2. Analysis or Model Title:

Description of Fracture Systems for External Criticality Reports

3. Document Identifier (including Rev. No. and Change No., if applicable):

ANL-NBS-GS-000010 REV 00

4. Revision/Change No.	5. Description of Revision/Change
00	Initial Issue

CONTENTS

Page

FIGURES

Page

FIGURES (continued)

Page

TABLES

Page

TABLES (continued)

Page

TABLES (continued)

Page

1. PURPOSE

The purpose of this Analysis/Model Report (AMR) is to describe probabilistically the main features of the geometry of the fracture system in the vicinity of the repository. They will be used to determine the quantity of fissile material that could accumulate in the fractured rock underneath a waste package as it degrades. This AMR is to feed the geochemical calculations for external criticality reports. This AMR is done in accordance with the technical work plan (BSC (Bechtel SAIC Company) 2001b).

The scope of this AMR is restricted to the relevant parameters of the fracture system. The main parameters of interest are fracture aperture and fracture spacing distribution parameters. The relative orientation of the different fracture sets is also important because of its impact on criticality, but they will be set deterministically. The maximum accumulation of material depends primarily on the fracture porosity, combination of the fracture aperture, and fracture intensity. However, the fracture porosity itself is not sufficient to characterize the potential for accumulation of a fracture system. The fracture aperture is also important because it controls both the flow through the fracture and the potential plugging of the system. Other features contributing to the void space such as lithophysae are also investigated. On the other hand, no analysis of the matrix porosity is done. The parameters will be used in sensitivity analyses of geochemical calculations providing actinide accumulations and in the subsequent Monte Carlo criticality analyses.

This AMR is associated with disposal criticality analysis and has been prepared in accordance with AP-3.10Q.

2. QUALITY ASSURANCE

An activity evaluation (BSC 2001b, p. 27), which was prepared per AP-2.21Q, *Quality Determinations and Planning for Scientific, Engineering, and Regulatory Compliance Activities*, determined that the Quality Assurance (QA) program (DOE 2000) applies to the activity under which this analysis was developed. Control of the electronic management of data was accomplished in accordance with the controls specified by BSC (2001b, p.47). The output Data Tracking Numbers (DTNs) have been prepared according to AP-SIII.3.Q, *Submittal and Incorporation of Data to the Technical Data Management System.*

3. COMPUTER SOFTWARE AND MODEL USAGE

3.1 COMPUTER SOFTWARE

3.1.1 Standard Software

The computer program *Microsoft Excel 97 SR-2* was used in the preparation of this analysis. This software item is appropriate for this application. *Microsoft Excel 97* was used to perform support calculations and is not a controlled source of information. Thus, it is not subject to software management per AP-SI.1Q, *Software Management. Microsoft Excel 97* is a commercial spreadsheet program designed to assist in routine calculations. The *Microsoft Excel 97 SR-2* applications can be verified by hand and algorithms, inputs and outputs are included in each specific file (Attatchment IV CD-

ROM). *Microsoft Excel 97 SR-2* also includes a graphics package to assist in data presentation. All plots and graphics were produced on *Microsoft Excel 97 SR-2*. Plots and graphics are exempt from software management per AP-SI.1Q, *Software Management*.

3.1.2 Software Approved for Quality Assurance Work

3.1.2.1 GAMV2 Module

The module GAMV2 from the GSLIB software package (GSLIB 1.0MGAMV2V1.201, STN 10087-GSLIB1.0MGAMV2V1.201 Lawrence Berkeley National Laboratory 1999) is approved and qualified under the STN 10087-1.0MGAMV2V1.201-00. GSLIB runs were performed on the YMP Sun Ultra-2 workstation otis ID#: 115491 running under Solaris 2.6 Unix and located in Building 10 of the Summerlin facilities in Las Vegas. The GAMV2 module was used to compute semi-variograms of the fracture spacing.

The software was obtained through the Software Configuration Management. The software is appropriate for use in this document and has been used within the range of parameters for which the software has been validated. Input and output files are in Attachment IV (CD-ROM) under the directory "variogram".

3.1.2.2 Add_Fracture Microsoft Excel Macro

The macro "Add_Fracture" software has been qualified under the AP-SI.1Q, *Software Management*, procedure under the Software Tracking Number 10498-1.0-00 and the Software Activity Number DUKE-2001-077 (BSC 2001a). The runs were performed on a Duke Engineering & Services Dell Pentium II computer (CPU# U998E located in the DE&S facilities, 9111 Research Boulevard, Austin, TX).

The software was obtained through the Software Configuration Management. The software is appropriate for use in this document and has been used within the range of parameters for which the software has been validated. Input and output files are in Attachment IV (CD-ROM) under the directory "MC_for_Multiple_Fracture_Spacing".

3.2 MODELS

None used.

4. INPUTS

4.1 DATA AND PARAMETERS

4.1.1 Fracture System Geometry

Data used in this work come from the Exploratory Studies Facility (ESF) and Enhanced Characterization of the Repository Block (ECRB) Detailed Line Surveys (DLS), Full-Periphery Geologic Maps (FPGM), and Small-Scale Survey (SSS) (Table 4-1). They are all qualified data. They are complemented (reference only data) as needed by borehole information or outcrop/pavement information presented in different earlier reports. DLSs of the North Ramp (00+00 to 18+00) and South Ramp (beyond 55+00) are of limited

interest in this calculation as they applies mainly to formations stratigraphically above the proposed repository.

Table 4-1. DLS, FPGM, and SSS Sources

Description of Data	Data Tracking Number	Unit
ESF DLS, Stations 18+00 to 26+00, Rev.01	GS971108314224.024	TSw33
ESF DLS, Stations 26+00 to 30+00, Rev.01	GS971108314224.025	TSw33 / TSw34
ESF DLS, Stations 30+00 to 35+00, Rev.00	GS960708314224.008	TSw34
ESF DLS, Stations 35+00 to 40+00, Rev.00	GS960808314224.011[a]	TSw34
ESF DLS, Stations 40+00 to 45+00, Rev.00	GS960708314224.010	TSw34
ESF DLS, Stations 45+00 to 50+00, Rev.01	GS971108314224.026	TSw34
ESF DLS, Stations 50+00 to 55+00, Rev.00	GS960908314224.014	TSw34
ESF DLS, Stations 55+00 to 60+00, Rev.01	GS971108314224.028	TSw34 / TSw35
ECRB DLS, Stations 00+00.89 to 14+95.18, Rev.00	GS990408314224.001	TSw33/TSw34
ECRB DLS, Stations 15+00.85 to 26+63.85, Rev.00	GS990408314224.002	TSw35/TSw36
ECRB FPGM Stations 0+10 to 10+00	GS990408314224.003	TSw33
ECRB FPGM Stations 10+00 to 15+00	GS990408314224.004	TSs34
ECRB FPGM Stations 15+00 to 20+00	GS990408314224.005	TSw35
ECRB FPGM Stations 20+00 to 26+81	GS990408314224.006	TSw35/TSw36
ECRB SSS (only horizontal traverses)	GS990908314224.009	TSw33 to TSw36
Fracture Attitude data for ECRB cross drift fracture clusters identified by Clustran analysis	GS991108314224.015; Table S99470_003	TSw33 to TSw36
ESF DLS, Stations 35+00 to 40+00, Rev.00	GS000608314224.004	TSw34

NOTE: [a]superseded by GS000608314224.004 with no impact

These DTNs provide fracture attitude, filling, roughness, and length. DTN GS960808314224.011 (ESF DLS, Stations 35+00 to 40+00) has been superseded by DTN GS000608314224.004 since this work was completed. The changes to the data set have no impact on the results because (1) most of the calculation uses data from the ECRB tunnel and not from the ESF; (2) the changes consist of adding one line (i.e., one fracture was missing) and of changing a fracture length from 3.6 to 3.62 m.

4.1.2 Fracture Characteristics

Other DTNs used in the analysis are displayed in Table 4-2. They relate mainly to both hydraulic and solute transport fracture apertures but also to lithophysae and fracture fillings.

Table 4-2. Miscellaneous DTNs

Description of Data	Data Tracking Number
Unsaturated zone hydrologic characteristics	LB971212001254.001
Unsaturated zone hydrologic characteristics	LB997141233129.001
Fracture properties (in particular fracture porosity)	LB990501233129.001
Fracture porosity from tracer tests	LB980912332245.002
Lithophysal abundance	GS991108314224.015, Table S99470_001
Fracture filling	GS991108314224.015, Table S99470_002
Secondary mineral abundance	GS980308315215.008

4.2 CRITERIA

There are no criteria from either Requirements Documents or System Description Documents that are applicable to this description of the fracture system.

4.3 CODES AND STANDARDS

No codes and standards are utilized in the preparation and completion of this document.

5. ASSUMPTIONS

5.1 It is assumed that the fracture porosity determined by tracer test in the TSw34 unit can be scaled to the TSw35 and TSw36 units. The rationale for this assumption is that, although there is no direct porosity measurement in units TSw35 and TSw36, fracture aperture is not expected to vary wildly between units and thus the fracture porosity is mainly a function of the fracture intensity. This assumption is used in Sections 6.3.3 and 6.9.7. This assumption requires no confirmation.

5.2 It is assumed that all fractures used in criticality calculations are either vertical or horizontal. The basis for this assumption is detailed in Section 6.5.1. This assumption is used in Sections 6.9.10 and 7.1.3. The computation itself does not make this assumption but the fracture spatial distribution being too complex to be represented accurately, it is assumed that the system is well-represented by composite continuous vertical fracture at least 1 m long and of same aperture and by a few horizontal fractures. This assumption requires no confirmation.

5.3 It is assumed that the fraction of each fracture size bin is constant and independent of fracture frequency. The basis for this assumption is that it is conservative. Details are given in the small-scale survey studies (see Section 6.9.6). This assumption is used in Section 6.9.6. This assumption requires no confirmation.

5.4 It is assumed that the fracture cutoff of 1m does not change the relative importance of the orientation clusters. The basis for this assumption is that, although small fractures are more randomly distributed than longer fractures, they still fall into the same fracture sets as longer fractures. This assumption is used in Section 6.5.1. This assumption requires no confirmation.

5.5 It is assumed that the fracture aperture distribution (both hydraulic and transport) follows a lognormal distribution. The basis for this assumption is that fracture aperture is bounded by zero and skewed towards small values. This assumption is used in Section 6.3.2. This assumption requires no confirmation.

5.6 It is assumed that the lithophysae size distribution follows a lognormal law. This assumption is reasonable because many natural parameters with skewed distribution follow this distribution. This assumption is used in Section 6.4. This assumption requires no confirmation.

5.7 It is assumed that the lithophysae porosity distribution follows a normal law. This assumption is reasonable because of the small range of variations in porosity. This assumption is used in Section 6.4. This assumption requires no confirmation.

5.8 It is assumed that both fracture spacing and fracture length follow a lognormal distribution. The basis for this assumption is that fracture spacing and length are bounded by zero, unbounded towards high values, and skewed towards small values. This assumption is used in Sections 6.8 and 6.9. This assumption will be relaxed in Section 6.9.2. This assumption requires no confirmation.

5.9 It is assumed that corrections for non-verticality of the fracture plane and non-orthogonality of the drift bearing and fracture plane can be applied to the average strike and dip rather than to individual fractures. The basis for this assumption is that corrections are small. This assumption is used in Section 6.9.5. This assumption requires no confirmation.

5.10 It is assumed that all the fractures are connected within a single network. The basis for this assumption is that it is conservative because it maximizes the amount of accumulation and that it is not overly conservative as demonstrated in Section 6.10. This assumption is used in Sections 6.3.3. and 6.10. This assumption requires no confirmation.

5.11 It is assumed that general results from lithophysae studies are applicable specifically to the TSw35 unit. The basis for this assumption is that mineral accumulation in lithophysae is more driven by chemical processes than by the physical location of the lithophysal cavity. This assumption is used in Section 6.11. This assumption requires no confirmation.

5.12 It is assumed that fracture spacing is not spatially correlated at a WP length scale, i.e., a tight fracture spacing does not infer that the next spacing will be either another tight spacing or a large spacing but rather that the next spacing can be chosen at random (independence of fracture spacing). The basis for this assumption is described in Section 6.9.3. This assumption is used in Section 6.9. This assumption requires no confirmation.

6. ANALYSIS/MODEL

The following sections present definitions and describe not only the processing methods used in this AMR but also the methods used to acquire the needed parameters because of their impact on the results. The following parameters will be described for each relevant stratigraphic unit:

- Fracture aperture [S]
- Lithophysae porosity [S]
- Fracture orientation
- Fracture roughness
- Fracture filling
- Fracture length [S]
- Fracture frequency [S]
- Fracture intensity [S]
- Relationship between fracture intensity and fracture frequency
- Fracture connectivity.

Statistical distributions are derived for the relevant parameters ("[S]" at end of line).

The screening criteria listed in the Screening Criteria for Grading of Data attachment in AP-3.15Q have been examined. This AMR is assigned a Level 3 importance.

6.1 CLASSIFICATION OF FRACTURES

Fractures are classified into:

- "Tectonic" fractures: they are openings of tectonic origin. They are by far the most numerous type of discontinuity > 1m (>90% in ESF (Albin et al. 1997, p. 22) - 81% in the ECRB (Mongano et al. 1999, p. 9).

- Cooling joints: they are due to stresses related to cooling of the rock after its deposition. They tend to be longer and smoother than "tectonic" fractures. Their identification as such is not easy most of the time and many are likely to appear with fractures in the fracture group. They account for at least 7% of the openings > 1m in the ECRB (Mongano et al. 1999, p. 9).

- Vapor-phase partings: They are discontinuities that consist of roughly linear accumulations of vapor-phase minerals and are parallel to sub-parallel to lithostratigraphic layering. They account for 4% of the openings > 1m in the ECRB (Mongano et al. 1999, p. 9).

- Shear and Faults: they are fractures with clear apparent offset. The magnitude of the movement (cutoff of 0.1 m) determines the subgroup. They account for 8% of the openings in the ECRB (Mongano et al. 1999, p. 9).

6.2 DESCRIPTION OF TSW33 TO TSW37 UNITS

The repository will be sheltered in the crystal-poor section of the Topopah Spring tuff (Tptp stands for Topopah Spring tuff crystal poor) formation that includes:

- The upper lithophysal unit (TSw33 within the project -w for welded- or Tptpul for the United States Geological Survey teams - ul for upper lithophysal-)
- The middle nonlithophysal unit (TSw34 or Tptpmn).
- The lower lithophysal unit (TSw35 or Tptpll)
- The lower nonlithophysal (TSw36 or Tptpln).
- The vitric unit (TSw37 or Tptpv3).

The current design (BSC 2001c, Table 18; Curry 2001, pp. 2-18 to 2-20, and Fig. 2-4) calls for the repository being in the TSw34 to TSw36 units (Table 6-1) but mainly in the TSw35 unit.

Table 6-1. Percentage of Each Unit in the Repository

Formation	% of Repository
TSw34	8.5%
TSw35	80.4%
TSw36	11.1%

Source: BSC (2001c, Table 18)

The ESF main drift (ESF for short) extends for about 8 km, and the TSw34 formation is visible from about station 27+00 (corresponding to a length of 2,700 m after the North Portal) to station 57+29. The TSw35 and TSw36 units have limited or no exposures (respectively) in the ESF, and earlier reports relied only on boreholes and outcrops. An additional 3 km of tunnel were then constructed across but slightly above the future location of the emplacement drifts (cross drift or ECRB tunnel). The ECRB tunnel is cut through the 3 main formations that will host the repository (TSw34, TSw35, and TSw36). Because the TSw34 unit was initially thought to host the repository, it has been studied more extensively and earlier than TSw35 and TSw36, and more information is available on it.

Because the drift direction is relevant to the final fracture spacing (see Section 6.9.5), a summary of successive drift bearings is presented in Table 6-2 and Table 6-3.

Table 6-2. ESF Drift Bearings

Stationing	Comments	Source
4+00 - 21+87	North Ramp - Bearing = 299°	Albin et al. 1997 p. 4
21+87 - 28+00	Curved Section	Albin et al. 1997 p. 4
28+00 - 59+35.47	Main Drift - Bearing = 183°	Albin et al. 1997 p. 4
59+35.47 - 64+25.21	Curved Section	Eatman et al. 1997 Fig. 2
64+25.21 - 78+77	South Ramp - Bearing = 091°	Eatman et al. 1997 Fig. 2

Table 6-3. ECRB Drift Bearings

Stationing	Comments	Source
0+00 - 1+82	Bearing = 254°	Mongano et al. 1999, p. 3
1+82 - NA	Curved Section	Mongano et al. 1999, p. 3
NA - 23+21	Bearing = 229°	Mongano et al. 1999, p. 3
23+21 - NA	Curved Section	Mongano et al. 1999, p. 6
NA - 26+81	Bearing = 289°	Mongano et al. 1999, p. 6

NOTE: NA=Not Available

6.2.1 TSw33 Unit

The TSw33 unit is visible in the ESF main drift from station 17+97 to 27+20, in the North Ramp from station 63+08 to 64+55 and 71+68 to 73+02 and at a few other occurrences in the South Ramp. The TSw33 unit is visible in the ECRB from station 00+00 to 10+15 and again from station 25+85 to 26+63.85 because of a fault.

6.2.2 TSw34 Unit

The TSw34 formation is visible in the ESF from about station 27+20 to station 57+29. ESF main drift fracture studies broke the TSw34 layer into 4 domains (Albin et al. 1997 - Fig. 6 p. 31 and pp. 34 and ff.). As far as fracture accumulation is concerned, these 4 domains collapse into 2 zones: the intensely-fractured zone (IFZ - from about 42+00 to 51+50 with a "quiet" zone in the middle) and the rest. The IFZ seems to be stratabound (more brittle because of the absence of lithophysae) and therefore was thought to possibly cover the whole repository.

The TSw34 formation is visible in the ECRB from about station 10+15 to station 14+40. ECRB studies have proven that the IFZ is a localized phenomenon (Mongano et al. 1999, p. 43) and that fracture frequency in the TSw34 layer in the ECRB is comparable to the fracture frequency of the same layer outside of the IFZ. Results using mainly information from the main drift are likely to overestimate the overall average frequency in this unit.

6.2.3 TSw35 Unit

The TSw35 unit has a limited exposure in the ESF main drift from station 57+29 to 58+78 but is visible in the ECRB from about station 14+40 to station 23+25.

6.2.4 TSw36 Unit

The TSw36 formation is visible in the ECRB only from about station 23+25 to station 25+85.

6.2.5 TSw37 Unit

Information about the TSw37 is only accessible through boreholes.

6.3 DISTRIBUTION OF FRACTURE APERTURES

The following sections deal with the hydraulic and transport apertures. Hydraulic aperture results rely mainly on older reports on the ESF while transport aperture results include newer tracer studies but still from the ESF. In addition to fractures themselves, lithophysae may locally, especially in lithophysal units, add significant porosity to the rock. Lithophysae are examined in Section 6.4.

6.3.1 Field Observations

While it is relatively easy to come up with fracture frequency and length with outcrop and drift observations, fracture aperture is not directly observable in a consistent way.

Field observations can typically only come up with the maximum aperture (Mongano et al. 1999, Figures 15 to 20) and are not appropriate to estimate average aperture. The classic way of obtaining fracture aperture is through either pneumatic or tracer tests. Most measured field fracture apertures vary from almost 0 to a few mm (Table 6-4). Table 4 of Albin et al. 1997 (p. 83) reports that in the TSw34-ESF the minimum fracture aperture follows an exponential distribution of mean 0.007 mm and standard deviation of 0.218 mm while the maximum aperture distribution follows a lognormal distribution of mean 0.582 mm and standard deviation of 2.824 mm.

Table 6-4. Field Measurements of Fracture Aperture

Unit	Minimum Aperture (mm)		Maximum Aperture (mm)		Comments	Source
	Mean	St. Dev.	Mean	St. Dev.		
TSw33 ECRB					Max=80 mm	Mongano et al. 1999, Fig. 17
TSw34 ESF	0.007	0.218	0.582	2.824	Min. Ap. is Exponential and Max. Ap. is lognormal	Albin et al. 1997 Table 4, p. 83
TSw34 ECRB					Max=520 mm	Mongano et al. 1999, Fig. 18
TSw35 ECRB					Max=200 mm	Mongano et al. 1999, Fig. 19
TSw36 ECRB					Max=110 mm	Mongano et al. 1999, Fig. 20

NOTE: Maximum opening does not include lithophysae in the fracture path.

6.3.2 Distributions of Hydraulic Apertures

Pneumatic test interpretation follows the cubic law (in other words, the parallel plate representation) (Domenico and Schwartz 1990 - pp. 86 and 87, Eq. 3-38). Air permeabilities k are obtained from the tests, and the average aperture $2b$ is then calculated from the following formula:

$$k = \frac{I(2b)^3}{12} \qquad \text{(Eq. 1)}$$

where I is the fracture intensity (m/m^2). This formulation considers also that the fractures are fully connected. This average aperture is called the hydraulic aperture (the correspondence between air and water permeability is direct because the pneumatic tests are done at fracture residual water saturation - about 0.01% at the repository level). These measurements are made in boreholes on small volumes isolated with packers (~ <10-m intervals).

Estimates of fracture hydraulic apertures have varied in the past. Most of the work had been devoted to estimating hydraulic aperture in the TSw34 unit, initially thought to be the main repository unit. In this unit, hydraulic apertures (in microns) follow a lognormal distribution of mean $\mu_{log10} = \log_{10}(98)$ and standard deviation $\sigma_{log} = 0.38$ (see details below) (this is decimal log – see Bodvarsson et al. 1997 - Table 7.12, top of p. 7-18). The mean of the distribution is obtained through local air permeability tests, while the standard deviation is obtained through core experiment and mountain scale parameter fitting. This work also assumes a lognormal distribution of the hydraulic aperture (Assumption 5.5).

6.3.2.1 Estimation of the Standard Deviation of the Fracture Hydraulic Apertures

The distribution of aperture within a fracture is related to the behavior of unsaturated flow in the fracture system while varying saturation because smaller openings retain water longer in desaturation experiments. Experiments on cores yield a curve of capillary pressure P_c ("h" in Maidment 1993, Table 5.1.1) versus saturation. This curve is characterized by the two parameters of the Van Genuchten formulation: m and α (Maidment 1993, Table 5.1.1 by expressing h as a function of S_e instead of S_e as a function of h and by expressing n as a function of m. The parameters m and n are both a function of λ, the pore-size index).

$$P_c = \frac{1}{\alpha}\left(S_e^{-1/m} - 1\right)^{1-m} \qquad \text{(Eq. 2)}$$

where S_e is the reduced saturation. Best fit on that curve yields m and α. In addition, the mountain-scale case also allows fitting of the fracture parameters but in that instance emphasis is on the matrix rather than the fracture. The parameter m is related to the standard deviation of the distribution of pore/opening size while the parameter α is related to the air-entry pressure. A clayey material has a large range of pore size and its curve-fitted m is on the low range of natural porous media. On the other hand, an uniform sand has a small pore size range and its curve-fitted m is in the higher range. The value of m=0.492 retained by the project (DTN: LB971212001254.001) for all formations between TSw33 and TSw37 corresponds to a standard deviation of 0.5 of the log-normal distribution of aperture. A larger value of m, as 0.667 used earlier in the project for unit TSw34, corresponds to a smaller distribution (standard deviation of 0.32) and was estimated from air-permeability data (Bodvarsson et al. 1997, Table 7.14). A value of 0.633 was more recently used in large-scale studies (DTN: LB990501233129.001) and a value of 0.608 was retained for the drift seepage calculations (DTN: LB997141233129.001). The value of 0.608 is thus taken to be the conservatively more accurate and yields by linear interpolation between the couples (0.492, 0.5) and (0.633, 0.32) a standard deviation of 0.38 (couple (0.608, 0.38)) (Table 6-5).

Table 6-5. Van Genuchten *m* Parameters and Hydraulic Aperture Standard Deviations

Unit	Van Genuchten *m*	Hydraulic Aperture Standard Deviation
TSw33	0.608	0.38
TSw34	0.608	0.38
TSw35	0.611	0.38
TSw36	0.610	0.38
TSw37	0.610	0.38

Source DTN: LB997141233129.001

This method uses information from large-scale studies and applies it to the drift scale. Therefore, one should be cautious when using its results. The method also seems to underestimate the true standard deviations as suggested at the beginning of Section 6.3.3.

6.3.2.2 Estimation of the Mean of the Hydraulic Fracture Aperture

The average aperture is characterized by the geometric mean, that is, the exponential of the mean of the log-transformed apertures. A value of 81 μm for TSw34 is given in Bodvarsson et al. 1997 (Table 7-12 p. 7-18) and is repeated at the top of p. 2-40 of the Total System Performance Assessment - Viability Assessment (CRWMS M&O 1998). This value includes both ESF and borehole measurements. However, the value of 140 μm appears in Table 7-12 of Bodvarsson et al. 1997. This value is derived from ESF measurements only. Table 6-6 summarizes the most recently mentioned values.

Table 6-6. Hydraulic Aperture Geometric Means

Unit	Geometric Mean Hydraulic Aperture (μm)
TSw33	230
TSw34	98
TSw35	150
TSw36	160
TSw37	160

Source DTN: LB990501233129.001

6.3.2.3 Example of Treatment

TSw34 is taken as an example and a CDF (cumulative distribution function) is provided (Table 6-7). Fracture hydraulic apertures (in microns) follow a lognormal distribution of mean $\mu_{\log 10} = \log_{10}(98)$ and standard deviation $\sigma_{\log} = 0.38$ (this is decimal log).

At "q" standard deviations, the aperture is:

$$\log\left(2b|_{q\sigma}\right) = \log\left(2b|_{mean}\right) + q\sigma$$

$$2b|_{q\sigma} = 2b|_{mean}\, 10^{(q\sigma)} \qquad \text{(Eq. 3)}$$

that is the geometric average hydraulic fracture aperture has a probability of 0.15% of being in excess of 1.35 millimeters and similarly of being below 7 μm.

Table 6-7. CDF of Fracture Hydraulic Apertures for Unit TSw34

TSw34 Fracture Hydraulic Aperture (μm)	CDF
54	0.25
98	**0.50**
122	0.60
155	0.70
205	0.80
301	0.90
413	0.95
750	0.99
1315	0.9985

6.3.3 Distribution of Solute Transport Aperture

It can be proven theoretically (Tsang 1992) that mass balance apertures are always larger than hydraulic apertures. A relationship between hydraulic and transport apertures is given by Gelhar (1993, Eq. 5.5.13) when apertures are lognormally distributed:

$$2b|_{Solute} = 2b|_{Hydraulic} \exp\left(\frac{\sigma_{ln}^2}{2}\right) \qquad \text{(Eq. 4)}$$

This suggests that the hydraulic aperture is a lower bound for the "physical" average aperture. This happens because flow does not "see" dead ends where solutes can diffuse and is mainly affected by the smallest apertures along the flow lines. In other words, if a fracture in the tuff can be envisioned as larger openings connected by constrictions, the hydraulic aperture relates to the constriction size while the transport aperture relates to the size of the larger openings or the overall fracture porosity. It is thus conservative and more physically sound to retain the transport aperture for the purpose of actinide accumulation but still relevant to study the hydraulic aperture for flow in the fracture and possible plugging.

One way to obtain the average solute transport aperture would be to apply Eq. 4 with results from Section 6.3.2, e.g., for unit TSw34:

$$2b|_{Solute} = 2b|_{Hydraulic} \exp\left(\frac{\sigma_{ln}^2}{2}\right) = 98 * \exp\left(\frac{(0.38*2.3)^2}{2}\right) = 144 \qquad \text{(Eq. 5)}$$

This number is lower than that given by the field experiments (see Table 6-11 in next section). Although an interpretation of the fracture porosity obtained through tracer tests is given in Table 6-8, it was felt more appropriate to go back to the original field data and redo the derivation.

Table 6-8. Processed Data for Fracture Porosity

Unit	Fracture Porosity (% of Total Rock)
TSw33	0.66
TSw34	1.0
TSw35	1.1
TSw36	1.5
TSw37	1.5

Source DTN: LB990501233129.001

NOTE: Only TSw34 porosity is obtained through field tests. Other values are scaled from that unit porosity and from permeability and fracture frequency values.

The tracer tests were done in Niche 3107 located in the ESF at station 31+07 and in Alcove 5 (the location of the Drift Scale Test block) at station 28+27. Results for the porosity calculations are given in DTN: LB980912332245.002 and reproduced in Table 6-9. Description of the geology of Alcove 5 in the ESF is given in the South Ramp report (Eatman et al. 1997 - pp. 161 to 166). It is stated that the geology of Alcove 5 is very similar to the geology of the nearby drift. The drift segment between stations 28+00 and

28+50 is thought to be the most representative of the geology of Alcove 5 (Table 6-10). Similarly the drift interval between stations 29+90 and 30+30 is representative of the geology of Niche 3107 (Table 6-10). Both Alcove 5 and Niche 3107 are within the TSw34 unit. There is, to date, no reportable tracer test data porosity for other units. Rather than do the scaling from the TSw34 unit to other units, it was felt more appropriate to assume that the fracture aperture derived for the TSw34 unit is also valid for the other units (Assumption 5.1).

Table 6-9. Tracer Test Data for Fracture Porosity

Tracer Test Location	Fracture Porosity (% of Total Rock)	Tracer Test Location	Fracture Porosity (% of Total Rock)
Alcove 5 (ESF)	1.8		
Alcove 5 (ESF)	0.6		
Alcove 5 (ESF)	1.5	Niche 3107 (ESF)	1.2
Alcove 5 (ESF)	1.1		
Average Alcove 5	1.25		

Source DTN: LB980912332245.002

Table 6-10. Fracture Spacing for Drift Intervals Located in the Vicinity of the Tracer Tests

Fractures > 1m Dip > 65°	Number of Fractures	Arithmetic Spacing (m)		Geometric Spacing (ln units)		Average Geometric Spacing (m)
		Mean	St. Dev.	Mean	St. Dev	
TSw34 ESF 27+20 to 42+00	2384	0.620	0.724	-1.111	1.285	0.329
Around Alcove 5 (28+00 to 28+50)	89	0.619	0.709	-1.116	1.294	0.328
Around Niche 3107 (29+90 to 30+30)	44	1.109	1.126	-0.539	1.380	0.583

Source: FILE (Att. IV CD-ROM): **Niche3107_Alcove5_forporosity.xls**

CRWMS M&O (2000d - Section 6.2.1) assumes that the distribution is lognormal and gives as the final result:

Table 6-11. Transport Aperture Distribution Parameters

Unit	Geometric Mean (mm)[a]	Geometric SD [-][b]	at - 2 σ	at + 2 σ
TSw34	0.739	1.615	0.28	1.93
TSw35	0.739[d]	1.9[c]	0.20	2.67
TSw36	0.739[d]	1.9[c]	0.20	2.67

NOTES: [a] from CRWMS M&O 2000d Table 3 Column 6
[b] from CRWMS M&O 2000d Table 4 Column 9
[c] No calculations were performed specifically on these units because of a lack of data. They were assigned the arithmetic average of the geometric standard deviations of all overlying units (CRWMS M&O 2000d Table 4 Column 9).
[d]: The values of 1.14 mm and 1.22 mm given in CRWMS M&O 2000d were not retained because they were obtained through fracture intensity scaling. The value of 0.739 mm was obtained through tracer tests (CRWMS M&O 2000d Table 3 Column 6).

DEVELOPED DTN: MO0109SPAFIE10.006

The average transport aperture needs to be adapted to this document's needs because its derivation is done assuming a porosity of 1% and a fracture cutoff of 0.3 m. Two

elements need to be addressed. The true porosity where the porosity was calculated is 1.25%; this will increase the fracture aperture. Assuming that the fracture system is well-connected (Assumption 5.10), the smallest fractures need to be incorporated, this will decrease the fracture aperture. Their fraction is about 33% (Table 6-40, row 19). Variations are small; a linear correction can be used. The correction goes: (2b) x (1.25% / 1%) x (0.67 / 1) = 0.84 (2b) where (2b) is the fracture aperture. This correction would yield a smaller fracture aperture than assumed in Table 6-11. The correction coefficient is thus conservatively set to 1 instead of 0.84.

The average aperture of the TSw34 unit is between 0.46 mm and 1.19 mm at 1 standard deviation. There is a 2.5% chance that the average aperture is over 1.615^2*0.739=1.93 mm and a 0.15% chance that the aperture is over 3.1 mm. Fracture apertures for other units are also available from CRWMS M&O 2000d (Tables 3 and 4). However, they were not calculated from field experiments but extrapolated from fracture intensity. That extrapolation did not take into account the most recent data from the ECRB. It was felt more appropriate to assume that the fracture aperture is the same in all units and use the new fracture intensity from the ECRB data. In any case, the apparent increase in the fracture aperture from the TSw34 to the TSw35 units from 0.739 mm to 1.14 mm (about 54%) may be due to the fact that more than 50% of the fracture length in the TSw35 unit is due to fractures < 0.3 m (Table 6-40) that are not considered in the extrapolation. The standard deviation is kept at 1.9 to take into account the increased uncertainty for the TSw35 and TSw36 units.

It is worth noting that fracture apertures are calculated ***without*** including the lithophysae, that is they truly represent fracture apertures and not an artificial average void space aperture. The average aperture numbers are derived from unit TSw34 poor in lithophysae (Table 6-14) and extrapolated to other units on the basis of fracture frequency (Assumption 5.1).

This translates into the following lognormal CDF (Table 6-12):

Table 6-12. CDF of Solute Fracture Apertures

	Fracture Solute Aperture (mm)		
CDF	TSw34	TSw35	TSw36
0.01	0.24	0.17	0.17
0.25	0.53	0.48	0.48
0.50	**0.74**	**0.74**	**0.74**
0.60	0.83	0.87	0.87
0.70	0.95	1.03	1.03
0.80	1.11	1.27	1.27
0.90	1.37	1.68	1.68
0.95	1.63	2.12	2.12
0.99	2.25	3.29	3.29
0.9985	3.07	4.96	4.96

Source: FILE (Att. IV CD-ROM): **Aperture_dist_tsw34.xls**

It is now straightforward to come up with the average aperture of a series of fracture if the apertures are not correlated (that is, a large-aperture fracture does not imply on

average that the next fracture is either also large (positive correlation) or small (negative correlation). Figure 6-1 displays an example of treatment for unit TSw35. The average of a larger and larger number of fractures tends to converge to the average of the distribution. The value of 0.88 mm, 0.94 mm, and 1.04 mm (for 40, 20, and 10 fractures respectively) for the upper bound of the average fracture aperture at 95% CDF is reasonable (Table 6-13).

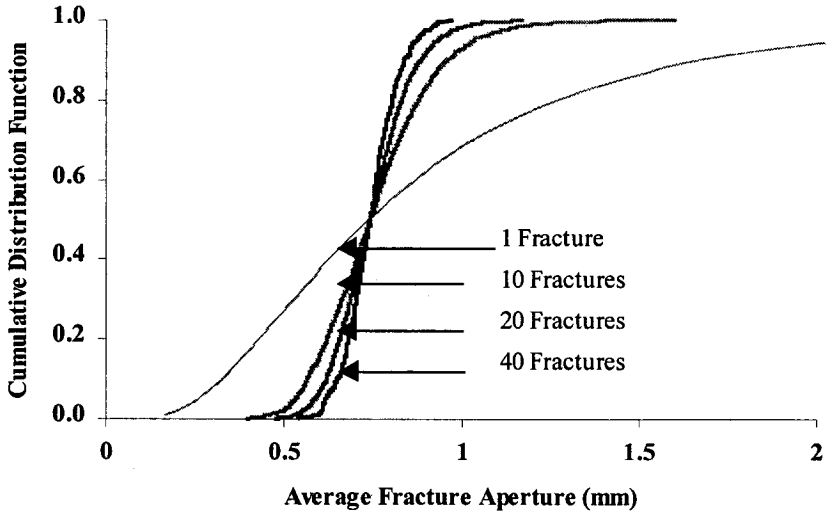

Source: FILE (Att. IV CD-ROM): **Aperture_distribution_TSw35-36_run1.xls**; worksheet: 40 fractures

Figure 6-1. Average Fracture Aperture (TSw35 unit) over 1, 10, 20, and 40 Fractures

The standard deviation for each set of fractures is given in Table 6-13. Table 6-13 can be used to set the maximum average aperture that fractures can have when the fracture intensity is high.

Table 6-13. Standard Deviation (in natural ln space) and Average Fracture Aperture for a Set of *n* Fractures (*n* = 5, 10, 20, 30, 40 or 80) - 2 runs

		1	2	3	4	5	6	7
	Unit	**Standard Deviations of Average Aperture**						
		1 fracture	5 fractures	10 Fractures	20 Fractures	30 Fractures	40 Fractures	80 Fractures
1	34	0.479	NC	0.150 - 0.148	0.108 - 0.104	0.086 - 0.084	0.075 - 0.075	0.074 - 0.074
2	35	0.642	0.284	0.202 - 0.197	0.141 - 0.140	0.114 - 0.115	0.101 - 0.098	0.070 - 0.071
3	36	Ibid. 35	Ibid. 35	Ibid. 35	Ibid. 35	Ibid. 35	Ibid. 35	Ibid. 35
		Average Aperture at 95%						
		1 fracture	5 fractures	10 Fractures	20 Fractures	30 Fractures	40 Fractures	80 Fractures
4	34	1.63	NC	0.94 - 0.95	0.87 - 0.88	0.85 - 0.87	0.83 - 0.83	0.81 - 0.81
5	35	2.12	1.17	1.04 - 1.04	0.93 - 0.94	0.88 - 0.88	0.88 - 0.88	0.83 - 0.83
6	36	Ibid. 35	Ibid. 35	Ibid. 35	Ibid. 35	Ibid. 35	Ibid. 35	Ibid. 35
		Average Aperture at 99.5%						
		1 fracture	5 fractures	10 Fractures	20 Fractures	30 Fractures	40 Fractures	80 Fractures
7	34	2.54	NC	1.09 - 1.11	0.95 - 0.99	0.93 - 0.97	0.91 - 0.89	0.85 - 0.85
8	35	3.86	1.52	1.30 - 1.30	1.08 - 1.08	1.04 - 1.04	0.94 - 0.94	0.87 - 0.88
9	36	Ibid. 35	Ibid. 35	Ibid. 35	Ibid. 35	Ibid. 35	Ibid. 35	Ibid. 35

Source: FILES (Att. IV CD-ROM): **Aperture_distribution_TSw34_run1.xls, Aperture_distribution_TSw34_run2.xls, Aperture_distribution_TSw35-36_run1.xls, Aperture_distribution_TSw35-36_run2.xls**

NOTES: NC = Non Calculated. Results from 2 Monte-Carlo runs are presented run1 - run2

DEVELOPED DTN: MO0109SPAFIE10.006

6.3.4 Influence of External Factors on Fracture Porosity

Several factors, which will be developed in this section, have an influence on the fracture porosity before any waste package breach occurs:

- Precipitation/dissolution of secondary minerals
- Mechanical influences of thermal stresses
- Mechanical influences of tectonic stresses.

The drift-scale thermal-hydrologic-chemical model (BSC 2001d, p. 222) shows that the fracture porosity is not affected by mineral precipitation/dissolution in the early history of the potential repository. It changes by less than 1% during the first 10,000 years (the calculations were done on the TSw34 unit with no waste package breach).

The thermal event affects porosity and permeability because of the mechanical effects of heat. CRWMS M&O 2000a, Section 5.4.1 shows in Table 2 that the maximum permeability multiplier for fractures within 2 drift diameters of the drift is 2.5 and 11 for normal and shear displacements, respectively. The permeability increase occurs during the cool down period (CRWMS M&O 2000a, Section 6, p.41). However, the permeability increase is not generalized but occurs only in some locations. It is also compensated by permeability decrease. Although not easily transferable to fractured media, the Kozeny-Carman equation (Bear 1988, Equation located between Eq. 5.10.18 and Eq. 5.10.19, p. 166), that relates porosity and permeability, can be used as a first approximation:

$$k = \frac{d_m^2 n^3}{180(1-n)^2} \qquad \text{(Eq. 6)}$$

where d_m is the mean particle size, k is the permeability and n the porosity. When the porosity is low (<10%), combining Eq. 6 for two states yields:

$$\frac{k_1}{k_x} = \left(\frac{n_1}{n_x}\right)^3 \qquad \text{(Eq. 7)}$$

where the subscript 1 indicates the starting condition and the subscript x the final condition. A change in permeability by one order of magnitude translates into a change in porosity by a factor 2. The thermal-hydrologic-mechanical model also assumes a low fracture frequency (0.1 to 0.5 fracture m^{-1}; CRWMS M&O 2000a, Section 5.1) on the basis that not all fractures are active. With more fractures to absorb the thermal stresses the change in fracture porosity will be less. A fracture frequency of 0.1 to 0.5 fracture.m^{-1} translates into a fracture spacing of 2 to 10 m. This fracture spacing is one order of magnitude lower that the fracture spacing computed in this document (see Figure 6-24). The limited changes in porosity (the factor 2 is a maximum that does not applied to all locations), that in addition occur both ways, suggest that they are already included in the fracture porosity variability as described in the previous sections. Therefore the thermal effects are not included in the rest of this document.

Possible tectonic stresses in the form of a seismic event with lasting effects on the fracture porosity have also be analyzed (CRWMS M&O 2000c). It has been determined that the mean displacements along the faults are 0.1 cm (7.8 and 32 cm) or less at a 10^{-5} annual exceedance probability, and on the order of 1 m (5 m) or less at 10^{-8} exceedance probability (the values into brackets refer to the Solitario Canyon fault and Bow Ridge fault, respectively) (CRWMS M&O 2000c, Section 6.1.2). Models for a fault displacement of 1 meter along the Solitario Canyon fault indicate a strain of 50 microns per meter two kilometers from the fault plane and 10 microns per meter about 6 kilometers from the fault (CRWMS M&O 2000c, Section 6.2.1.5). If the conservative assumption that all the strain accumulates in the fractures is made, then an estimate of the change in aperture can be made. The value of 50 microns per meter is retained because most of the potential repository is within two kilometers of the Solitario Canyon fault. This value can be scaled to any displacement along the fault because of the linearity of the elastic model. The lower bound for the fracture frequency for fractures > 0.3 m is 4.3 fractures/m (Table 6-40). This translates into an increase in fracture aperture of 50 microns distributed over 4.3 fractures or 50/4.3=12 microns per fracture (still for a fault displacement of 1 meter). Thus a seismic event is not likely to significantly change the fracture aperture; 12 microns is 1.6% of the average aperture of about 740 microns and falls well within the uncertainty of the tracer test methodology.

6.4 LITHOPHYSAE

Lithophysae are well-developed in the lithophysal units (TSw33 and TSw35). However, they are not evenly distributed even when they are abundant (Table 6-15) and may be absent for tens of meters. The volume percentage of lithophysae in each unit is given in Table 6-14. Lithophysae have variable shape, from almost spherical to ellipsoidal and to lenticular or irregular shape. Most lithophysae have diameters smaller than 20 cm, but cavities with diameters that vary from 20 cm to greater than 1 meter are scattered throughout the proposed repository. Lithophysal units have typically a lower fracture frequency for fractures > 1m (Fig. 13 of Mongano et al. 1999, p. 77) as lithophysae seem to inhibit the fracture propagation. On the other hand, lithophysal formations have a higher number of small-length fractures.

6.4.1 Lithophysae Porosity

Table 6-14 gives the lithophysae porosity for the different units in the vicinity of the proposed repository while Table 6-15 gives some details about lithophysae abundance of the main repository unit. More details are available on the lithophysae of TSw35 in Table 3 of Mongano et al. (1999) which is reproduced and modified in Table 6-15.

Available information about lithophysae is more descriptive than quantitative and the following description is a first attempt to quantify the importance of lithophysae on criticality issues. When weighed by the interval length, the mean percentage of the rock (TSw35) occupied by lithophysae is about 8.5% and the mode is about 5%. Although the lithophysae shape can be quite irregular, a spherical shape is more conservative and is assumed in this section. The size of a lithophysal cavity will be represented by its diameter. The geometric mid-size of the lithophysae is 18.5 cm. This value was obtained by assuming a lognormal distribution of the lithophysae size (Assumption 5.6) and assuming that the extreme values of the range correspond to the same number of standard

deviations from the mean (no value for this parameter needs to be specified to compute the mean). These numbers yield about 27 lithophysae per m^3 if evenly distributed, that is 3 in each direction (3 levels of 3 rows and 3 lines, i.e., a total of 27), that is a spacing of 0.33 m between the center of the lithophysae in all three directions.

Table 6-14. Percentage of Lithophysae in Each Unit

Unit	% Lithophysae	Source
TSw33 ESF	3 - 40	Eatman et al. 1997 p. 45 (south ramp)
TSw33 ECRB	25 - 40	Mongano et al. 1999, p. 17
TSw34 ESF	0 - 3 0 - 2	Albin et al. 1997 p. 15 (main drift) Eatman et al. 1997 p. 47 (south ramp)
TSw34 ECRB	0 - 1	Mongano et al. 1999, p. 20
TSw35 ESF	15 - 25 5 - 15 (locally 1 - 5)	Albin et al. 1997 p. 19 (main drift) Eatman et al. 1997 p. 49 (south ramp)
TSw35 ECRB	5 - 30	Mongano et al. 1999 p. 25
TSw36 ECRB	0 - 5 (Typically <1)	Mongano et al. 1999 p. 34

The "Rock Properties" model, integrating many sources of information but mainly cores, gives for lithophysae porosity a mean of 14.6%, a standard deviation of 7.6%, a minimum of ~0% and a maximum of 55.1% for the *whole* TSw formation (CRWMS M&O 2000e, Table 13). This result is consistent with this study as the TSw35 unit is only the third interval in importance of lithophysal porosity (e.g., CRWMS M&O 2000e, Fig. 12).

Table 6-15. Lithophysae Distribution in TSw35 ECRB

Interval Stationing	*Interval Length (m)*	Range of Volume % of Lith.	*Mid-Range of volume % of Lith.*[a]	Size Range (cm)	*Geometric Mid Size (cm)*[b]	Comments Mineral Coatings (Mongano et al. 1999, pp. 26 to 29)
14+44 14+62	*18*	3 - 7	*5*	7 - 30	*14.5*	Mode = 20 cm 1 - 3 cm VPM
14+62 - 15+16	*54*	12 - 15	*13*	10 - 30	*17.3*	
15+16 - 15+84	*68*	5 - 15	*10*	10 - 120	*34.6*	2 - 3 cm VPM
15+84 - 15+98	*14*	5 - 10	*8*	15 - 100	*38.7*	
15+98 - 16+30	*32*	20 - 30	*25*	15 - 130	*44.1*	Thin or No VPM
16+30 - 17+00	*70*	5 - 10	*8*	0 - 20	*11.0*[c]	<1 - 3 cm VPM
17+00 - 17+23	*23*	3 - 5	*4*	10 - 70	*26.5*	
17+23 - 17+97	*74*	10 - 20	*15*	6 - 75	*21.2*	
17+97 - 19+50	*153*	7 - 10	*9*	6 - 40	*15.5*	Thin, Drusy Coatings of VPM
19+50 - 20+65	*115*	4 - 6	*5*	5 - 30	*12.2*	
20+65 - 21+31	*66*	4 - 6	*5*	7 - 50	*18.7*	
21+31 - 22+82	*151*	3 - 7	*5*	7 - 40	*16.7*	
22+82 - 23+26	*44*	3 - 5	*4*	15 - 100	*38.7*	Drusy Coatings of VPM
Weighed Average			*8.5*		*18.5*	

Source DTN: GS991108314224.015; Table S99470_001
FILE (Att. IV CD-ROM): **lithophysae.xls**

NOTES: Plain text: information reproduced from Table 3, Mongano et al. 1999, p. 29 (also in DTN) except comments
Text in italics: Computed information
[a] Assumes a uniform distribution within the range
[b] Assumes a lognormal distribution (see text)
[c] Assumes a lower bound for size of 6 cm.
VPM = Vapor-phase Minerals

The full periphery geologic maps (FPGM) map lithophysae with a diameter larger than 1 m (DTNs: GS990408314224.003, GS990408314224.004, GS990408314224.005, and GS990408314224.006). There is a total of 170 mapped lithophysae with a diameter larger than 1 m in the TSw35 unit (Figure 6-2).

The cross drift has a diameter of 5 m (Mongano et al. 1999; p. 3). The large lithophysae are mapped from springline to the ceiling to springline, i.e., a half-circle segment of 7.85 meters and along 885 meters of tunnel. Those numbers yield an approximate surface density of 170/885/7.85=0.025 large lithophysal cavity per square meter of drift footprint or about one large lithophysal cavity per waste package length on average. On the other hand, only 56.2% of the 10-m intervals have large lithophysae (see file **Lithophysae.xls**)

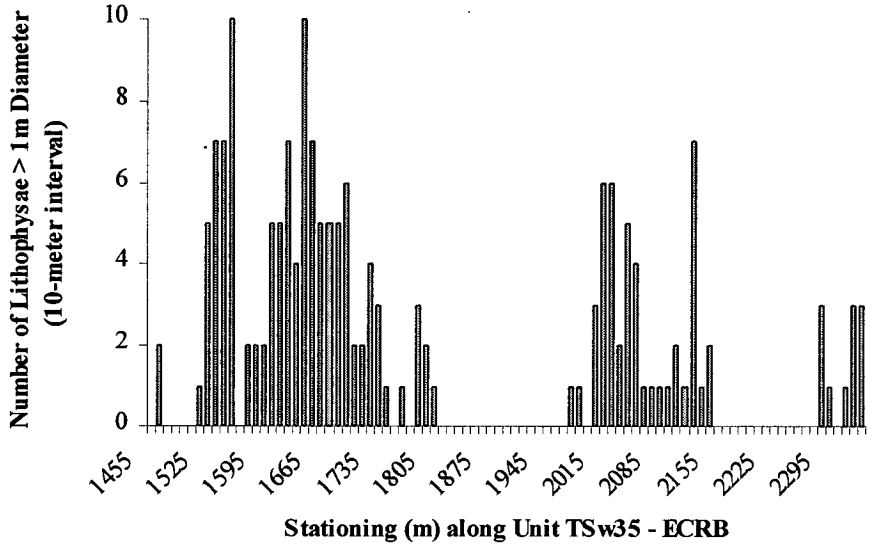

Source: DTNs: GS990408314224.003, GS990408314224.004, GS990408314224.005, and GS990408314224.006
FILE (Att. IV CD-ROM): **Lithophysae.xls**; worksheet: litho larger than 1m

Figure 6-2. Distribution of Lithophysae with a Diameter Larger than 1 Meter (Unit TSw35)

6.4.2 Lithophysae Morphology

The ECRB report (Mongano et al. 1999; p. 26) gives only a qualitative description of the lithophysae morphology. They tend to be lenticular or ellipsoidal. The cavity interior may be smooth but often irregularly shaped with blocky features. The shape of the largest lithophysae is not systematically spherical but more often oblate. The lithophysae may locally blend with the matrix without clear discontinuity.

6.4.3 Lithophysae and Fracture Network

Lithophysae are relevant for criticality calculations only if they are connected to the general fracture network. The DLS provides termination mode for fractures. One common mode is junction to a lithophysae. Table 6-16 gives the number of fractures

ending in lithophysae, but there is no explicit information on how many lithophysae are intercepted by fractures.

Although not explicitly stated in Mongano et al. (1999) it makes sense to assume that the larger the lithophysae, the more likely it is to have one or several fracture terminations. Unit TSw34 with little lithophysae (3% maximum) has about 5% of its fractures ending in lithophysae. Table 6-40 (row 11) suggests that the fracture intensity stays about the same in the different units. A lower fracture intensity for fracture >1m is compensated by a larger number of small fractures. Table 6-41 suggests that the total fracture intensity is still higher when the fracture frequency for fractures >1m is higher (by 12.5% in this case). For the only unit with abundant lithophysal cavities (TSw35), Table 6-42 shows that the average spacing for fractures longer than 0.4 m is 0.12 m or smaller (6+2+0=8 fractures, 11+5+1=17 fractures, and 2+2+4=8 fractures for the three Small Scale Survey intervals; and 1 m /8 fractures =0.12 m). This value is smaller than the average lithophysae spacing of 0.33 m (see Section 6.4.1). It is thus conservative but still plausible to assume that all lithophysae are intercepted by fractures and hence connected to the general fracture network..

Table 6-16. Percentage of Fractures Ending on Lithophysae

Unit	Discontinuity (Fractures, VPP) Length Interval	Fraction of Fractures Ending on Lithophysae	Comments
TSw35	0.0 - 1.0 m	42 / 372 = 11.3%	From small scale study FILE (Att. IV CD-ROM): **ECRB_smallfract_spacing.xls** worksheet: ll lithophysae
TSw35	> 1 m	65 / 268 = 24.3%	From all ECRB exposures FILE (Att. IV CD-ROM): **ECRB_study_TSw35.xls** worksheet: lithophysae all fractures >65
TSw34	> 1 m	40 / 848 = 4.7%	From all ECRB exposures FILE (Att. IV CD-ROM): **ECRB_study_TSw34.xls** worksheet: lithophysae all fractures >65

6.4.4 Lithophysae Size and Lithophysae Porosity Distributions

A calculation of lithophysae size and porosity distribution was attempted with information only from Table 6-15 (see file **lithophysae.xls** in Att. IV CD-ROM). Synthetic distributions were built making the following assumptions:

- Lithophysae size is lognormally distributed while lithophysae porosity is normally distributed both in their given interval and along the total length of the drift (for unit TSw35) (Assumptions 5.6 and 5.7).
- Each length interval (each row from Table 6-15) is weighted by its length for lithophysae porosity distribution and by the lithophysae volume for the lithophysae size distribution.
- Each length interval is characterized by a range of values assumed to exactly encompass 4 standard deviations (2 on each side of the mean). Each interval is then represented by its mean (geometric for size and arithmetic for porosity), by one value at 12% of the cumulative distribution function, and by one value at 12%

of the complementary cumulative distribution function. That is, the mean has a weight of 2 and represents values between 25 and 50% of the CDF, while each of the other values has a weight of 1 and represents the more extreme values of the distribution. A value of 12% for the CDF corresponds to a standard deviation of 1.175.

- The final distributions are constructed by combining the 3 values yielded by each length interval into one single distribution.

Figure 6-3 and Figure 6-4 display data and analytical curve for the lithophysae size and porosity distribution. The analytical curve was constructed by assuming a normal distribution with the same mean and standard deviation as the data. The correlation coefficient between mid-range of porosity and geometric mid-size (column 4 and 6 of Table 6-15) is 0.41. A larger porosity is in general due to the presence of larger lithophysae, but this is just a general trend as the correlation coefficient is not very high.

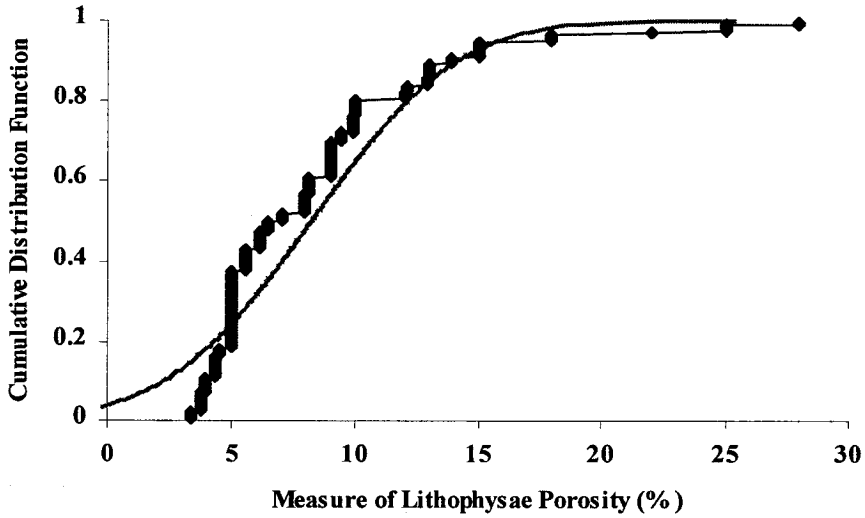

Source: FILE (Att. IV CD-ROM): **Lithophysae.xls**; worksheet: litho pro dist
DEVELOPED DTN: MO0102SPALIT10.001

Figure 6-3. CDF of Lithophysae Porosity

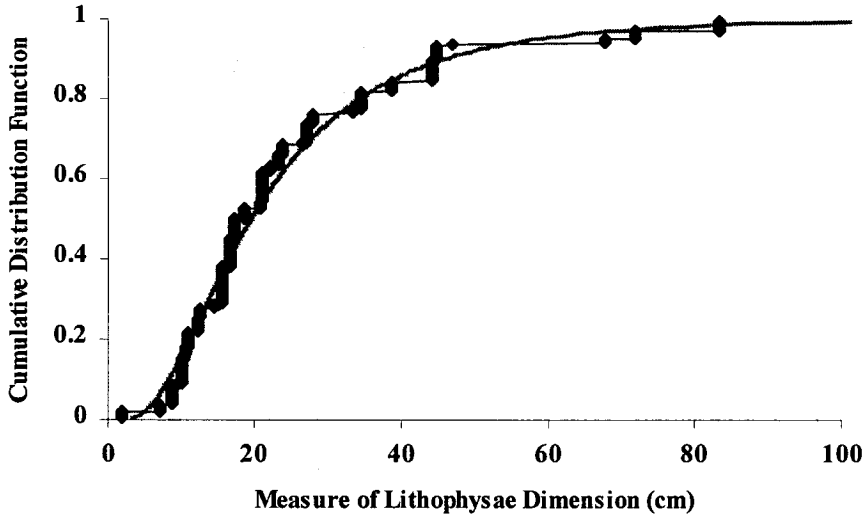

Source: FILE (Att. IV CD-ROM): **Lithophysae.xls**; worksheet: litho size dist
DEVELOPED DTN: MO0102SPALIT10.001

Figure 6-4. CDF of Lithophysae Size

Although an attempt was made to fit the resulting CDFs to a parametric distribution (Table 6-17), it is felt more appropriate to use the CDF directly in the lookup table available in the developed DTN: MO0102SPALIT10.001.

Table 6-17. Lithophysae Size and Porosity Distribution Parameters (TSw35 unit)

	Type	Average	Standard Deviation
L. Porosity	Normal	8.2%	4.6%
L. Size	Lognormal	(Geom) 19.6 mm	0.67(ln transformed values)

6.4.5 Lithophysae Fillings

Table 6-15 (column 7) displays the quantitative comments about the lithophysae fillings of the TSw35 unit. They are mainly vapor-phase minerals whose composition is consistent with what is observed in the fractures (see Table 6-26 to Table 6-28). The vapor phase partings consist mainly of silica polymorphs (tridymite, high temperature form of silica, often transformed into quartz or cristobalite) and less common sanidine (Barr et al. 1996, p. 116), type of potassium feldspar. Rarely, stibnite (Barr et al. 1996, p. 116) and fluorite (Albin et al. 1997, p. 23) have also been found. Specular hematite sometimes appears in addition to the very common silica polymorphs. Secondary infilling, such as calcite and opal, is sometimes present in larger cavities (Eatman et al. 1997, p. 46; Albin et al. 1997, p. 18 and p. 23 on TSw34). Fine-grained hematite and manganese oxides sometimes also coat the vapor-phase partings. Both manganese oxides and hematite can be either primary or secondary, but they are minor components most of the time. The first generation of the depositional sequence bears little genetic resemblance to potential actinide accumulation. The second generation (coarse, tabular calcite, and opal) is clearly of meteoric origin (Moscati and Whelan 1996, p. 5) and resembles more the expected settings of actinide accumulation.

About 105 meters of ECRB drift (about 12%) have significant filling up to 3 cm. The average can be estimated at 1.5 cm. About 71% (626 m over 882 m) of the TSw35 have lithophysae with thin coatings that can be estimated at 0.3 cm. The rest (17%) has no infillings (Table 6-18).

Marshall et al. 2000, p. 3 states that between 1 and 40% of the lithophysae have calcite coatings in the TSw33 unit. This wide range can be compared to the calcite abundance in the fractures of units TSw34 to TSw36 (Table 6-26 to Table 6-28). Calcite is relatively abundant in the TSw34 unit where it can be recognized in 10% of the fractures. Calcite is one order of magnitude less abundant in the TSw35 unit fractures. It appears that calcite is preferentially deposited in the lithophysae rather than in the fractures. Thickness of secondary minerals will be developed in Section 6.11. A summary of the results is presented in Table 6-18.

Table 6-18. Summary of Lithophysae Infillings in ECRB

Infilling	Fraction	Nature
PRIMARY		
Thick VPP (1.5 cm)	12%	Silica, $KAlSi_3O_8$
Thin VPP (0.3 cm)	71%	Silica, $KAlSi_3O_8$
No VPP	17%	Silica, $KAlSi_3O_8$
Sum	100%	
SECONDARY		
Calcite (0 - 2 cm)	1 - 40%	Calcite
UNDIFFERENTIATED		
Mn (and Fe) oxides (0 - 0.3 cm)		Mn Oxides, Hematite.

6.5 FRACTURE ORIENTATION

Fracture orientations are obtained through individual measurements of strike and dip. Results are plotted on stereographic nets, and visual inspection/statistical analyses are performed. The fractures are then grouped into sets or families that are characterized by the arithmetic average of dip and strike. All orientation sets are presented in the "strike/dip" format.

6.5.1 Average Orientation

Visual inspection of Fig. 8 to 12 of Mongano et al. (1999) in addition to cluster analysis of the ECRB data (fracture cutoff is 1 m) is summarized in Table 6-19 through Table 6-24. Another cluster analysis on the ECRB data is presented in the drift degradation analysis (CRWMS M&O 2000b, Section 6.3.2). Both analyses are in good agreement. The fracture set numbers given in the following tables correspond to the tectonic analysis of the ESF fracture system. Overall information is extracted from Table 8 from Mongano et al. (1999) for ECRB data and from Table 1 from Albin et al. 1997, for ESF data. The shorthand notations "EW", "NS", "NE-SW", and "NW-SE" stand for East-West, North-South, Northeast-Southwest, and Northwest-Southeast, respectively. The ECRB sets are assigned to ESF sets when appropriate. The few fracture sets of the ECRB not present in the ESF have been assigned to the closest ESF set.

- Unit TSw33 (Fig. 8 of Mongano et al. 1999): two main, nearly vertical sets of fractures crossing at an angle of approximately 80°.

Table 6-19. Orientation of TSw33 Fracture Sets (373 fractures) - ECRB

Set Orientation	# of Entries	Percentage	Proportion	ESF Geologic Set
088/86 (Vertical "EW")	23	6%	5	
122/83 (Vertical "EW")	79	21%		Set 1
195/83 (Vertical "NS")	178	48%	10	Set 2
302/38 (Horizontal)	93	25%	5	Sets 3&4

Sources: DTN GS991108314224.015; Table S99470_003 for "Set Orientation" column
Mongano et al. (1999, Table 7) for # of entries.

- Unit TSw34 (Fig. 9 of Mongano et al. 1999): two main, nearly vertical sets of fractures crossing at an angle of approximately 75°. The fractures can be modeled as 2 perpendicular sets of vertical fractures. A TSw34 unit fracture count indicates that one set is more abundant that the other set (by about a factor of 2 - Table 6-20). Set 1 is the well-developed fracture set in the IFZ of the ESF (Table 6-22).

Table 6-20. Orientation of TSw34 Fracture Sets (930 fractures) - ECRB

Set Orientation	# of Entries	Percentage	Proportion	ESF Geologic Set
122/84 (Vertical "EW")	585	63%	10	Set 1
195/85 (Vertical "NS")	286	31%	5	Set 2
306/09 (Horizontal)	59	6%	1	Sets 3&4

Sources: DTN: GS991108314224.015; Table S99470_003 for "Set Orientation" column
Mongano et al. (1999, Table 7) for # of entries

ESF data outside of the IFZ show a similar trend (Table 6-21) although set 1 is already more preponderant than in the ECRB. The increase in fracturation in the IFZ is entirely due to set 1 because set 2 has about the same intensity: 0.30 fracture/m outside the IFZ (that is, 532 fractures in 1750 m) and 0.23 fracture/m in the IFZ (that is, 215 fractures in 950 m). Set 1 shows a three-fold increase: 1 fracture/m outside the IFZ (that is, 1766 fractures in 1750 m) and 3.1 fracture/m in the IFZ (that is, 2951 fractures in 950 m).

Table 6-21. Orientation of TSw34 Fracture Sets (2523 fractures) - ESF Outside the IFZ

Set Orientation	# of Entries	Percentage	Proportion	ESF Geologic Set
Vertical "EW"	1766	70%	7	Set 1
Vertical "NS"	532	21%	2	Set 2
Horizontal	225	9%	1	Sets 3&4

NOTE: Values obtained by summing results from domains 1, 2 and 4 from Table 1, Albin et al (1997) (Total drift length of 1750 m). The random orientation group (25% of total) is not included and is assumed not to change the relative importance of the other groups.

Table 6-22. Orientation of TSw34 Fracture Sets (3187 fractures) - ESF - IFZ

Set Orientation	# of Entries	Percentage	Proportion	ESF Geologic Set
Vertical "EW"	2951	93%	13	Set 1
Vertical "NS"	215	7%	1	Set 2
Horizontal	21	0%	0	Sets 3&4

NOTE: Values from domain 3 from Table 1, Albin et al. (1997) (Total drift length of 950 m). The random orientation group (20% of total) is not included and is assumed not to change the relative importance of the other groups.

The relative orientation of sets 1 and 2 is slightly more open in the ESF than in the ECRB. The two sets are 90° apart outside the IFZ and 82 ° within the IFZ.

- Unit TSw35 (Fig. 10 of Mongano et al. 1999): fracture directions are more spread out but with a clear dominant fracture direction around N115E. The 3 remaining sets can be approximated by an average set whose deviation from the main set is the average deviation of each individual set weighted by the number of fractures in that set: [(157-032)*8+(157-070)*14+(157-097)*40]/62=74. CRWMS M&O 2000b, Table 5, presents an analysis with 2 sets 35° apart.

Table 6-23. Orientation of TSw35 Fracture Sets (300 fractures) - ECRB

Set Orientation	# of Entries	Percentage	Proportion	ESF Geologic Set
032/84 (Vertical "NE-SW")	8	2.7%	2	Set 2
070/85 (Vertical "NE-SW")	14	4.7%		
097/84 (Vertical "EW")	40	13.3%		
157/80 (Vertical "NW-SE")	218	72.6%	7	Set 1
340/06 (Horizontal)	20	6.7%	1	Sets 3&4

Sources: DTN: GS991108314224.015; Table S99470_003 for "Set Orientation" column
Table 7 of Mongano et al. 1999 for # of entries

- Unit TSw36 (Fig. 10 of Mongano et al. 1999):

Table 6-24. Orientation of TSw36 Fracture Sets (199 fractures) - ECRB

Set Orientation	# of Entries	Percentage	Proportion	ESF Geologic Set
027/77 (Vertical NE-SW")	7	3.5%		Set 2
198/82 (Vertical "NS")	76	38%	4	Set 2
134/80 (Vertical "NW-SE")	99	50%	5	Set 1
336/17 (Horizontal)	17	8.5%	1	Sets 3 & 4

Sources: DTN: GS991108314224.015; Table S99470_003 for "Set Orientation" column
Mongano et al. (1999, Table 7) for # of entries

The results are summarized in Table 6-25. The low or high dip value justifies the assumption of a fracture being either horizontal or vertical respectively (Assumption 5.2). In Table 6-25, the main set has a hypothetical orientation of 0°, and the other sets make the given angle with the main set:

Table 6-25. Summary of Fracture Orientation Starting from an Arbitrary Orientation of 0 (NOT for the same hypothetical volume of rock)

Unit	TSw33 ECRB	TSw34 ECRB and outside IFZ	TSw34 ESF-IFZ	TSw35 ECRB	TSw36 ECRB
Main set	5 fractures at 0°	10 fractures at 0°	13 fractures at 0°	7 fractures at 0°	5 fractures at 0°
Secondary sets	4 fractures at 80°	5 fractures at 70°	1 fracture at 80°	2 fractures at 74°	4 fractures at 64°
	4 horizontal fractures	1 horizontal fracture		1 horizontal fracture	1 horizontal fracture

DEVELOPED DTN: MO0109SPAFIE10.006

Those results are assumed applicable to all fractures including fractures < 1m (Assumption 5.4).

6.5.2 Orientation Variations

The analysis of TSw34 unit fracture system leaves no choice but to break up all data into 2 fracture sets. On the other hand, TSw35 and TSw36 units have a more diffuse range of fracture orientations that renders not unlikely the possibility of having 3 fractures of different orientations intersecting at the same location. This is true for fracture set 1 of the TSw35 unit (Fig. 10 of Mongano et al. 1999) where the case of 3 fractures 30° apart should be considered in sensitivity analysis. This is also the case for fracture set 2 of unit TSw36 (Fig. 11 of Mongano et al. 1999).

6.6 FRACTURE ROUGHNESS

Fracture roughness gives an indication of the contact area between the fracture water and the fracture walls. Fracture roughness is estimated on a scale from 1 to 6. Roughness characterizes the small-scale asperities of a fracture surface on a scale from 1 to 6. R1 designates a stepped surface with near-normal steps and ridges. R6 designates a very smooth, shiny, and polished surface. The other states are detailed below (introduction text of DTNs: GS990408314224.001 and GS990408314224.002):

R1: Stepped, near-normal steps and ridges occur on the fracture surface
R2: Rough, large, angular asperities can be seen
R3: Moderately rough asperities are clearly visible, and fracture surface feels abrasive
R4: Slightly rough, small asperities on the fracture surface are visible and can be felt
R5: Smooth, no asperities, smooth to the touch
R6: Polished, extremely smooth and shiny

A bar chart of cross drift fracture roughness (Fig. 22, Mongano et al. 1999) illustrates that the most common roughness recorded was R3 (just over 750 occurrences), followed by R4 (just under 700 occurrences).

6.7 FRACTURE FILLINGS

Most fractures have some vapor-phase minerals deposited while the ash pile was still warm, but only a few have low-temperature minerals such as calcite suggesting that only part of the fracture network has been active in the groundwater flow. Carlos et al. (1995) give an overview of the fracture-lining minerals in the Yucca Mountain area. Figures 23

and 24 of Mongano et al. (1999) give spatial distribution and thickness of fracture infillings in the cross drift. It should be noted that the fracture aperture computed in Section 6.3 represents the void space aperture and does not include the infillings. Table 6-26 and Table 6-28 give results for fractures > 1m and fracture < 1m respectively. Table 6-27 is equivalent to Table 6-26, and results are the same except for manganese oxide that is present as a minor mineral in many fractures. Table 6-26 was provided for comparison purposes with Table 6-28.

Table 6-26. Major Infillings for Fractures > 1m (ECRB)

Unit	TSw34 - ECRB		TSw35 - ECRB		TSw36 - ECRB	
	A	B	A	B	A	B
Total	931	100%	301	100%	198	100%
No minerals	70	7.5%	92	30.6%	40	20.2%
Crushed Rock / Fault Material	13	1.4%	41	13.6%	28	14.1%
Calcite	**110**	**11.8%**	**5**	**1.7%**	**2**	**1.0%**
Manganese Oxides	47	5.1%	10	3.3%	20	10.1%
Vapor-Phase Minerals	691	74.2%	152	50.5%	108	54.5%
Quartz	0	0%	1	0.3%	0	0%

Sources: DTNs: GS990408314224.001 and GS990408314224.002
FILES (Att. IV CD-ROM): **ECRB_study_TSw34.xls, ECRB_study_TSw35.xls,** and **ECRB_study_TSw36.xls** (by using the "filter option" on column " Infill (mm)" of "all fractures" worksheet)
NOTES: The table is only qualitative and values have to be taken as order of magnitude.
A: Number of fractures
B: Fraction of fractures with that particular mineral

Table 5 of Mongano et al. (1999) is reproduced below (Table 6-27). It includes all minerals present in a fracture; consequently, the percentages add up to more than 100%.

There is no significant difference between large and small fractures (Table 6-26 and Table 6-28) suggesting that they are both part of the same fracture network (see Section 6.10 on connectivity). Mongano et al. 1999 (p. 79) state that vapor-phase minerals are about 1-3 mm thick followed in abundance by manganese oxides which tend to be less than 1 mm thick.

Table 6-27. Infillings for Fractures > 1m (ECRB)

Unit	TSw34 - ECRB	TSw35 - ECRB	TSw36 - ECRB
No minerals	8.0%	37.8%	25.2%
Opal	**0.2%**	**0.6%**	**0.0%**
Calcite	**11.5%**	**1.6%**	**1.0%**
Manganese Oxide	24.4%	14.3%	41.4%
Vapor-Phase Minerals	84.0%	46.7%	49.5%

Sources: DTN: GS991108314224.015
Mongano et al. (1999, Table S99470_002 and Table 5)

Using other arguments, it has been suggested that 18% to 27% of the fracture network is currently active (Liu et al. 1998) leading to the conclusion that not all active fractures have calcite deposits.

Table 6-28. Major Infillings for Fractures < 1m (ECRB)

Unit	TSw34 - ECRB		TSw35 - ECRB		TSw36 - ECRB	
	A	B	A	B	A	B
Total	192	100%	374	100%	120	100%
No minerals	36	18.8%	164	43.9%	63	52.5%
Crushed Rock / Fault Material	17	8.9%	40	10.7%	9	7.5%
Calcite	**6**	**3.1%**	**2**	**0.5%**	**7**	**5.8%**
Manganese Oxide	7	3.6%	2	0.5%	5	4.2%
Vapor-Phase Minerals	114	58.9%	158	42.2%	34	28.3%
Quartz	0	0.0%	4	1.1%	2	1.7%

Source: DTN: GS990908314224.009
NOTES: The table is only qualitative, and values have to be taken as order of magnitude.
A: Number of fractures
B: Fraction of fractures with that particular mineral

6.8 FRACTURE LENGTH

Fractures are three-dimensional objects, but they are typically modeled as two-dimensional disks (Bear et al. 1993; pp. 250 to 264). Outcrop and drift studies yield the intersection of the "fracture disk" with the observation plane. If the measurements are abundant enough, a study of the "observation plane" yields an accurate representation of the overall fracture size distribution. The latter is typically strongly skewed towards small lengths, and a cutoff on the fracture length is generally imposed. The different studies related to the Yucca Mountain project are not consistent in that sense. Cutoff values vary from 0.3 m to 1.5 m and also include 0.5 and 1 m (most common value). A limited data set, used in this work, includes all the fractures independently of their size (ECRB SSS; DTN: GS990908314224.009).

Between Station 28+00 and 37+80 of the ESF, all fractures with trace lengths longer than 30 cm were reported in the survey. Beginning at 37+80, the minimum trace length for the DLS was raised to 1m. Data on shorter fractures, 30 cm to 1 m, were collected in 50-m intervals every 500 m, between 45+00 and 45+50, and between 50+00 and 50+50. A comparison of data 30-cm cutoff versus 1-m cutoff (Albin et al. 1997, p. 40) suggests that about 50% of fractures >0.3m are in the 0.3 - 1 m range for the TSw34 unit (result corroborated by this work's results in Table 6-30). Their distribution in orientation and location is similar for both groups, but smaller fractures show a tendency to be more evenly distributed (that is more frequent between predefined sets). Similarly, the ECRB DLS used a fracture length cutoff of 1.0 m, but "small-scale" surveys recording ALL fractures were performed locally on 6-meter intervals: stations 11+15 to 11+21 and 13+00 to 13+06 for TSw34, 15+25 to 15+31, 17+35 to 17+41, and 22+15 to 22+21 for TSw35 and 24+25 to 24+31 for TSw36. Table 6-29 displays a summary of the results. Both arithmetic and geometric means are displayed to show the sensitivity of the results to the assumed distribution law. This work assumes a lognormal distribution of the fracture length (Assumption 5.8).

Table 4 of Albin et al. 1997 (p. 83) reports that in the TSw34-ESF, the mean fracture length is 2.098 m and follows a lognormal distribution with a standard deviation of 4.292 (for fractures > 1 m). Table 6-30 to Table 6-32 provide the distribution of the fracture length, counting all fractures along the SSS, for the three units hosting the repository (source DTN: GS990908314224.009).

Table 6-29. Distribution Parameters of Fracture Length (cut-off = 1m)

Unit	Arithmetic		Geometric		Mean Length[b]
	Mean μ_L	St. Dev. σ_L	Mean $\mu_{ln(L)}$	St. Dev. $\sigma_{ln(L)}$	$\exp[\mu_{ln(L)}]$
TSw33 - ECRB	3.25	3.39	0.88	0.69	2.40
TSw34 - ECRB	2.61	2.14	0.77	0.56	2.15
TSw34 - ESF North of IFZ	2.56	3.06	0.71	0.58	2.03
TSw34 - ESF IFZ	2.37	1.59	0.73	0.49	2.07
TSw34 - ESF South of IFZ	2.86	2.29	0.86	0.58	2.37
TSw35 - ECRB	3.52	3.84	0.86	0.81	2.36
TSw35 - ESF[a]	5.26	6.20	1.19	0.92	3.28
TSw36 - ECRB	4.32	4.59	1.03	0.87	2.81

Source: FILES (Att. IV CD-ROM): Organized by following the row order of the table:
ECRB_study_TSw33.xls; worksheet ul all fractures >65 DIST,
ECRB_study_TSw34.xls; worksheet mn all fractures >65 DIST, **ESF27.20-42.00.xls**, **ESF42.00-51.50.xls**, **ESF51.50-57.29.xls**
ECRB_study_TSw35.xls; worksheet ll all fractures >65 DIST, **ESF_study_TSw35.xls**; worksheet ll all fractures >65 DIST,
ECRB_study_TSw36.xls; worksheet ln all fractures >65 DIST.

NOTES: [a] This represents the minimum mean length because some terminations are not exposed in the drift or are hidden by engineering structures.
[b] An outlier (length = 43 m) was removed

Table 6-30. Distribution by Length Intervals for the TSw34 Unit (for a total of two SSS intervals)

Length Interval (m)	Number of Discontinuities	Average Length (arithmetic) (m)
0.0 - 0.1	48	0.074
0.1 - 0.2	54	0.15
0.2 - 0.3	24	0.24
0.3 - 0.4	15	0.35
0.4 - 0.5[d]	5	0.45
0.5 - 1.0[d]	12	0.72
> 1 m[a]	34	
> 1 m[b]	28.6	2.16 (geometric)
> 1 m[c]	31.3	2.23 (geometric)

Sources: DTN: GS990908314224.009
FILE (Att. IV CD-ROM): **Percentage_SSS.xls**; worksheet : all units

NOTES: [a] Over the same interval stationing.
[b] Averaged over the whole TSw34 exposure and scaled to 10 m (848 fractures > 1 m over 427.24 m). TSw34 is visible for 4 meters and 6 meters in the SSS (Only for fractures >1m & dip>65).
[c] Averaged over the whole TSw34 exposure and scaled to 10 m (931 fractures >1m over 427.24 m). TSw34 is visible for 4 meters and 6 meters in the SSS (for all discontinuities > 1m)
[d] Results subject to caution because of the limited number of fractures in this range

Table 6-31. Distribution by Length Intervals for the TSw35 Unit (for a total of three 6-meter intervals)

Length Interval (m)	Number of Discontinuities	Average Length (arithmetic) (m)
0.0 - 0.1	92	0.073
0.1 - 0.2	127	0.15
0.2 - 0.3	73	0.25
0.3 - 0.4	44	0.36
0.4 - 0.5	19	0.44
0.5 - 1.0[c]	9	0.60
> 1 m	5	
> 1 m[a]	5.5	2.35 (geometric)
> 1 m[b]	6.2	2.51 (geometric)

Sources: DTN: GS990908314224.009
FILE (Att. IV CD-ROM): **Percentage_SSS.xls**; worksheet : all units

NOTES: [a] Averaged over the whole TSw35 exposure and scaled to 18 m (267 fractures > 1 m over 879.29 m) (only for fractures > 1m & dip>65)
[b] Averaged over the whole TSw35 exposure and scaled to 18 m (301 fractures >1m over 879.29 m) (for all discontinuities > 1m)
[c] Results subject to caution because of the limited number of fractures in this range

Table 6-32. Distribution by Length Intervals for the TSw36 Unit (for a total of one 6-meter interval)

Length Interval (m)	Number of Discontinuities	Average Length (arithmetic) (m)
0.0 - 0.1	17	0.075
0.1 - 0.2	33	0.15
0.2 - 0.3	30	0.25
0.3 - 0.4	12	0.35
0.4 - 0.5[c]	4	0.47
0.5 - 1.0	17	0.60
> 1 m	7	
> 1 m[a]	5.1	2.81 (geometric)
> 1 m[b]	5.6	2.63 (geometric)

Sources: DTN: GS990908314224.009
FILE (Att. IV CD-ROM): **Percentage_SSS.xls**; worksheet : all units

NOTES: [a] Averaged over the whole TSw36 exposure and scaled to 6 m (178 fractures > 1 m over 210.75 m) (only for fractures > 1m & dip>65)
[b] Averaged over the whole TSw36 exposure and scaled to 6 m (198 fractures > 1m over 210.75 m) (for all discontinuities > 1m)
[c] Results subject to caution because of the limited number of fractures in this range

It should be noted that the length given for long fractures is a minimum length because of the bias introduced by the inability to follow all fractures to their two terminations. Table 6-33 displays the breakup of the fractures both in terms of number and total cumulative length. It is apparent that fractures < 0.3 m do make an important percentage of the total fracture length and cannot be neglected (see also Section 6.10 about connectivity).

Table 6-33. Distribution of Fractures by Frequency and Length

	TSw34		TSw35		TSw36	
Fracture Size	% (Length)	% (Number)	% (Length)	% (Number)	% (Length)	% (Number)
< 0.3 m	33.1	65.6	57.4	79.1	39.8	66.7
>0.3 & < 1.0 m	28.0	16.7	38.7	19.5	47.8	27.5
> 1m	38.9	17.7	3.9	1.4	12.4	5.8

Sources: DTN: GS990908314224.009
FILE (Att. IV CD-ROM): **Percentage_SSS.xls**; worksheet : all units

NOTE: All fractures longer than 0.6 meters have been set to 0.6 m because the remainder of the fracture is most likely outside of the band of interest. Corrections for no verticality were not done to compute the total length; therefore the numbers are only qualitative.

6.9 FRACTURE FREQUENCY AND INTENSITY

Single fracture spacing and fracture frequency are inverse of each other. They are typically obtained through a detailed line survey. A physical line is drawn on the drift wall in the vicinity of the springline or on the outcrop, and every fracture (depending on the cutoff) present within a 60 cm-wide band centered on the line is recorded (Mongano et al. 1999, p. 9). It is obvious that fractures more or less parallel to the DLS will be underestimated. Adjustments are done to correct this problem (the so-called "Terzaghi" correction - Albin et al. (1997, p. 29 similar to Eq. 9).

Fracture frequency and spacing are typically modeled with lognormal distribution laws (Assumption 5.8). Note that the inverse of a lognormal distribution is also lognormal and that

$$\mu_{\ln X^{-1}} = -\mu_{\ln X} \quad and \quad \sigma_{\ln X^{-1}} = \sigma_{\ln X} \qquad \text{(Eq. 8)}$$

That is, fracture frequency and fracture spacing are both lognormal, and both distributions are very simply related. It should be also noted that if single fracture spacing and frequency are inverse of each other, this is only true of their geometric average but not their arithmetic average.

Fracture frequency and fracture intensity are related but not interchangeable words. Typically fracture frequency represents the number of fractures intersecting a line along a given distance. Fracture intensity on the other hand typically represents the total length or surface of fracture found in 1 m^2 cross-section of the rock or in 1 m^3 volume of the rock respectively. The fracture intensity I can strictly be expressed in several ways: in number of fracture/m ($=I_1$ or fracture frequency), in m/m^2 ($=I_2$), or in m^2/m^3 ($=I_3$). Because most of the fractures in this study are vertical (Sweetkind et al. 1997, Appendix 2 and 3 Tables), I_2 and I_3 are numerically equivalent. Fracture frequency is a particular expression of the fracture intensity. The distinction is important because most studies report their measurements in terms of fracture frequency, but only fracture intensity I_2 or I_3 matter for accumulation. We restrict the definition of fracture intensity to the fracture intensity I_2 while the fracture intensity I_1 will be called fracture frequency.

There is no general analytical relationship between fracture frequency and intensity. In some particular cases such as infinite fracture length, an expression can be derived (Bear et al. 1993, p. 174).

$$I_3 = I_2 = \frac{I_1}{\sin\theta} \qquad \text{(Eq. 9)}$$

where θ is the angle in the horizontal plane between the vertical fracture and the horizontal DLS (or equivalently the fracture strike and the drift orientation). Equation 9 can be extended to several fracture sets by computing I_2 for each set and by doing the weighed sum.

Fracture intensity will be conservatively estimated from the following formula:

$$I_2 = \frac{1}{0.6}\sum_{i=1}^{N}\frac{n_i \bar{l}_i}{L_i} \qquad \text{(Eq. 10)}$$

where i=1,2...N represents the number of length bins, n_i is the number of fractures in bin i, $\bar{l}_i$ is the average fracture length in bin i, and L_i is the drift interval length over which bin i is measured. The value of 0.6 represents the drift band width in meters on which the measurements are done.

6.9.1 Results of Previous Collection of Information

As a general rule, the non-lithophysal units (TSw34 and TSw36) are recognized as more densely fractured because lithophysae inhibit fracture growth (Fig. 13 of Mongano et al. 1999, p. 77). Stresses are accommodated by deformation of the lithophysae rather than by growing long fractures. Figure 6-5 to Figure 6-9 (see file **ECRB_spacing.xls** in Att. IV CD-ROM for data) illustrate that TSw34 has the highest fracturation for fractures > 1m. The locations of the small scale surveys are also indicated on the figures. Table 6-34 and Table 6-35 summarize the different data collected from earlier reports in addition to new results from this work.

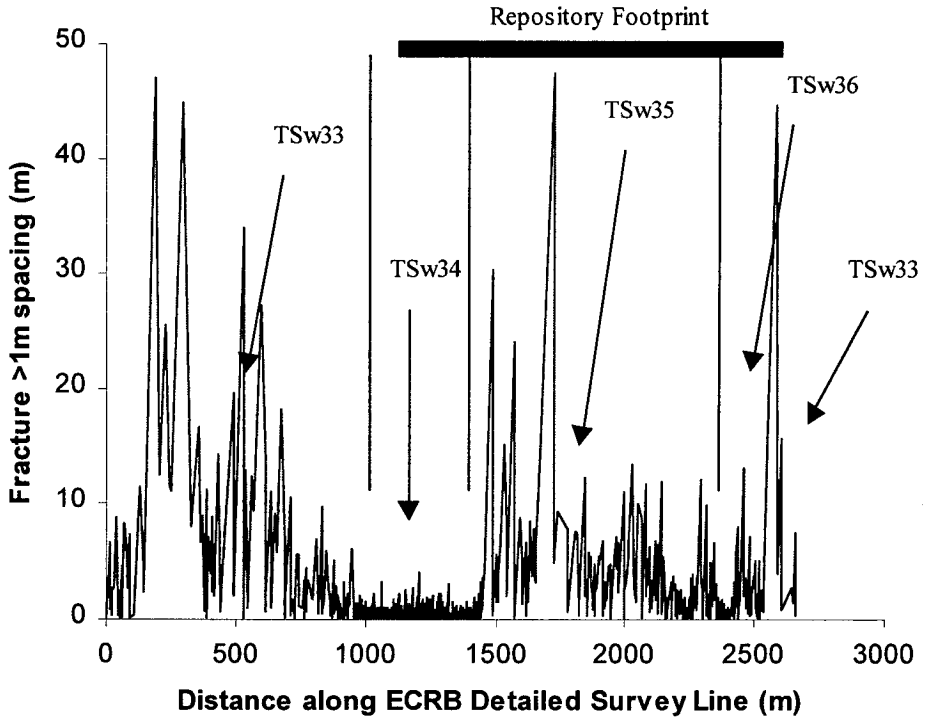

Sources: DTN: GS990408314224.001 and GS990408314224.002
FILE (Att. IV CD-ROM): **ECRB_spacing.xls**; worksheet: all points

Figure 6-5. Fracture Spacing for Fracture > 1m along ECRB

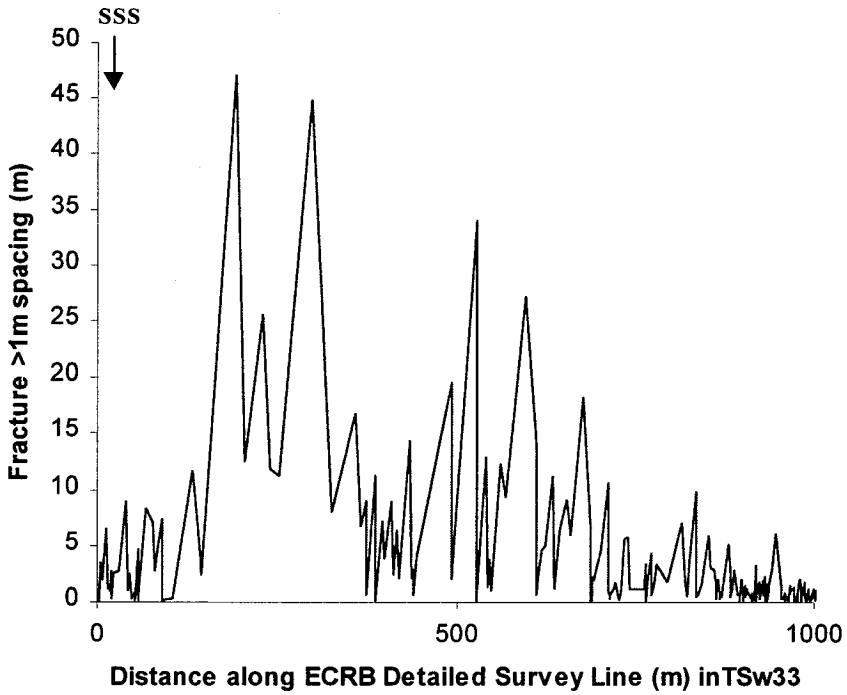

Sources: DTN: GS990408314224.001 and GS990408314224.002
FILE (Att. IV CD-ROM): **ECRB_spacing.xls**; worksheet: all points

Figure 6-6. Fracture Spacing for Fracture > 1m along TSw33 - ECRB

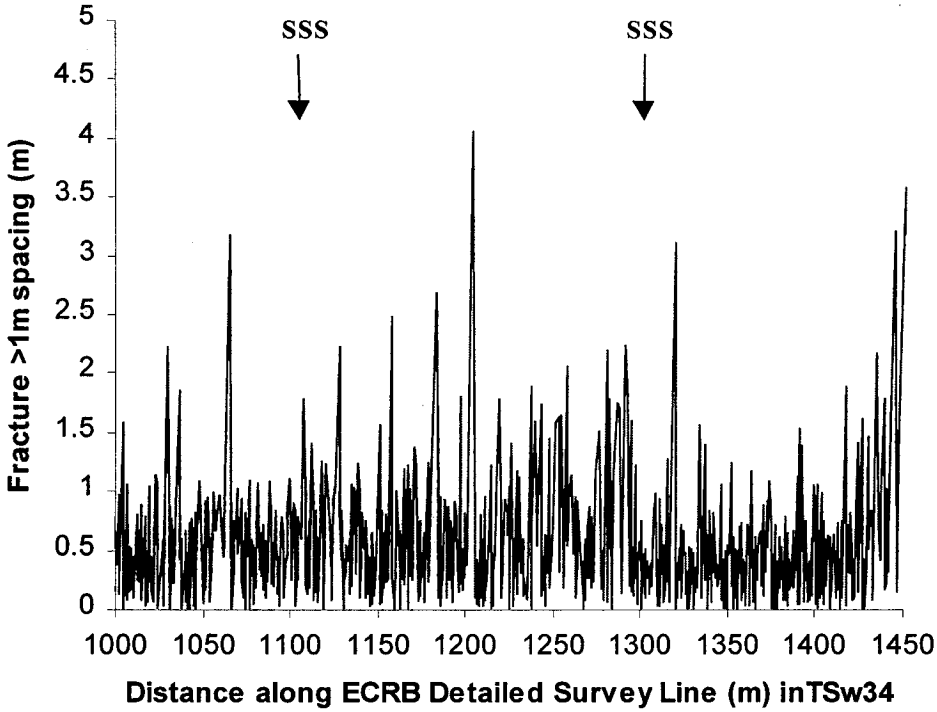

Sources: DTN: GS990408314224.001 and GS990408314224.002
FILE (Att. IV CD-ROM): **ECRB_spacing.xls**; worksheet: all points

Figure 6-7. Fracture Spacing for Fracture > 1m along TSw34 - ECRB

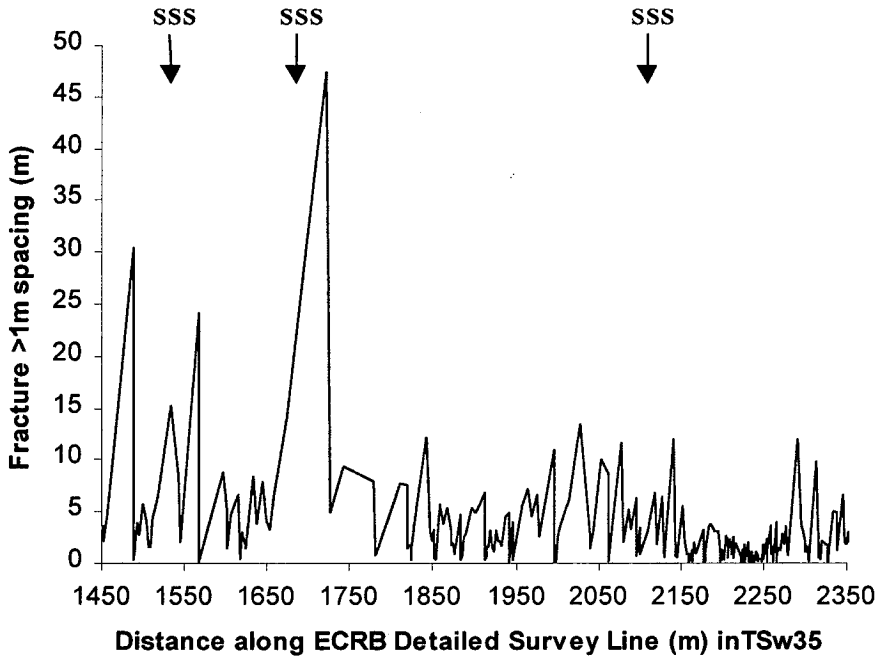

Sources: DTN: GS990408314224.001 and GS990408314224.002
FILE (Att. IV CD-ROM): **ECRB_spacing.xls**; worksheet: all points

Figure 6-8. Fracture Spacing for Fracture > 1m along TSw35 - ECRB

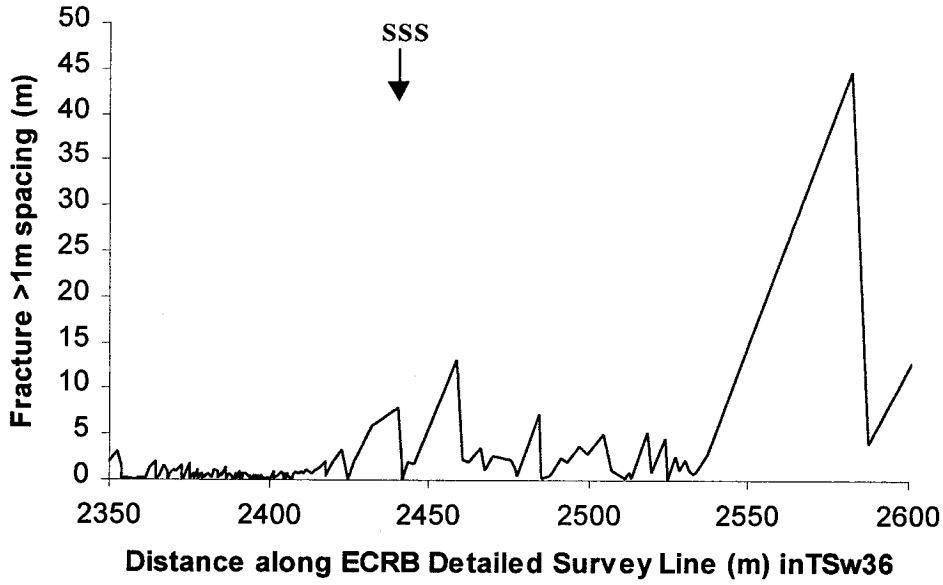

Sources: DTN: GS990408314224.001 and GS990408314224.002
FILE (Att. IV CD-ROM): **ECRB_spacing.xls**; worksheet: all points

Figure 6-9. Fracture Spacing for Fracture > 1m along TSw36 - ECRB

The fracture frequency is reported from earlier studies as 1.880, 1.810, and 2.10 fracture/meter in TSw34, TSw35, and TSw36, respectively, for fractures having a trace length larger than 1m (Bodvarsson et al. 1997, Tables 7.7 and 7.10). TSw34 data were provided by ESF data, while borehole results were used for underlying units. The fracture frequency for unit TSw34 is corroborated by Fig. 7.5 p. 7-24 of Bodvarsson et al. (1997), which shows 4 fracture/meter along the survey line, and by more recent studies (Mongano et al. 1999). It is apparent, however, from more recent studies (South Ramp, Eatman et al. 1997; ECRB, Mongano et al. 1999) that fracture frequency for fracture > 1m in the TSw35 and TSw36 units had been overestimated (Table 6-35).

6.9.1.1 Unit TSw34

Results are presented in Table 6-34. The value of 4 for fractures > 0.3 m (Fig. 7.5 p. 7-24 of Bodvarsson et al. 1997) is consistent with the previous value of 1.88 for fractures > 1 m because the number of fractures increases twofold from fracture > 1 m to fractures > 0.3 m. Some areas of the ESF are more densely fractured because fracture frequency as high as 1/0.23=4.35 fracture/meter for fracture > 1 m are sustained for several meters of the main drift in TSw34 (Sweetkind et al. 1997, Table 13). They can even reach 8 fracture/m (Sweetkind et al. 1997, Fig.4b) in the IFZ along at least 10 meters of drift and a maximum of 19 fractures > 1m per meter (Albin et al. 1997, p. 58).

As mentioned earlier, fracture frequency is only part of the picture as the average trace length needs to be incorporated into the characterization process. Both fracture frequency and average trace length, and to a lesser degree fracture orientations, come together to compose fracture intensity (or I_2). Although fracture intensity can be derived

from the parameters mentioned above either analytically or through numerical simulation, direct outcrop or ESF measurements are more accurate. Outcrop measurements may not be representative of the subsurface environment as shown by the fracture intensity measurements in the TSw34 formation (Sweetkind et al. 1997, Appendix 2 Tables) and give a fracture intensity of 1.7 m/m^2 for fractures > 1.5 m (Sweetkind et al. 1997 - p. 102). Anna, 1998, (Table 3 for FSU3 unit equivalent to the TSw34 and TSw35 horizons) mentions I_1=1.82 fracture/meter and I_2=1.22 m/m^2 from ESF studies for fracture greater than 1.5 m in length.

6.9.1.2 Units TSw35 and TSw36

Results are presented in the second half of Table 6-35. Little data existed for these units before the making of the ECRB, and they were provided mainly through borehole studies.

Table 6-34. Compilation of Fracture System Geometry Parameters for Unit TSw34

	Interval –Zone	Fracture Spacing (m)/ Frequency (1/m)	Standard Deviation	Fracture Length (m)	Standard Deviation	Fracture Intensity I2 (m/m^2)	Standard Deviation	Comments - References
1	TSw34 (ESF) 27+20.0 – 34+93.0	NA / 1.88[a] (geom=2.91)	0.62 / N/A	2.82	3.58	0.89[b]	N/A	Fractures > 1 m Table 7.7 Bodvarsson et al. 1997
2	TSw34 (ESF) 27+20.0 – 34+93.0	NA./ ~4	N/A	N/A	N/A	N/A	N/A	Fractures > 0.3 m Fig. 7.5a Bodvarsson et al. 1997
3	FSU3[c] 27+00.0 – 40+00.0 (Simulated data & only connected fractures)	N/A / 1.339	NA / 0.105	N/A	N/A	1.293	0.109	Fractures > 1.5 m Table 2 Anna 1998
4	TSw34 (ESF)	NA / 1.82	N/A	N/A	N/A	1.22	N/A	Fracture > 1.5 m Table 3 Anna 1998
5	TSw34 (ESF)	NA / 3.73	N/A	N/A	N/A	N/A	N/A	Fractures > 0.3 m Table 8 Sweetkind and Williams-Stroud 1996, p. 55
6	TSw34 (P2001)	N/A	N/A	N/A	N/A	1.70	N/A	Fracture > 1.5 m Table 8 and Fig. 25C Sweetkind and Williams-Stroud 1996
7	TSw34 (P2001)	N/A	N/A	N/A	N/A	1.01	N/A	Fracture > 1.5 m Table 9 and Fig. 25B Sweetkind and Williams-Stroud 1996
8	TSw34 (P2001)	N/A	N/A	N/A	N/A	0.96	N/A	Fracture > 1.8 m Table 9 and Fig. 25C Sweetkind and Williams-Stroud 1996
9	TSw34 (ESF) North of IFZ <42+00 Within IFZ (42+00 to 51+50) South of IFZ >51+50	 0.52 / NA 0.23 / NA 0.40 / NA	 N/A N/A N/A	 2.5 – 4 N/A 2.5-4	 N/A N/A N/A	 N/A N/A N/A	 N/A N/A N/A	Fracture > 1 m Table 13 Sweetkind et al. 1997
10	TSw34 (ESF) 28+00 - 55+00			2.098	4.292			Fractures > 1 m Albin et al. 1997, p. 83
11	TSw34 (ESF) (up to 37+00)	0.231 / 4.32	NA / 3.4	NA	NA	NA	NA	Fracture > 0.3 m DTN: LB990501233129.001
12	TSw34 (ECRB) (10+15 to 14+40)	NA / 2.2[a]	NA / NA	NA	NA	NA	NA	Fracture > 1 m Mongano et al. 1999, p. 44

NOTES: All distributions are lognormal unless noted.
[a] This is the arithmetic average.
[b] For a 3-m-high band above and below centerline (Bodvarsson et al. 1997, p. 7.10).
[c] FSU= Fracture SubUnit. FSU3 corresponds approximately to units TSw33 to TSw35.

Table 6-35. Compilation of Fracture System Geometry Parameters for Units TSw33, TSw35, and TSw36

	Interval –Zone	Fracture Spacing (m)/ Frequency (1/m)	Standard Deviation	Fracture Length (m)	Standard Deviation	Fracture Intensity I2 (m/m^2)	Standard Deviation	Comments - References
1	TSw33 (ESF) 17+17 - 27+20	1.46 / 0.69[a]	1.90 / N/A	3.7	4.40	0.42	N/A	Fractures > 1 m Table 7.7 Bodvarsson et al. 1997
2	TSw33 (ESF) 17+17 - 27+20	NA / ~1.3	N/A	N/A	N/A	N/A	N/A	Fractures > 0.3 m Fig. 7.5a Bodvarsson et al. 1997
3	TSw33 (ESF) 17+17 - 18+00	N/A / 1.23	N/A	N/A	N/A	N/A	N/A	Fractures > 0.3 m Table 8 Sweetkind and Williams-Stroud 1996, P. 55
4	TSw33 (P2001)	N/A / N/A	N/A	N/A	N/A	0.64 or 0.54 (typo)	N/A	Fracture > 1.5 m Table 8 and Fig. 25C Sweetkind and Williams-Stroud 1996
5	TSw33 (ESF) 17+17 - 27+20 63+08 - 65+00	1.45 / N/A	N/A	3.0 - 3.5	N/A	N/A	N/A	Fracture > 1 m Table 12 Sweetkind et al. 1997
1	TSw35 (Boreholes)	NA / 1.81						Fractures > 1 m Table 7.10 Bodvarsson et al. 1997
2	TSw35 (ESF) 57+30 - 58+78	NA / 3.34	N/A	2.5 - 5	N/A	N/A	N/A	Table 14 Sweetkind et al. 1997
3	TSw35 (ESF) 57+30 - 58+78	0.316 / 3.16	N/A	N/A	N/A	N/A	N/A	Fracture > 0.3 m DTN: LB990501233129.001
1	TSw36 (Boreholes)	NA / 2.10	N/A	N/A	N/A	N/A	N/A	Fractures > 1 m Table 7.10 Bodvarsson et al. 1997
2	TSw36	0.249 / 4.02	N/A	N/A	N/A	N/A	N/A	Fracture > 0.3 m DTN: LB990501233129.001

NOTES: All distributions are lognormal unless noted.
[a] This is the arithmetic average.

6.9.2 Distribution of Fracture Frequency

DTN LB990501233129.001, used for flow models, assumes that the fracture frequency distribution is lognormal (Assumption 5.8) with the parameters presented in Table 6-36. Note that this DTN does not use information from the ECRB and uses information from only part of the ESF. In addition some information is inferred from borehole studies. Table 6-37 presents results from this work mainly for fractures > 1 m (a few fractures > 0.3m and < 1m were also considered). When actual tunnel data were used in Table 6-36 (layer TSw33 and TSw34), results are in good agreement. There are deviations for the other formations.

Table 6-36. Distribution Parameters of Fracture Frequency for Fracture >0.3 m

Layer	Geometric Mean Fracture Spacing /Frequency (m / 1/m)	(Arithmetic) SD of Fracture Frequency
TSw33	1.23 / 0.81	1.03
TSw34	0.231 / 4.32	3.42
TSw35	0.316 / 3.16	NC
TSw36	0.249 / 4.02	NC
TSw37	0.249 / 4.02	NC

Source: DTN: LB990501233129.001
NOTE: NC=Not Calculated

Table 6-37. Distribution Parameters of Fracture Spacing/Frequency for Fractures > 1m (This work) (no correction for sampling bias - see Section 6.9.5)

Unit	Arithmetic		Geometric		Mean spacing $\exp[\mu_{ln(sp)}]$	Mean frequency $1/\exp[\mu_{ln(sp)}]$
	Mean μ_{sp}	St. Dev. σ_{sp}	Mean $\mu_{ln(sp)}$	St. Dev. $\sigma_{ln(sp)}$		
TSw33 - ECRB	4.04	7.24	0.26	1.65	1.30	0.77
TSw34 - ECRB	**0.51**	**0.52**	**-1.20**	**1.16**	**0.30**	**3.31**
TSw34 - ESF North of IFZ	0.62	0.72	-1.11	1.28	0.33	3.0
TSw34 - ESF IFZ	0.24	0.28	-1.99	1.14	0.14	7.14
TSw34 - ESF South of IFZ	0.46	0.49	-1.37	1.26	0.25	4.0
TSw34 - ESF Outside of IFZ[a]	0.57	0.64	-1.20	1.27	0.30	3.31
TSw34 -ESF[b]	**0.46**	**0.52**	**-1.46**	**1.23**	**0.23**	**4.31**
TSw35 - ECRB	**3.33**	**5.55**	**0.31**	**1.45**	**1.36**	**0.74**
TSw35 - ESF	**3.90**	**5.97**	**0.55**	**1.39**	**1.73**	**0.58**
TSw36 - ECRB	**1.19**	**1.72**	**-0.68**	**1.44**	**0.51**	**1.97**

Sources: DTNs: GS971108314224.024, GS971108314224.025, GS960708314224.008, GS960808314224.011, GS960708314224.010, GS971108314224.026, GS960908314224.014, GS971108314224.028, GS990408314224.001, and GS990408314224.002.
FILES (Att. IV CD-ROM): **ESF27.20-42.00.xls; ESF42.00-51.50.xls, ESF51.50-57.29.xls, ESF_study_TSw35.xls, ECRB_study_TSw33.xls, ECRB_study_TSw34.xls, ECRB_study_TSw35.xls, ECRB_study_TSw36.xls**

NOTES: [a] Weighted average of North of IFZ (2/3) and South of IFZ (1/3) corresponding to the number of fractures in each zone (2384 and 1258 respectively)
[b] Weighted (by drift length) average of all ESF data (1/3 IFZ - 2/3 remaining)

A lognormal distribution may not be conservative for criticality studies as demonstrated by the following normal probability plots (Figure 6-10 to Figure 6-13). Deviation from linearity at the lower left hand-side of the plot means that smaller spacings are underestimated while the deviation at the upper right side suggests that large spacings are overestimated. It is thus more conservative for the criticality Monte-Carlo simulations to directly use the raw data rather than to go through the extra-step of fitting a distribution law through the data (Section 6.9.7).

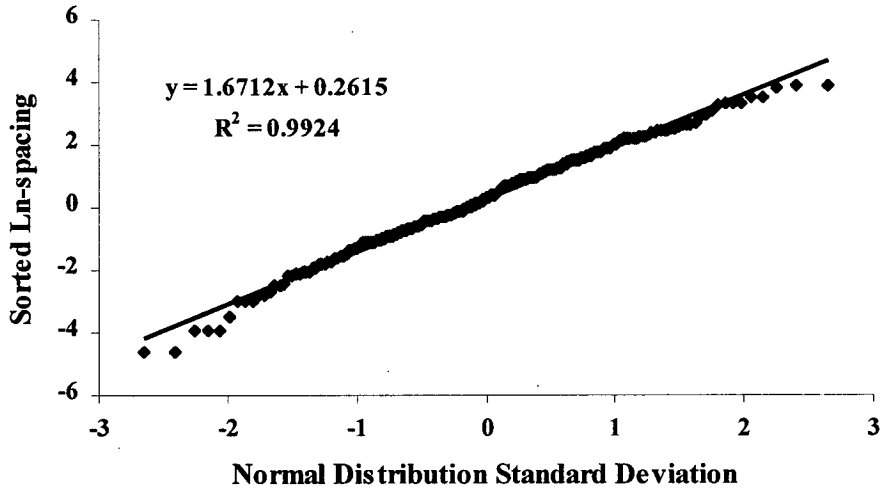

Sources: DTN: GS990408314224.001
FILE (Att. IV CD-ROM): **ECRB_study_TSw33.xls**; worksheet: ul all fractures >65 DIST

Figure 6-10. Probability Plot of the Fracture Spacing Distribution (all ECRB fracture sets - TSw33 - fractures > 1 m)

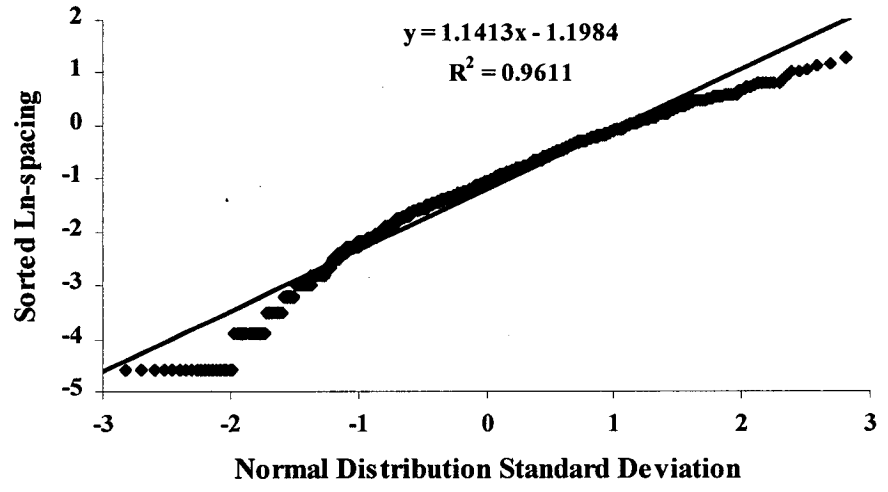

Sources: DTN: GS990408314224.001
FILE (Att. IV CD-ROM): **ECRB_study_TSw34.xls**; worksheet: mn all fractures >65 DIST

Figure 6-11. Probability Plot of the Fracture Spacing Distribution (all ECRB fracture sets - TSw34 - fractures > 1 m)

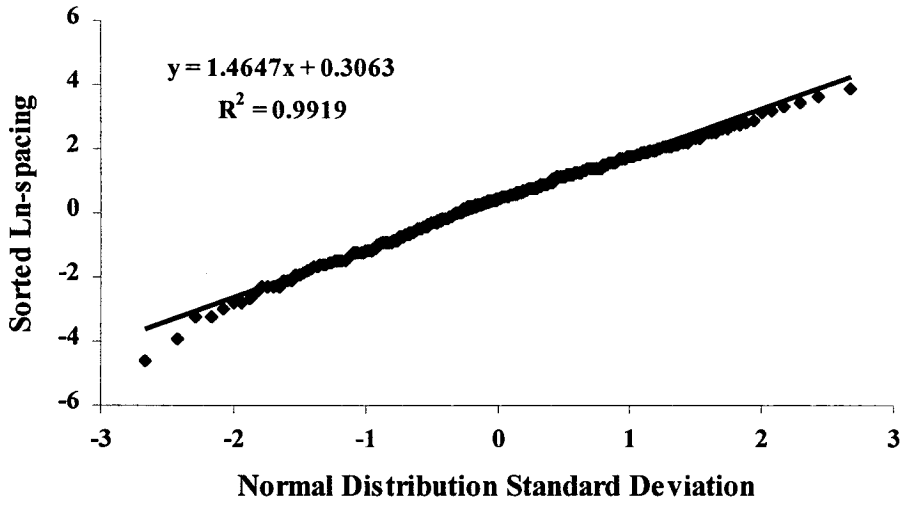

Sources: DTN: GS990408314224.001 and GS990408314224.002
FILE (Att. IV CD-ROM): **ECRB_study_TSw35.xls**; worksheet: ll all fractures >65 DIST

Figure 6-12. Probability Plot of the Fracture Spacing Distribution (all ECRB fracture sets - TSw35 - fractures > 1 m)

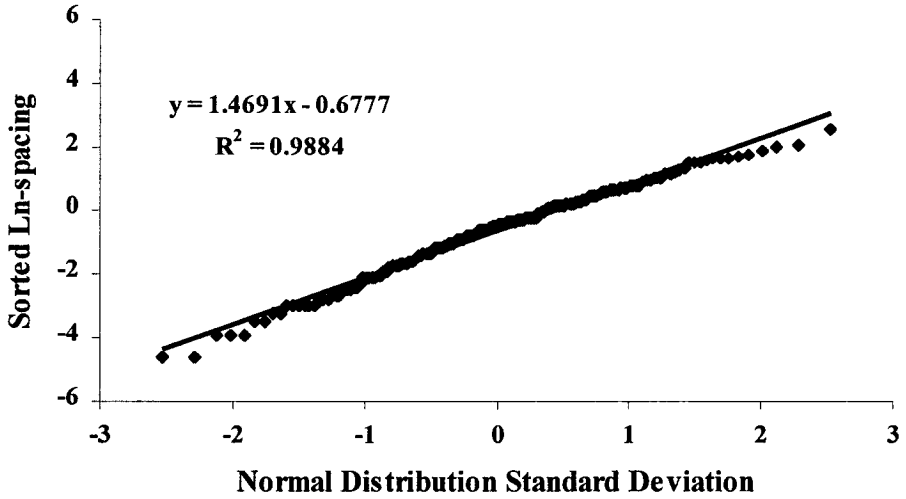

Sources: DTN:GS990408314224.002
FILE (Att. IV CD-ROM): **ECRB_study_TSw36.xls**; worksheet: ln all fractures >65 DIST

Figure 6-13. Probability Plot of the Fracture Spacing Distribution (all ECRB fracture sets - TSw36 - fractures > 1 m)

6.9.3 Geostatistical (Spatial Correlation) Analysis

The assumption of independence of fracture spacing (Assumption 5.12) is potentially not conservative because a high fracture frequency may extend for a few meters. Geostatistical tools can be used to compute the spatial correlation of fracture spacing and justify the assumption of independence. Additional studies of correlation factors confirm that the spacing distances are independent or negatively correlated on a small distance (that is, a short spacing tends to be followed by a larger spacing). A Fourier analysis tried to determine a short range periodic

pattern and failed. Figure 6-14 to Figure 6-22 display semi-variograms for the three repository units. When needed, the fracture data has been analyzed by orientation sets.

6.9.3.1 TSw34 Unit

The assumption of independence of the fracture spacing (Assumption 5.12) is reasonable for the TSw34 unit as suggested by the almost flat semi-variogram of fracture set 1 (Figure 6-14). It is also conservative if the hole effect seen in Figure 6-15 is real. Data from Figure 6-15 are more closely examined in Figure 6-16. The hole effect may be an artifact but in any case the semi-variogram quickly converges to the variance, also suggesting independence of fracture spacing in this unit.

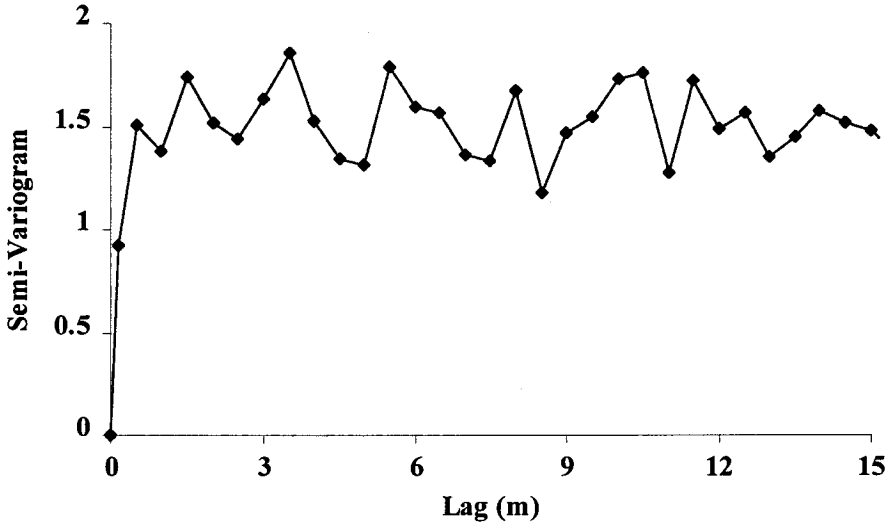

Sources: DTN: GS990408314224.001
FILE (Att. IV CD-ROM): **ewbis_lag=0.5_tol=0.25.xls**
NOTE: The semivariogram quickly converges to the variance (~1.5) (lag=0.5 m - 0.25 m lag tolerance) and has a definite nugget effect.

Figure 6-14. Semivariogram of the TSw34 EW Fracture Set (set 1 - fractures > 1 m)

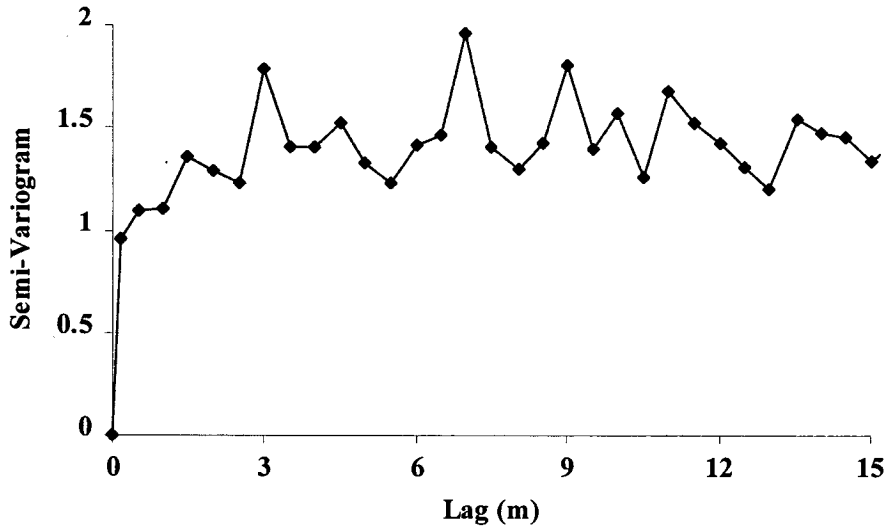

Sources: DTN: GS990408314224.001
FILE (Att. IV CD-ROM): **nsbis_lag=0.5_tol=0.25.xls**
NOTE: The semivariogram converges to the variance (~1.5) with a possible small hole effect (lag=0.5 m - 0.25 m lag tolerance) and has a definite nugget effect at this scale.

Figure 6-15. Semivariogram of the TSw34 NS Fracture Set (set 2 - fractures > 1 m)

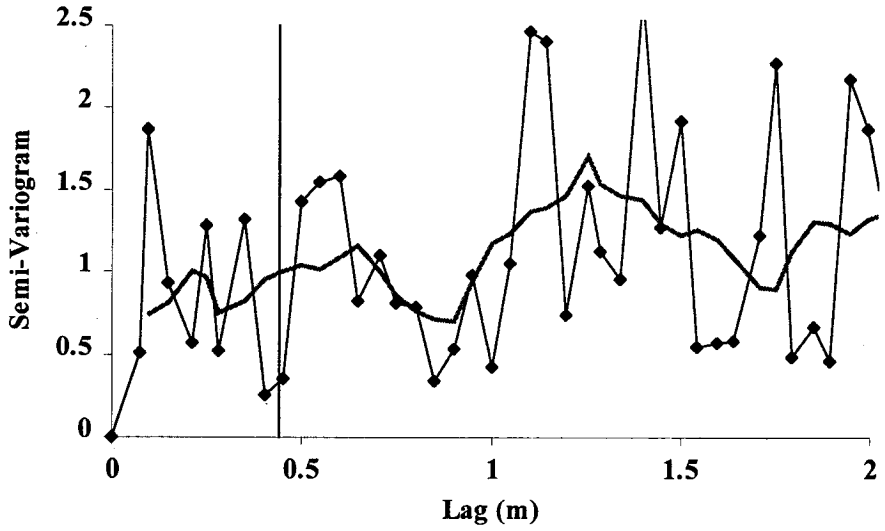

Sources: DTN: GS990408314224.001
FILE (Att. IV CD-ROM): **nsbis_lag=0.05_tol=0.025.xls**
NOTE: Beyond the vertical line, each point represents at least 20 lag pairs and is thus significant. The hole effect could be between 0.5 and 1m lag. The bold line represents a running average over 7 points.

Figure 6-16. Hole Effect in the Semivariogram of the TSw34 NS Fracture Set (set 2 - fractures > 1 m) (lag=0.05 m - 0.025 m lag tolerance)

6.9.3.2 TSw35 Unit

Figure 6-17 and Figure 6-19 show a definite spatial correlation in addition to a definite nugget effect on the fracture set 1 comprising most of the fractures. This correlation is already visible in Figure 6-8 and is mainly due to the presence or absence of lithophysae that has a big effect on

the number of fractures > 1 m. Figure 6-19 is overwhelmed by the high frequency zone because that zone has more fractures than the exposures of the rest of the unit. Figure 6-18 shows no spatial correlation in the "low" fracture frequency zone. The semivariogram of the less abundant fracture set (set 2) (Figure 6-20) shows no spatial correlation. When there is a correlation, the nugget effect is very high at more than 50% of the variance.

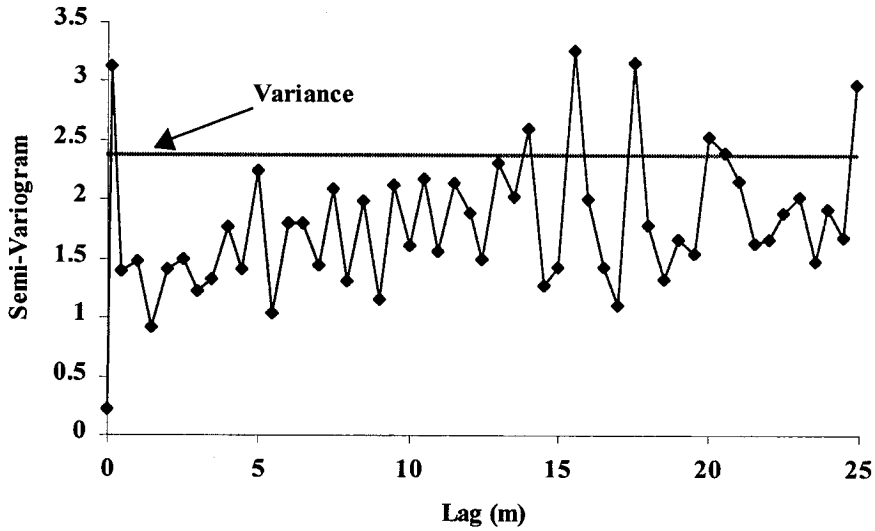

Sources: DTN: GS990408314224.001 and GS990408314224.002
FILE (Att. IV CD-ROM): **ew35-2_lag=0.5_tol=0.25.xls**
NOTE: The semivariogram has a definite nugget effect at this cale (lag=0.5 m - 0.25 m lag tolerance).

Figure 6-17. Semivariogram of the TSw35 EW Fracture Set (set 1 - fractures > 1 m - stations > 18+50 - higher fracture frequency)

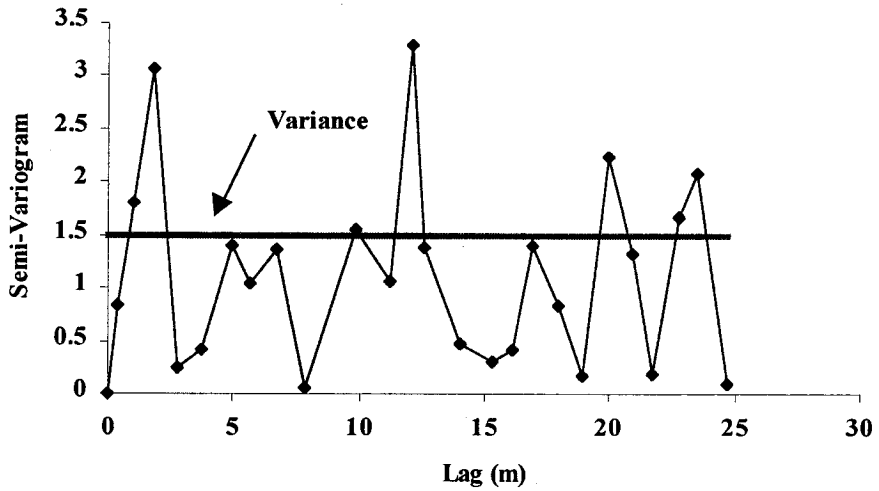

Sources: DTN: GS990408314224.001 and GS990408314224.002
FILE (Att. IV CD-ROM): **ew35-1_lag=1.0_tol=0.5.xls**
NOTE: The semivariogram has a definite nugget effect at this scale (lag=1.0 m - 0.5 m lag tolerance).

Figure 6-18. Semivariogram of the TSw35 EW Fracture Set (set 1 - fractures > 1 m - stations < 18+50 - lower fracture frequency)

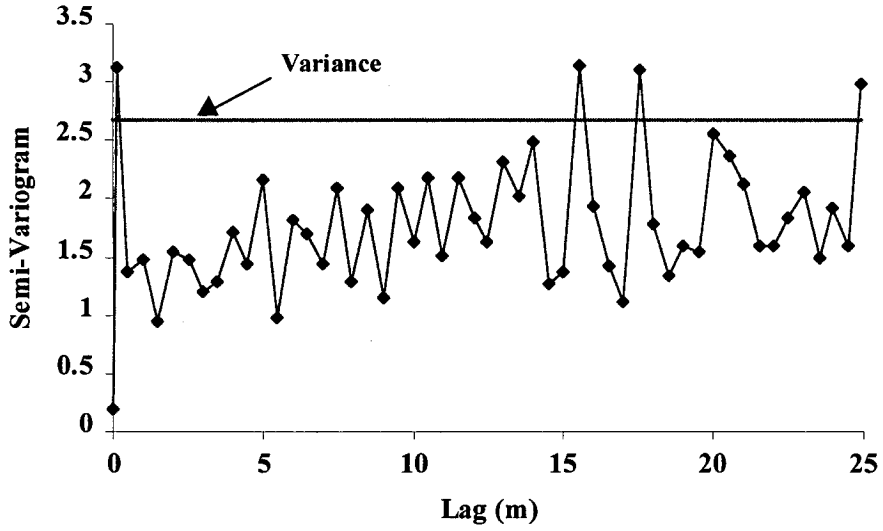

Sources: DTN: GS990408314224.001 and GS990408314224.002
FILE (Att. IV CD-ROM): **ew35_lag=0.5_tol=0.25.xls**
NOTE: The semivariogram has a definite nugget effect at this scale and very slowly converges to the variance (lag=0.5 m - 0.25 m lag tolerance).

Figure 6-19. Semivariogram of the TSw35 EW Fracture Set (set 1 - fractures > 1 m - all stations)

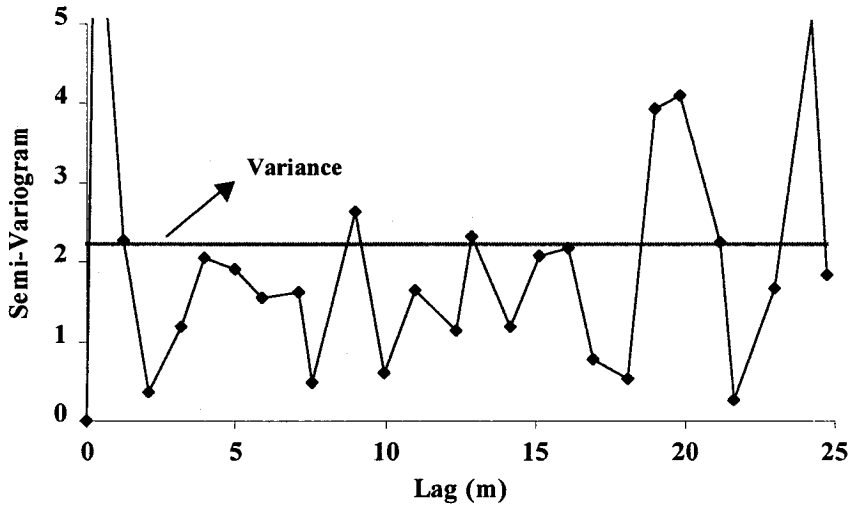

Sources: DTN: GS990408314224.001 and GS990408314224.002
FILE (Att. IV CD-ROM): **ns35_lag=1.0_tol=0.5.xls**
NOTE: The semivariogram has a definite high nugget effect at this scale (lag=1.0 m - 0.5 m lag tolerance).

Figure 6-20. Semivariogram of the TSw35 NS Fracture Set (set 2 - fractures > 1 m - all stations)

6.9.3.3 TSw36 Unit

In the case of the TSw36 unit, Figure 6-9 shows that the whole data set cannot be considered stationary and must be divided into two subsets (from station 14+50 to 24+20 and from station 24+20 to the end) according to the average fracture frequency. Both semivariograms (Figure 6-21 and Figure 6-22) show high nugget effect and very little spatial correlation.

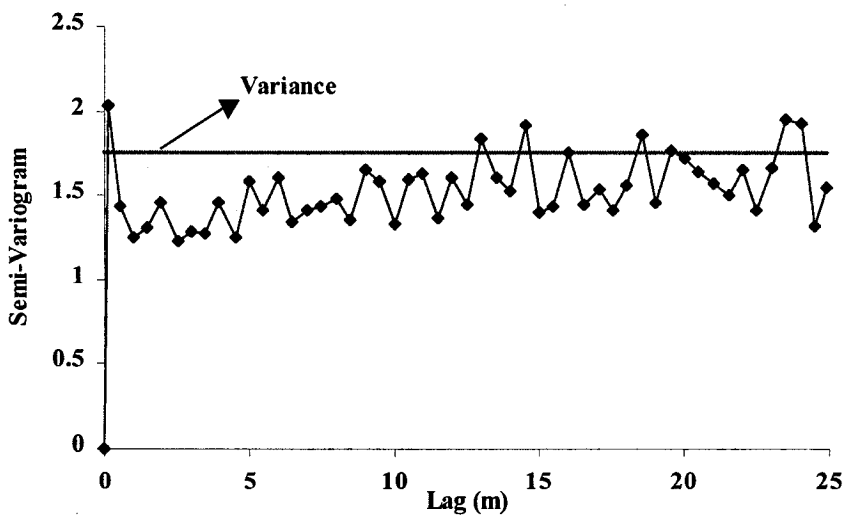

Sources: DTN:GS990408314224.002
FILE (Att. IV CD-ROM): **ewns36-1_lag=0.5_tol=0.25.xls**
NOTE: The semivariogram has a definite high nugget effect at this scale (lag=0.5 m - 0.25 m lag tolerance).

Figure 6-21. Semivariogram of the TSw36 all Fracture Sets (set 2 - fractures > 1 m - stations < 24+20 higher fracture density)

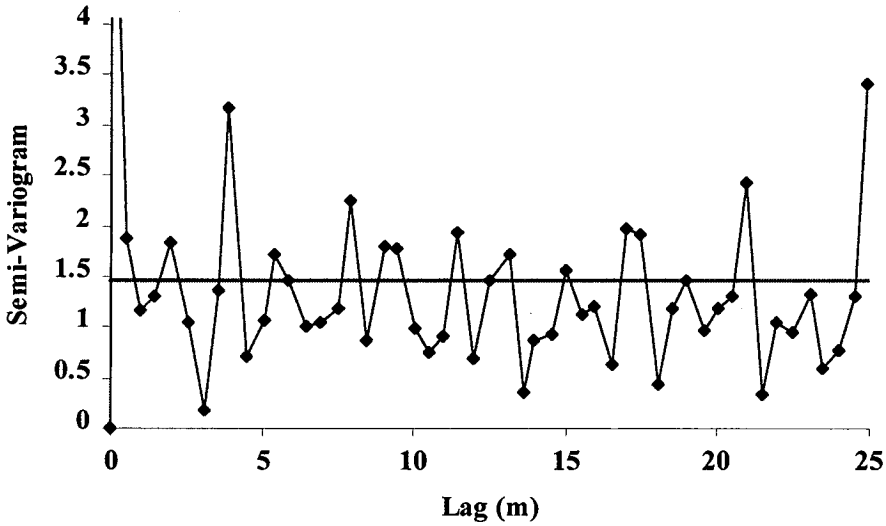

Sources: DTN:GS990408314224.002
FILE (Att. IV CD-ROM): **ewns36-2_lag=0.5_tol=0.25.xls**
NOTE: The semivariogram has a definite high nugget effect at this scale (lag=0.5 m - 0.25 m lag tolerance).

Figure 6-22. Semivariogram of the TSw36 all Fracture Sets (set 2 - fractures > 1 m - stations > 24+20 lower fracture density)

6.9.3.4 Conclusion of Geostatistical Analysis

The assumption of fracture independence (Assumption 5.12) is justified by the geostatistical results of units TSw34 and TSw36. An important conclusion follows from this observation. A tight spacing as given by 3 standard deviations from the mean of the log-spacing cannot be

extended over a large distance. That is, the standard deviation of the average fracture spacing over a given distance is less than the standard deviation given by considering only two fractures as demonstrated by Table 6-38.

When spacing between two fractures is considered, the standard deviation can be high. However, when one considers the average spacing over a given distance, the standard deviation decreases. If a lognormal distribution is assumed, the problem reduces to find the distributions of a sum of lognormal distributions. There is no analytical representation of this solution. Instead, a Monte-Carlo analysis was performed to estimate how the spacing standard deviation changes with the averaging distance (Table 6-38). Each Monte-Carlo simulation involved 1000 realizations.

In the 1-m case the reduction in standard deviation is not such that the distribution of individual fractures cannot be used. However, if a full waste package footprint is considered, it is overly conservative to assume that the highest fracture frequency (at two or three standard deviations above the mean) can be sustained for 5 m.

The case of unit TSw35 is different because it shows some spatial correlation on the 10-20 m range (Figure 6-17) for a set of fracture. However, the nugget effect is very high (1.5/2.38=63% of the variance), the drift length for which this result is applicable is small (~1m), and the other fracture set does not show a spatial correlation (Figure 6-20). For all these reasons, the assumption of independence (Assumption 5.12) is also justified.

Table 6-38. Standard Deviation of the Fracture Spacing for Different Drift Intervals and Different MC Realizations (unit TSw34)

Drift Interval	Any 2 fractures	1 m	2 m	5 m	10 m	20 m	50 m
Average	0.93	0.89	0.87	0.78	0.53	0.31	0.10
Run 1		0.849	0.921	0.859	0.662	0.379	0.102
Run 2		0.761	0.908	0.821	0.587	0.164	0.100
Run 3		1.029	0.902	0.747	0.384	0.520	
Run 4		0.845	0.841	0.805	0.534	0.330	
Run 5		0.978	0.759	0.656	0.466	0.175	

Source: FILE (Att. IV CD-ROM): **FractSp_stat_00a_sp=yy_zz.xls** where **yy** represents the spacing and **zz** the run number and **FractSp_stat_00a_sp_summary.xls**.

6.9.4 CDF of Fracture Spacing

CDF for the ECRB and ESF relevant units are plotted on Figure 6-23. It can be clearly seen that fracture data from the different locations of the TSw34 unit agree pretty well with each other except the IFZ area. The main body of the proposed repository is hosted in the TSw35 unit that has the lowest fracture > 1m frequency. However, when the small-length fractures are also taken into account, the lower frequency of the TSw35 unit disappears (Figure 6-24). This point will be developed in more detail in the following sections.

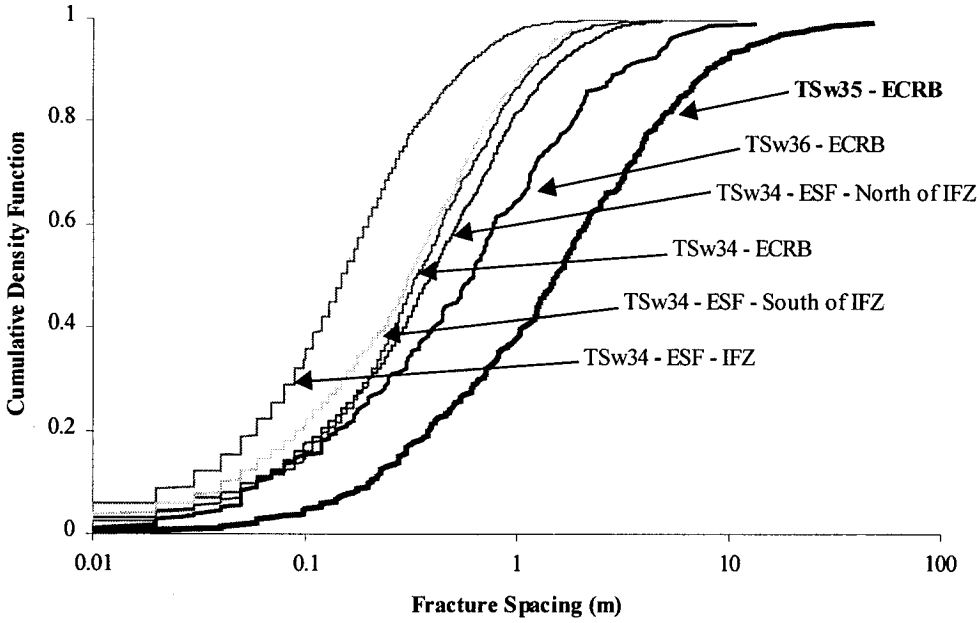

Sources: DTNs: GS971108314224.024, GS971108314224.025, GS960708314224.008, GS960808314224.011, GS960708314224.010, GS971108314224.026, GS960908314224.014, GS971108314224.028, GS990408314224.001, and GS990408314224.002
FILE (Att. IV CD-ROM): **CDF_Fracturespacing&intensity.xls**, worksheet: fracture spacing all units L>1m.
DEVELOPED DTN: MO0109SPAFIE10.006

Figure 6-23. CDF of Individual Fracture Spacing (fracture > 1 m)

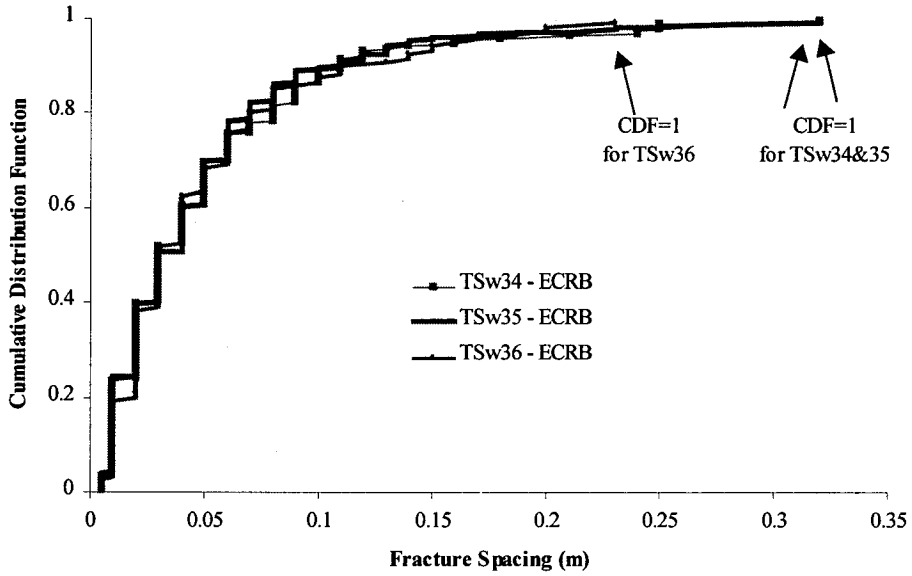

Sources: DTN: GS990908314224.009
FILE (Att. IV CD-ROM): **CDF_Fracturespacing&intensity.xls**, worksheet: fract spacing all units all fr
DEVELOPED DTN: MO0109SPAFIE10.006

Figure 6-24. CDF of Individual Fracture Spacing for all Fractures within the SSS

6.9.5 Terzaghi Correction

True spacing between fractures can only be expressed as the orthogonal distance between 2 fractures of the same set. The Terzaghi correction has little impact on the results of the different units (Table 6-39) because when the correction factor is higher it applies to the less frequent fracture set.

The Terzaghi correction is strictly applicable only to individual fractures. Application to the mean orientation as done here is only approximate (Assumption 5.9). More realistic corrections were proposed by Dershowitz and Herda (1992). They were not used, however, because they are believed to be lost in other conservative assumptions made in the course of this work.

The Terzaghi correction was not applied to sub-horizontal fracture sets. Although sub-horizontal fractures are an important feature of a well-connected network, their numerical importance is small (summary of fracture orientation in Table 6-25).

Table 6-39. Terzaghi Correction Factors

Fracture Set	Mean Set Orientation (Table 6-19 to Table 6-24)	Drift Bearing (Table 6-2 and Table 6-3)	Angle	Fracture Set Correction Factor[a]
TSw33 - ECRB Set 1	122	Curved Section Average = 242	57	1.19
TSw33 - ECRB Set 2	195	Curved Section Average = 242	60	1.15
TSw34 - ECRB Set 1	122	229	73	1.05
TSw34 - ECRB Set 2	195	229	44	1.44
TSw34 - ECRB Weighed Average (See Table 6-25): (1.05*10+1.44*5)/15 = **1.18**				
TSw35 - ECRB Set 1	157	229	72	1.05
TSw35 - ECRB Set 2	97	229	48	1.35
TSw35 - ECRB Weighed Average (See Table 6-25): (1.05*7+1.35*2)/9 = **1.12**				
TSw36 - ECRB Set 1	134	Curved Section: Average = 259	55	1.22
TSw36 - ECRB Set 2	198	Curved Section: Average = 259	61	1.14
TSw36 - ECRB Weighed Average (See Table 6-25): (1.22*5+1.14*4)/9 = **1.18**				

NOTE: [a] obtained with Eq. 9 (correction factor = 1/sin(angle))

6.9.6 Correspondence between Fracture Frequency and Intensity

Because the Total System Performance Assessment - Viability Assessment gives a distribution law only for the fracture frequency and because we are interested in the fracture intensity, some kind of relationship (which is site specific) must be devised between the two parameters. Bodvarsson et al. 1997 reports that a fracture frequency of 1.88 corresponds to a fracture intensity of 0.89 m/m^2 (Row 1 of Table 6-34) but Row 4 of Table 6-34 shows that fracture intensity can be as high as 1.22. These fracture intensity values disregard at least two parameters important for criticality accumulations: 1) Fracture smaller than 1 m or 0.3 m have to be taken into account as they are in general connected to the fracture network (see Section 6.10 on

connectivity) and, 2) Fracture orientations deviate from verticality and are not perpendicular to the DLS, both factors increasing the value of fracture intensity. This will be developed in the next paragraphs. In addition, if fracture frequency distribution for fractures > 1 m can be accurately predicted from ECRB mapping, this is not the case for the distribution of all fractures because their mapping has been done only in limited drift intervals. One needs to devise a conservative mean to go from the fracture frequency distribution for fractures > 1 m to the fracture intensity that includes all fractures.

The basic assumption is that the percentage of each fracture size bin is constant and independent of fracture frequency (Assumption 5.3). That is, if the fracture frequency of fracture > 1m is doubled, the fracture intensity is also doubled. This approach is conservative as a higher number of fracture > 1m is likely due to the growth and coalescence of smaller fractures.

Information from Table 6-30 to Table 6-32 can be summarized in Table 6-40 with one small change. Because fracture intensities are computed from a 0.6-meter-wide band, all fracture length outside of that band is not relevant to the fracture intensity, that is, all fractures longer than 0.6 meter are truncated to 0.6 meter and the correction for nonverticality is done by adding 10% of the final value. The value of 10% was chosen because an overwhelming number of fractures have a dip larger than 65° and the extra-length added by nonverticality is 1/sin(65)~1.1. The Terzaghi correction coefficients that take into account non-normality between DLS and fracture are taken from Table 6-39.

When all the fractures are taken into account, it appears that the three repository units have a similar fracture frequency. When the TSw34 unit is studied in more detail (Table 6-41), it also suggests that the fracture frequency stays about the same within the same formation even if the number of long fractures varies as explained next. The total fracture length for all fractures is 4.78 and 5.55 m/m of drift (row 11 and both columns 4 of Table 6-41) for the two SSS segments but the fracture frequency for fracture > 1 m is 1.5 and 4.67 /m of drift (row 16 of Table 6-41), respectively. A lower fracture frequency for fracture >1m is compensated by a larger number of small fractures. However, the total fracture frequency is still higher when the fracture frequency for fractures >1m is higher (by 12.5% is this case).

The TSw35 unit must be examined more thoroughly (Table 6-42) because of (1) its preponderance in the repository, and (2) because of a more complex set of data with zones of apparent higher and lower fracture frequency (related to the lithophysae abundance). Application of the principle detailed in the last paragraph would lead to unrealistic fracture intensity in the zones with higher fracture frequency of fractures > 1m (Table 6-43).

Table 6-40. Details of Fracture Intensity Calculations for Units TSw34 to TSw36

		TSw34 - ECRB (10 meters of SSS)			TSw35 - ECRB (18 meters of SSS)			TSw36 - ECRB (6 meters of SSS)		
	1	2	3	4	2	3	4	2	3	4
1	0.0 - 0.1	48	0.074	3.54	92	0.073	6.71	17	0.075	1.28
2	0.1 - 0.2	54	0.15	8.02	127	0.15	18.68	33	0.15	4.84
3	0.2 - 0.3	24	0.24	5.79	73	0.25	18.22	30	0.25	7.40
4	0.3 - 0.4	15	0.35	5.23	44	0.36	15.69	12	0.35	4.16
5	0.4 - 0.5	5	0.45	2.23	19	0.44	8.28	4	0.47	1.86
6	0.5 - 1.0	12	0.60	7.20	9	0.60	5.40	17	0.60	10.20
7	> 1 m	34	0.60	20.40	5	0.60	3.00	7	0.60	4.20
8	Total Length along SSS			52.40			75.98			33.93
9	# fractures > 0.3 m	66			77			40		
10	Length along SSS for fractures > 0.3 m			35.06			32.37			20.42
11	Total Length/m of drift			5.24			4.22			5.65
12	After 10% Correction			5.76			4.64			6.22
13	After 1/0.6 Correction			9.61			7.74			10.37
14	After Terzaghi Correction			9.61 x 1.18 = **11.34**			7.74 x 1.12 = **8.67**			10.37 x 1.18 = **12.24**
15	Length Due to Fractures > 1 m			20.40/ 52.40 = **39%**			3.00/ 75.98 = **4%**			4.2/ 33.93 = **12.4%**
16	Fracture Frequency for Fracture > 1 m	34/ 10= **3.4**			5/ 18 = **0.28**			7/ 6 = **1.17**		
17	Length Due to Fractures > 0.3 m			35.06/ 52.40 = **66.9%**			32.37. 75.98 = **42.6%**			20.42/ 33.93 = **60.2%**
18	Fracture Frequency for Fracture > 0.3 m	66/10= **6.6**			77/18= **4.3**			40/6= **6.7**		
19	Length Due to Fractures < 0.3 m			(52.40 - 35.06)/ 52.40 = **33.1%**			(75.98 - 32.37)/. 75.98 = **57.4%**			(33.93 - 20.42)/ 33.93 = **39.8%**

Sources: DTN: GS990908314224.009
FILE (Att. IV CD-ROM): **Percentage_SSS.xls**

NOTES: Fracture lengths higher than 0.6 m are truncated to 0.6
1 Length Interval (m)
2 Number of Discontinuities (Table 6-30, Table 6-31, and Table 6-32)
3 Average Length (arithmetic) (m) (Table 6-30, Table 6-31, and Table 6-32)
4 Total Length in Each Bin (m) (= "2" x "3")

Table 6-41. Details of Fracture Intensity Calculations for Unit TSw34

		TSw34 - ECRB (4 meters of SSS) 11+15 to 11+19			TSw34 - ECRB (6 meters of SSS) 13+00 to 13+06		
	1	2	3	4	2	3	4
1	0.0 - 0.1	27	0.073	1.96	21	0.075	1.58
2	0.1 - 0.2	30	0.15	4.52	24	0.15	3.49
3	0.2 - 0.3	11	0.24	2.61	13	0.24	3.18
4	0.3 - 0.4	8	0.35	2.83	7	0.34	2.40
5	0.4 - 0.5	0	0.00	0.00	5	0.45	2.23
6	0.5 - 1.0	6	0.60	3.60	6	0.60	3.60
7	> 1 m	6	0.60	3.60	28	0.60	16.80
8	Total Length along SSS			19.12			33.28
9	# fractures > 0.3 m	20			46		
10	Length along SSS for fractures > 0.3 m			10.03			25.03
11	Total Length / m of Drift			4.78			5.55
12	After 10% Correction			5.26			6.10
13	After 1/0.6 Correction			8.76			10.17
14	After Terzaghi Correction (= 1.18)			8.76 x 1.18= **10.34**			10.17 x 1.18= **11.79**
15	Length Due to Fractures > 1 m			3.60/ 19.12= **18.8%**			16.80 / 33.28= **50.5%**
16	Fracture Frequency for Fracture > 1 m	6/4= **1.5**			28/6= **4.67**		
17	Length Due to Fractures > 0.3 m			10.03/ 19.12 = **52.4%**			25.03/ 33.28 = **75.2%**
18	Fracture Frequency for Fracture > 0.3 m	20/4= **5**			46/6= **7.67**		

Sources: DTN: GS990908314224.009
FILE (Att. IV CD-ROM): **Percentage_SSS.xls**

NOTES: Fracture lengths higher than 0.6 m are truncated to 0.6
1 Length Interval (m)
2 Number of discontinuities - details in referenced file (column M)
3 Average Length (arithmetic) (m) - details in referenced file (column M)
4 Total Length in Each Bin (m) (= "2" x "3")

Table 6-42. Details of Fracture Intensity Calculations for Unit TSw35

	TSw35 - ECRB (6 meters of SSS) 15+25 to 15+31			TSw35 - ECRB (6 meters of SSS) 17+35 to 17+41			TSw35 - ECRB (6 meters of SSS) 22+15 to 22+21		
1	2	3	4	2	3	4	2	3	4
0.0 - 0.1	12	0.071	0.85	59	0.071	4.20	21	0.079	1.66
0.1 - 0.2	42	0.15	6.25	53	0.14	7.66	32	0.15	4.78
0.2 - 0.3	22	0.25	5.46	33	0.26	8.43	18	0.24	4.34
0.3 - 0.4	21	0.36	7.50	18	0.35	6.39	5	0.36	1.80
0.4 - 0.5	6	0.43	2.58	11	0.43	4.75	2	0.48	0.95
0.5 - 1.0	2	0.55	1.09	5	0.57	2.87	2	0.60	1.20
> 1 m	0	0.60	0.00	1	0.60	0.60	4	0.60	2.40
Total Length along SSS			23.73			34.89			17.12
# fractures > 0.3 m	29			35			13		
Length along SSS for fractures > 0.3 m			11.17			14.61			6.35
Total Length / m of Drift			3.95			5.81			2.85
After 10% Correction			4.35			6.40			3.14
After 1/0.6 Correction			7.25			10.66			5.23
After Terzaghi Correction (= 1.12)			7.25 x 1.12= **8.12**			10.66 x 1.12= **11.94**			5.23 x 1.12= **5.86**
Length Due to Fractures > 1 m			0/ 23.73= **0%**			0.60/ 35.89= **1.7%**			2.4/ 17.12= **14%**
Fracture Frequency for Fracture > 1 m	0/6= **0**			1/6= **0.17**			4/6= **0.67**		
Length Due to Fractures > 0.3 m			11.17/ 23.73= **47.1%**			14.61/ 34.89= **41.9%**			6.35/ 17.12= **37.1%**
Fracture Frequency for Fracture > 0.3 m	29/6= **4.83**			35/6= **5.83**			13/6= **2.17**		

Sources: DTN: GS990908314224.009
File: **Percentage_SSS.xls**

NOTES: Fracture lengths higher than 0.6 m are truncated to 0.6
1 Length Interval (m)
2 Number of discontinuities (Table 6-31)
3 Average Length (arithmetic) (m) (Table 6-31)
4 Total Length in Each Bin (m) (= "2" x "3")

6.9.7 CDF of Fracture Intensity

The CDFs of the fracture intensity can be built from the CDF of the corrected fracture frequency with Assumption 5.1. The first data row of Table 6-43 indicates that to obtain the numerical value of fracture intensity for all fractures (in m/m^2) from the numerical value of fracture frequency of fracture > 1m (in m^{-1}) for unit TSw34, one has to multiply the latter by 3.34. Similarly, coefficients of 10.45 and 8.75 are used for the units TSw36 and TSw35 with high

fracture intensity respectively. The value of 11.94 is used in the TSw35 unit when the fracture frequency of fracture > 1m is lower than 11.94/8.75=1.36 m^{-1}.

Table 6-43. Correction Factor from Fracture Frequency to Fracture Intensity

Unit	Fracture Frequency of Fracture >1 m (Table 6-40 and Table 6-42)	Total Fracture Intensity for all Fractures (Table 6-40 and Table 6-42))	Final Correction	Comments
TSw34 - ECRB	3.4	11.36	(11.36/3.4=) 3.34	Used for entire TSw34 unit
TSw35 - ECRB	0.28	8.67	(8.67/0.28=) 30.96	Not used, leads to unrealistic fracture intensity (see below for segment specific values used instead)
TSw36 - ECRB	1.17	12.23	(12.23/1.17=) 10.45	Used for entire TSw36 unit
TSw35 - ECRB 15+25/31	0.0	8.12	N/A	Not used; the next row was retained as more conservative
TSw35 - ECRB 17+35/41	0.17	11.94	11.94 See Note	Used for low fracture (> 1m) frequency, i.e., within lithophysal sections
TSw35 - ECRB 22+15/21	0.67	5.86	(5.86/0.67=) 8.75	Used for high fracture (> 1m) frequency, i.e., outside of lithophysal sections

NOTE: Because there are very few fractures > 1m when lithophysae are present, it is conservatively assumed that the fracture intensity is always at least 11.94 m^{-1} (see Figure 6-26), the correction of 8.75 is used only when the fracture frequency is above 1.36 fracture > 1m / m (1.36=11.94/8.75)

Figure 6-25 to Figure 6-29 were constructed by: (1) constructing the distribution of the average fracture frequency of fractures > 1 m over a given drift interval from the individual fracture frequency data (worksheets "xx all fract. >65 - aver. on 1m" from file **ECRB_study_TSw3x.xls** in Att. IV CD-ROM where xx stands for ul, mn, and ll, and **x** stands for 3, 4, 5, or 6 respectively), and (2) scaling the fracture frequency of fracture > 1 m according to the correction factors presented in Table 6-43. In the case of unit TSw35, the correction factor computed for high fracture frequency was used for high intensity and the maximum of the high and low fracture frequency correction factors for lower fracture frequencies. This section supposes that the multipliers are constant. This approach is conservative and will be relaxed in Section 6.9.8.

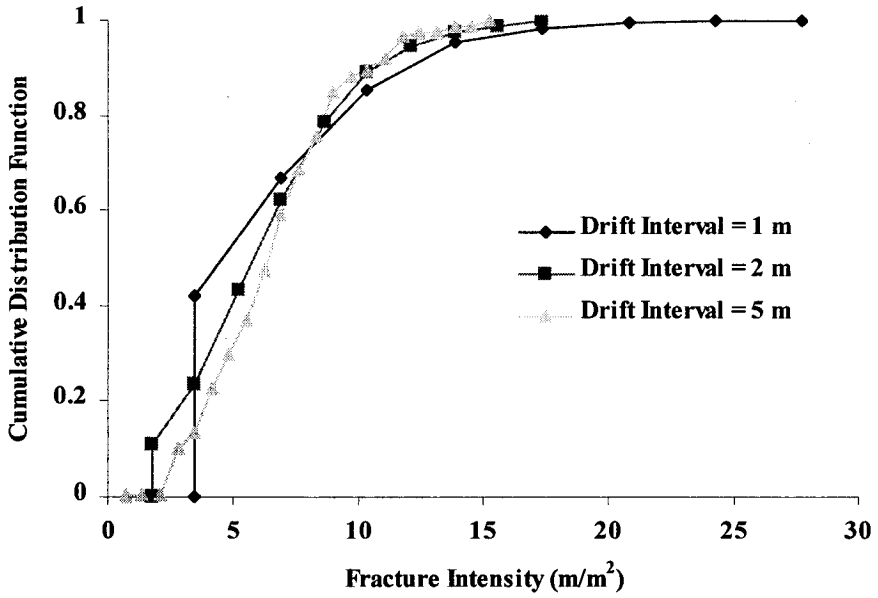

Sources: DTN: GS990408314224.001 and GS990408314224.002
FILE (Att. IV CD-ROM): **CDF_Fracturespacing&intensity.xls**, worksheet: fracture intensity TSw34

Figure 6-25. CDF of Fracture Intensity for TSw34 Unit along Different Drift Intervals

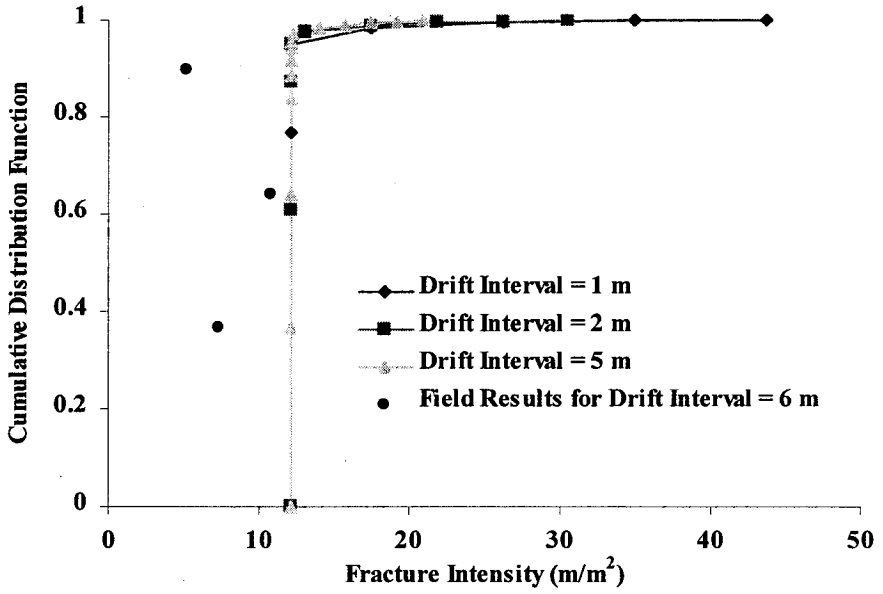

Sources: DTN: GS990408314224.001 and GS990408314224.002
FILE (Att. IV CD-ROM): **CDF_Fracturespacing&intensity.xls**, worksheet: fracture intensity TSw35
NOTE: Combination of lithophysal and non/less lithophysal sections.

Figure 6-26. CDF of Fracture Intensity for TSw35 Unit along Different Drift Intervals

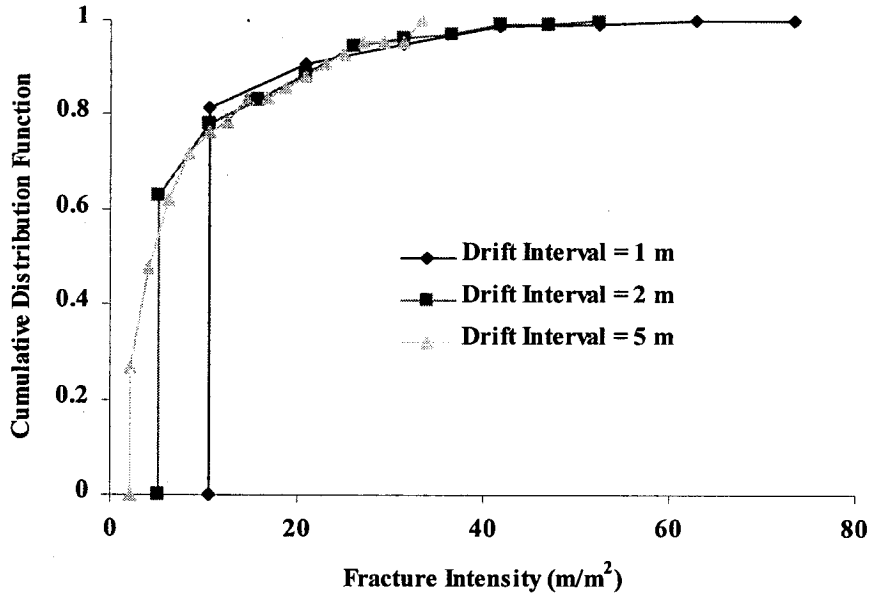

Sources: DTN: GS990408314224.001 and GS990408314224.002
FILE (Att. IV CD-ROM): **CDF_Fracturespacing&intensity.xls**, worksheet: fracture intensity TSw36
NOTE: Constant multipliers are used

Figure 6-27. CDF of Fracture Intensity for TSw36 Unit along Different Drift Intervals

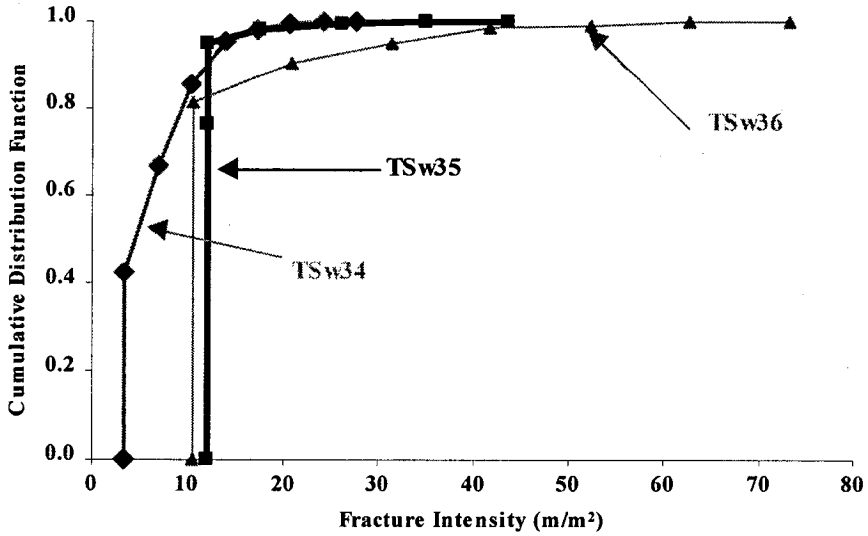

Sources: DTN: GS990408314224.001 and GS990408314224.002
FILE (Att. IV CD-ROM): **CDF_Fracturespacing&intensity.xls**, worksheet: fract. int. all drift inter.=1m
NOTE: Constant multipliers are used
DEVELOPED DTN: MO0109SPAFIE10.006

Figure 6-28. CDF of Fracture Intensity for the Three Repository Units along a Drift Interval=1 m

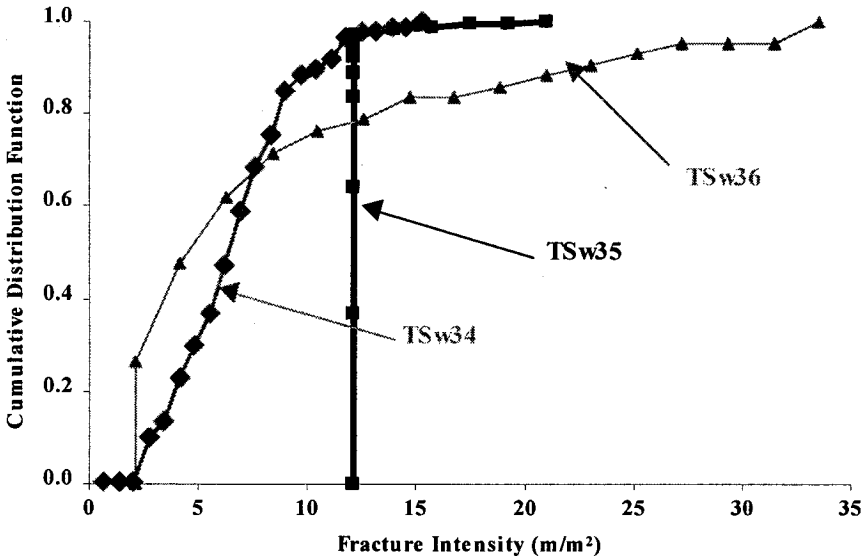

Sources: DTN: GS990408314224.001 and GS990408314224.002
FILE (Att. IV CD-ROM): **CDF_Fracturespacing&intensity.xls**, worksheet: fract. int. all drift inter.=5m
NOTE: Constant multipliers are used
DEVELOPED DTN: MO0109SPAFIE10.006

Figure 6-29. CDF of Fracture Intensity for the Three Repository Units along a Drift Interval=5 m

Table 6-44 reproduces the data plotted on Figure 6-28.

Table 6-44: Cumulative Distribution Functions for Units TSw34 to TSw36

	1	2	3	4	5	6	7	8
	TSw34		TSw35 (low)[a]		TSw35 (all)		TSw36	
	Fracture Intensity (m/m2)	Cumulative Distribution Function	Fracture Intensity (m/m2)	Cumulative Distribution Function	Fracture Intensity (m/m2)	Cumulative Distribution Function	Fracture Intensity (m/m2)	Cumulative Distribution Function
1	3.34	0.422						
2	6.68	0.668					10.45	0.813
3	10.02	0.853	11.94	0.766	11.94	0.766	20.90	0.905
4	13.36	0.954	11.94	0.952	11.94	0.952	31.35	0.950
5	16.7	0.984			17.50	0.984	41.80	0.987
6	20.04	0.996			26.25	0.996	52.25	0.993
7	23.38	0.998			35.00	0.999	62.70	0.999
8	26.72	~1	18.1[b]	~1	43.75	~1	73.15	~1

Sources: DTN: GS990408314224.001 and GS990408314224.002
FILE (Att. IV CD-ROM): **CDF_Fracturespacing&intensity.xls**, worksheet: fract. int. all drift inter.=1m
NOTE: [a] low stands for low fracture intensity for fracture > 1 m.
[b] obtained by assuming that the highest fracture intensity with no fracture > 1 m (=11.94 m/m^2) is applicable to the highest recorded fracture frequency in the SSS in the TSw35 unit (=0.67 fracture > 1 m /m)

The very high fracture intensity of unit TSw36 is simply due to the fact that the scaling factor that takes into account small fractures is computed from a drift length with few long fractures; however, some other areas of TSw36 have a higher frequency of long fractures. The combination of those two factors generates a high fracture intensity that may be artificial because long fractures tend to form by coalescence of small fractures, but a true increase in fracture frequency cannot be ruled out. It is thus conservatively kept.

6.9.8 Extrapolation and CCDF of Fracture Intensity

The Complementary Cumulative Distribution Function (CCDF) for high fracture intensity, not observed in the tunnels, is derived in this section. The probability of fracture frequency for fracture > 1 m for each unit is given in Table 6-46. Field measurements yield the fracture frequency, and thus the probability, of up to 8 fractures/m. This probability can be extrapolated to any number *n* of fractures according to the following equation (Eq. 11) (:

$$\Pr(\text{average number of fractures (> 1m) /m} > n) = \exp(a*n+b) \qquad \text{(Eq. 11)}$$

whose coefficients *a* and *b* are displayed in Table 6-45.

Table 6-45. Coefficients for Equations for Prob(average number of fractures (> 1m) /m >n)

Unit	a	b	SOURCE
TSw34	-0.8272	+0.2758	File: **FractureIntensityNew.xls**; worksheet: TSw34
TSw35	-1.3546	-0.1084	File: **FractureIntensityNew.xls**; worksheet: TSw35 for fractures
TSw36	-0.9533	-0.3356	File: **FractureIntensityNew.xls**; worksheet: TSw36

NOTE: coefficients *a* and *b* are extracted from regression equations on plots of the referenced worksheets
DEVELOPED DTN: MO0109SPAFIE10.006

Table 6-46. CCDF of the Average Number of Fracture (>1 m) / m

Fracture Frequency for Fracture >1 m	Unit TSw34	Unit TSw35	Unit TSw36
1	5.781E-01	2.344E-01	1.874E-01
2	3.324E-01	4.807E-02	9.490E-02
3	1.469E-01	1.650E-02	4.982E-02
4	4.623E-02	3.697E-03	1.305E-02
5	1.638E-02	1.138E-03	7.117E-03
6	4.096E-03	*2.649E-04*	1.186E-03
7	2.320E-03	*6.837E-05*	*9.040E-04*
8	*1.014E-03*	*1.764E-05*	*3.485E-04*
9	*4.436E-04*	*4.553E-06*	*1.343E-04*
10	*1.940E-04*	*1.175E-06*	*5.178E-05*
11	*8.482E-05*	*3.032E-07*	*1.996E-05*

Sources: File: **FractureIntensityNew.xls**; worksheet: Summary
NOTE: Values in italics are extrapolated using Equations from Table 6-45
DEVELOPED DTN: MO0109SPAFIE10.006

Figure 6-30 displays field results for the CCDF of the number of fractures in a given interval (Table 6-45 only shows results for an interval of 1 m). The tail of the distribution fits an exponential distribution.

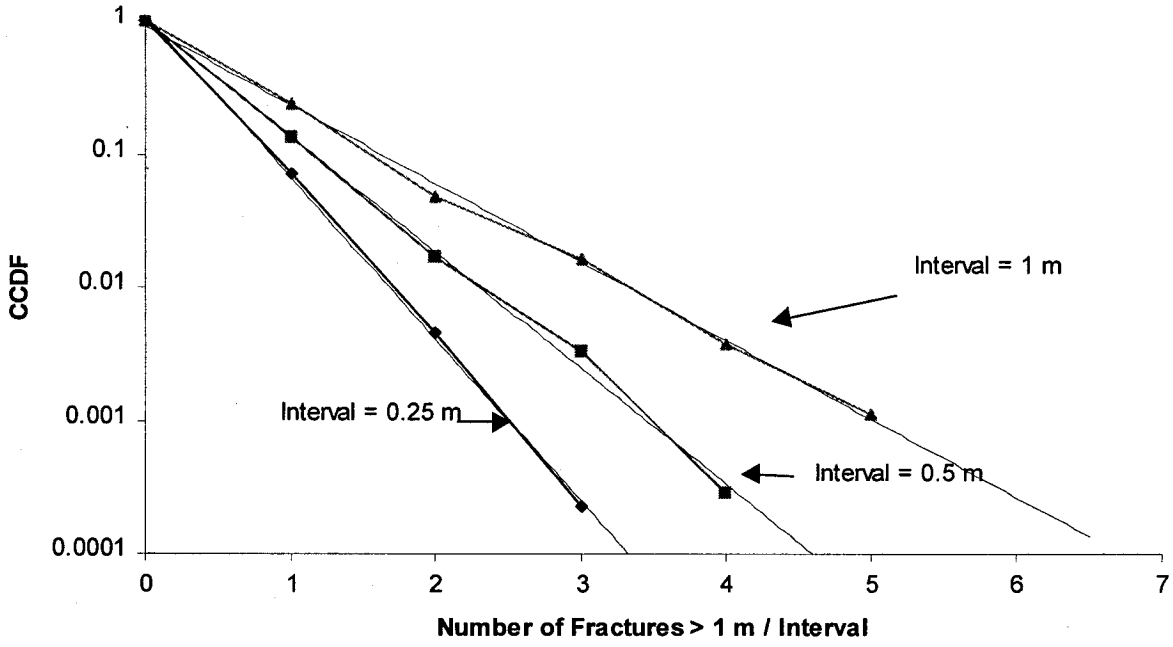

Source: FILE (Att. IV CD-ROM): **FractureIntensityNew.xls**; worksheet: TSw35 for fractures
NOTE: Dotted lines represent data, straight lines represent linear regression basis for extrapolation

Figure 6-30. CCDF of TSw35 by Extrapolation of Field Data

As mentioned in Section 6.9.7, the approach of having a constant multiplier when going from fracture spacing/frequency to fracture intensity is too conservative in the case of high fracture frequency/low fracture spacing. The following paragraphs describe a less conservative approach where the constant multiplier is broken down into several multipliers, each applicable to a group of fracture length bins (> 1 m, 0.3 < < 1 m, and < 0.3 m). To go from fracture intensity for fractures > 1m to corrected fracture intensity, multiply by u_{ACCI} as given in Table 6-47. The parameter u_{ACCI} is the product of the correction for non-verticality, the correction for survey bias (or Terzaghi correction) (drift not normal to fracture planes) and the correction for fractures smaller than 0.3 m for non lithophysal units.

Table 6-47. Correction Factor for Fracture Intensity for Fractures > 1m

	TSw34	TSw35	TSw36	Source
Non-verticality	1.1	1.1	1.1	Section 6.9.6
Survey bias	1.18	1.12	1.18	Section 6.9.5 and Table 6-39
Smaller fractures	1.33		1.40	Computed Table 6-40 Row 19[a]
Smaller fractures		1.0		No correction for TSw35 (see text)
u_{ACCI}	**1.726**	**1.232**	**1.817**	

NOTE: [a] Table 6-40 gives the results of 33.2% and 39.8% higher for TSw34 and TSw36, respectively, i.e., a correction factor of 1.33 and 1.40
DEVELOPED DTN: MO0109SPAFIE10.006

There is a difference in treatment for fractures whose length is between 1 and 0.3 m in lithophysal (TSw35) and non lithophysal (TSw34 and TSw36) units. It has been determined for non-lithophysal units that the total number of fracture for fractures 0.3 <-< 1 m is independent of the fracture frequency on the 1 meter scale. The correlation coefficient is ~0.05 (see cell B36 in

Complement_to_ESF26-60.xls/text) for the TSw34 unit. The TSw36 unit is taken to follow the same pattern. The probability of the uncorrected fracture intensity for fractures 0.3 <-< 1 m can be extrapolated to any number of fractures as given in Table 6-48 according to Eq. 12 (coefficients computed in **Complement_to_ESF26-60.xls**; worksheet "sorted for drift int.=1m"; regression on plot located on cell AH58 and vicinity):

$$\Pr(\text{Av. Uncorrected Fracture Intensity for Fractures } 0.3<-<1 \text{ m / meter} > L) = \exp(-1.0769L + 0.7893) \quad \text{(Eq. 12)}$$

Table 6-48. CCDF of Uncorrected Fracture Intensity for Fractures with Length 0.3<-<1m (TSw34 unit)

Uncorrected Fracture Intensity (m/m^2)	CCDF
1	5.5440E-01
2.1	2.1848E-01
3	7.5993E-02
4	2.6770E-02
5.04	7.7720E-03
6.1	4.3178E-03
7.21	8.6356E-04
8	*3.9926E-04*
9	*1.3601E-04*
10	*4.6331E-05*
11	*1.5783E-05*
12	*5.3764E-06*
13	*1.8315E-06*

Sources File: **Complement_to_ESF26-60.xls**; worksheet: text
NOTE: Extrapolated data in italics
DEVELOPED DTN: MO0109SPAFIE10.006

The lithophysal unit (TSw35) has a different treatment because there are very few measurements with both fracture of length > 1 m and fractures of length < 1 m. Therefore, the assumption of independence between those two distributions cannot then be used. However the distribution for uncorrected fracture length < 1 m (that is, that includes both fractures 0.3 <-< 1 m and fractures < 0.3 m) has been determined (see **Complement_to_ECRB_smallfract_spacing.xls**; worksheet "text"). When more than 1 fracture > 1 m /m are present, the total fracture intensity is the product (instead of the sum as in the non-lithophysal unit case) of the fracture frequency fracture > 1 m to the corrected fracture intensity of fracture < 1 m. It is most likely that large fractures result from the coalescence of smaller ones. This would make the approach conservative, there is however a lack of field data to support that conclusion. The probability of the uncorrected fracture intensity for fractures < 1 m can be extrapolated to any number of fractures as given in Table 6-49 according to Eq. 13 (coefficients computed in **Complement_to_ECRB_smallfract_spacing.xls**; worksheet "Results length"; regression on plot):

$$\Pr(\text{Av. Uncorrected Fracture Length for Fractures } <1 \text{ m / meter} > L) = \exp(-0.5048L + 1.2004) \quad \text{(Eq. 13)}$$

Because the distribution already takes into account fractures < 0.3 m, the correction factors u_{ACC1} and u_{ACC2} for unit TSw35 do not include a correction for small fractures (Table 6-47 and Table 6-50, middle row, column TSw35).

Table 6-49. CCDF of Uncorrected Fracture Intensity of Fractures with Length <1m (TSw35 unit)

Uncorrected Fracture Intensity (m/m2)	CCDF	Uncorrected Fracture Intensity (m/m2)	CCDF
0.29	9.286E-01	8	*5.854E-02*
2.774	8.571E-01	9	*3.534E-02*
2.984	7.857E-01	10	*2.133E-02*
3.053	7.143E-01	11	*1.288E-02*
3.855	6.429E-01	12	*7.772E-03*
4.21	5.714E-01	13	*4.692E-03*
4.525	5.000E-01	14	*2.832E-03*
4.55	4.286E-01	15	*1.709E-03*
4.64	3.571E-01	16	*1.032E-03*
4.963	2.857E-01	17	*6.229E-04*
5.19	2.143E-01	18	*3.760E-04*
6.56	1.429E-01	19	*2.269E-04*
7.415	7.143E-02	20	*1.370E-04*

Source: File: **Complement_to_ECRB_smallfract_spacing.xls**; worksheet: text
NOTE: Extrapolated data in italics
DEVELOPED DTN: MO0109SPAFIE10.006

To go from uncorrected fracture intensity for fractures < 1 m to corrected fracture intensity for fractures < 1 m, multiply by u_{ACC2} as given in Table 6-50.

Table 6-50. Correction Factor for Fracture Intensity for Fractures < 1m

	TSw34	TSw35	TSw36	Source
Survey bias	1.18	1.12	1.18	Section 6.9.5 and Table 6-39
Survey area	1/0.6	1/0.6	1/0.6	Eq. 10 and underneath. The study area is only 0.6-m wide. This correction scales the results to 1 m^2.
Smaller fractures	1.33	1.0	1.4	Table 6-40 Row 19
u_{ACC2}	**2.616**	**1.867**	**2.753**	

DEVELOPED DTN: MO0109SPAFIE10.006

The parameter u_{ACC2} is the product of the correction for survey bias (drift not normal to fracture planes) and the correction for survey area (0.6 m wide) and the correction for fracture smaller than 0.3 m for non lithophysal units. The correction for non-verticality is not needed in this case because this factor is already taken into account in the total fracture length.

Table 6-51 summarizes the previous results. It will be used to stochastically generate fracture intensity. Two random numbers between 0 and 1, *rdn1* and *rdn2*, need to be generated. Taking TSw34 as an example, also valid for TSw36, *rdn1* will provide the fracture intensity due to fractures > 1 m sampled from Table 6-46 (find *rdn1* in column 2 and then the corresponding value of fracture intensity in column 1). This value needs to be corrected as described above. The correction factor is 1.726 as read from Table 6-47. The random number *rdn2* will initiate the sampling of the fracture intensity due to fractures < 1 m. The value is read from Table 6-48. It also needs to be corrected by the multiplicative factor 2.616 as read in Table 6-50. Because those two distributions are independent (as shown at the beginning of this section), the resulting total fracture intensity is the sum of the fracture intensities of fractures > 1 m and fractures < 1 m. In the case of the TSw35 unit, because fracture intensities of fractures > 1 m and fractures < 1 m cannot be proven independent, the relationship is multiplicative instead of additive. The fracture intensity for fractures < 1 m is sampled from Table 6-49, corrected by the coefficient of 1.867 read in Table 6-50. Unlike units TSw35 and TSw36, the fracture intensity for fractures < 1

m needs to be further corrected by multiplying by the fracture intensity for fractures > 1 m. This is equivalent to say that fracture intensity for both types of fractures increase in a constant ratio (instead of being independent as in units TSw34 and TSw36). The rest of the calculation proceeds as in the TSw34 and TSw365 cases by adding that fracture intensity due to fractures > 1 m (value read from Table 6-46 and coefficient of 1.232 read from Table 6-47).

Table 6-51. Summary of Fracture Intensity for Stochastic Sampling

	Accumulation
TSw34	1.726*"Table 6-46" + 2.616*"Table 6-48"
TSw35	1.232*"Table 6-46"+1.867*"Table 6-49"*"Table 6-46"
TSw36	1.817*"Table 6-46" + 2.753*"Table 6-48"

NOTE: "Table 6-46", "Table 6-48" and "Table 6-49" stand for the sampled table numbers. The coefficients are given in Table 6-47 and Table 6-50.

DEVELOPED DTN: MO0109SPAFIE10.006

6.9.9 Impact of Large Faults

The zone of influence of large faults is limited to a few meters, and number of fractures > 1 m does not increase in the vicinity of a large fault (Sweetkind et al. 1997, p. 67), but there might be an increase in the number of fractures < 1 m. In the TSw34 layer, faults do not have more than 1 or 2 m of influence. Likewise, the ECRB report (Mongano et al. 1999, pp. 51-65) concludes that faults have a minimal impact on fracturation. In addition, waste packages will be kept away from the immediate vicinity of the faults.

6.9.10 Review of "Field" Results

This section presents a review of "field" results. This section is untitled "field" results as opposed to extrapolated results presented in Section 6.9.8. It combines fracture intensity and orientation to yield the following results for the worst-case, 95% confidence interval case, and median case scenarios over 1 m^3 of each unit. It should be noted that the 95% confidence interval case represent the 95% confidence interval of each of the property (intensity, aperture and lithophysae abundance). Although those properties may be somewhat correlated, the correlation is not perfect (i.e., a high fracture intensity does not infer a high aperture or a high lithophysae abundance) and may even be negative. Thus the true probability of a case similar to the case untitled 95% confidence interval or worse is much less than 0.05 (it would be $0.05 \times 0.05 = 2.5 \times 10^{-3}$ for fracture intensity and aperture if they were independent and less if negatively correlated). Table 6-52 presents the source of the information used in this section.

Table 6-52. Summary of Final Results

	TSw34	TSw35	TSw36
Fracture Aperture	Interpolation of Table 6-11, Table 6-12 and Table 6-13	Interpolation of Table 6-11, Table 6-12 and Table 6-13	Interpolation of Table 6-11, Table 6-12 and Table 6-13
Fracture Orientation	Table 6-25 Column 3	Table 6-25 Column 5	Table 6-25 Column 6
Fracture Intensity	Table 6-44		
Fracture Porosity	= Fracture Aperture x Fracture Intensity		
Lithophysae Porosity	NA	Table 6-17 or file Lithophysae.xls / litho pro dist	NA

The worst case is defined as the maximum possible fracture intensity as defined in Table 6-44, the fracture aperture and lithophysae porosity being at 99.5% of the cumulative frequency distribution. The number of fractures is given by the fracture intensity. This assumes a composite fracture system (Assumption 5.2). Because of the downstream use of the results in criticality runs, the number of fractures has to be integer. The rounding is done by trying to keep the original proportion between the two sets of horizontal fractures. This is done sometimes by neglecting the horizontal set, by accepting a total number of fractures slightly higher or lower than the total presented in Table 6-44, or by not rounding to the closest integer.

- TSw34 has 18 vertical fractures in set 1, 9 vertical fractures in set 2, and 1 horizontal fracture as explained next. Column 1, row 8 of Table 6-44 =26.72~27 combined with column 3 of Table 6-25 that gives proportion of 10, 5 and 1 yields for the different sets 26.72x10/16=16.7~18 (see comment above), 26.72x5/16=8.35~9 and 26.72x1/16=1.67~1. All fractures have an aperture of 0.97 mm as explained next. This number is obtained by using results of Table 6-13. Table 6-13 yields 0.95 mm/0.93 mm and 0.99 mm/0.97 mm for 20/30 fractures for run1 and run2 respectively. The value of 0.99 mm was retained as representative for 26.72 fractures. The fracture porosity is then 2.7% (fracture intensity times average fracture aperture). There is no lithophysae. This case corresponds to the ECRB TSw34. If new developments suggest that the IFZ is more widespread than currently assumed, data from the ESF-IFZ TSw34 should be used.
- TSw35(1) has 13 vertical fractures in set 1, 4 vertical fractures in set 2, and 1 horizontal fracture as explained next. Column 3, row 8 of Table 6-44 =18.1~18 combined with column 5 of Table 6-25 that gives proportion of 7, 2 and 1 yields for the different sets 18.1x7/10=12.67~13, 18.1x2/10=3.62~4 and 18.1x1/10=1.81~1. All fractures have an aperture of 1.12 mm as explained next. Row 8, column 3 of Table 6-13 shows that the average aperture at 99.5% confidence is 1.30 mm for 10 fractures. Similarly, row 8, column 4 of Table 6-13 yields 1.08 mm for 20 fractures. Linear interpolation for 18.1 fractures between the couples (10, 1.30) and (20,1.08) yields (18.1, 1.12). The fracture porosity is 2.0% [18.1x(1.12×10^{-3} m^3) over 1 m^3 = 2.0%]. The lithophysae porosity is about 27% at 99.6% of the CDF (file Lithophysae.xls).
- TSw35(2) has 31 vertical fractures in set 1, 9 vertical fractures in set 2, and 3 horizontal fractures as explained next. Column 5, row 8 of Table 6-44 =43.75 combined with column 5 of Table 6-25 that gives proportion of 7, 2 and 1 yields for the different sets 43.75x7/10=30.6~31, 43.75x2/10=8.7~9 and 43.75x1/10=4.4~3. All fractures have an aperture of 0.94 mm as explained next. Row 8, column 6 of Table 6-13 shows that the average aperture at 99.5% confidence is 0.94 mm for 40 fractures. Similarly, row 8, column 7 of Table 6-13 yields 0.88 mm for 80 fractures. Linear interpolation for 43.75 fractures yields 0.94 mm. There are no lithophysae. The total porosity is 4.1% [43.75x(0.94×10^{-3} m^3) over 1 m^3 = 4.1%].
- TSw36 has 37 vertical fractures in set 1, 29 vertical fractures in set 2, and 7 horizontal fractures as explained next. Column 7, row 8 of Table 6-44 =73.15 combined with column 6 of Table 6-25 that gives proportion of 5, 4 and 1 yields for the different sets 73.15x5/10=36.6~37, 73.15x4/10=29.3~29 and 73.15x1/10=7.3~7. All fractures have an aperture of 0.89 mm as explained next. Row 8, column 6 of Table 6-13 shows that the average aperture at 99.5% confidence is 0.94 mm for 40 fractures. Similarly, row 8, column 7 of Table 6-13 yields 0.88 mm for 80 fractures. Linear interpolation for 73.22

fractures yields 0.89 mm. There are no lithophysae. The total porosity is 6.5% [73.15x(0.89x10^{-3} m^3) over 1 m^3 = 6.5%].

The case at 95% is defined with all the parameters at 95% on the cumulative frequency curve.

- TSw34 has 8 vertical fractures in set 1, 4 vertical fractures in set 2, and 1 horizontal fracture as explained next. Column 1, row 4 of Table 6-44 =13.36 combined with column 3 of Table 6-25 that gives proportion of 10, 5 and 1 yields for the different sets 13.36x10/16=8.3~8, 13.36x5/16=4.2~4 and 13.36x1/16=0.83~1. All fractures have an aperture of 0.92 mm as explained next. Row 4, column 3 of Table 6-13 shows that the average aperture at 95% confidence is 0.94/0.95 mm for 10 fractures. Similarly, row 4, column 5 of Table 6-13 yields 0.87/0.88 mm for 20 fractures. Linear interpolation for 13.36 fractures yields 0.92 mm. There are no lithophysae. The fracture porosity is 1.2% [13.36x(0.92x10^{-3} m^3) over 1 m^3 = 1.2%]. This case corresponds to the ECRB TSw34. If new developments suggest that the IFZ is more widespread than currently assumed, data from the ESF-IFZ TSw34 should be used.
- TSw35(1) has 8 vertical fractures in set 1, 3 vertical fractures in set 2, and 1 horizontal fracture as explained next. Column 3, row 4 of Table 6-44 =11.94 combined with column 5 of Table 6-25 that gives proportion of 7, 2 and 1 yields for the different sets 11.94x7/10=8.5~8, 11.94x2/10=2.4~3 and 11.94x1/10=1.2~1. All fractures have an aperture of 1.02 mm as explained next. Row 5, column 3 of Table 6-13 shows that the average aperture at 95% confidence is 1.04 mm for 10 fractures. Similarly, row 5, column 4 of Table 6-13 yields 0.94 mm for 20 fractures. Linear interpolation for 11.94 fractures between the couples (10, 1.04) and (20,0.94) yields (11.94, 1.02). The fracture porosity is 1.2% [11.94x(1.02x10^{-3} m^3) over 1 m^3 = 1.3%]. The lithophysae porosity is about 18% at 95% of the CDF (file Lithophysae.xls).
- TSw35(2) is not possible. Fracture intensity and lithophysae abundance are negatively correlated. The fracture intensity is now low enough to be consistent with presence of lithophysal cavities.
- TSw36 has 16 vertical fractures in set 1, 13 vertical fractures in set 2, and 3 horizontal fractures as explained next. Column 7, row 4 of Table 6-44 =31.35 combined with column 6 of Table 6-25 that gives proportion of 5, 4 and 1 yields for the different sets 31.35x5/10=15.7~16, 31.35x4/10=12.5~13 and 31.35x1/10=3.1~3. All fractures have an aperture of 0.88 mm as explained next. Row 5, column 5 of Table 6-13 shows that the average aperture at 95% confidence is 0.88 mm for 30 fractures. Similarly, row 5, column 6 of Table 6-13 yields 0.88 mm for 40 fractures. There are no lithophysae. The total porosity is 2.8% [31.35x(0.88x10^{-3} m^3) over 1 m^3 = 2.8%].

The median case is defined with all the parameters at 50% on the cumulative frequency curve.

- TSw34 has 3 vertical fractures in set 1, 2 vertical fractures in set 2, and 0 horizontal fracture as explained next. Interpolation of column 1, rows 1 and 2 of Table 6-44 =4.4 combined with column 3 of Table 6-25 that gives proportion of 10, 5 and 1 yields for the different sets 4.4x10/16=2.7~3, 4.4x5/16=1.4~2 and 4.4x1/16=0.3~0. All fractures have an aperture of 0.74 mm (median aperture, Table 6-12). There are no lithophysae. The fracture porosity is 0.4% [4.4x(0.74x10^{-3} m^3) over 1 m^3 = 0.33%]. This case corresponds to the ECRB TSw34. If new developments suggest that the IFZ is more widespread than currently assumed, data from the ESF-IFZ TSw34 should be used.

- TSw35(1) has 8 vertical fractures in set 1, 3 vertical fractures in set 2, and 1 horizontal fracture as explained next. These values are identical to the 95% confidence interval case (see Figure 6-28). All fractures have an aperture of 0.74 mm. The fracture porosity is 0.9% [12.12x(0.74x10^{-3} m^3) over 1 m^3 = 0.9%]. The lithophysae porosity is about 7.1% at 50% of the CDF (file Lithophysae.xls).
- TSw35(2) is not possible. Fracture intensity and lithophysae abundance are negatively correlated. The fracture intensity is now low enough to be consistent with presence of lithophysal cavities.
- TSw36 has 5 vertical fractures in set 1, 4 vertical fractures in set 2, and 1 horizontal fracture as explained next. Column 7, row 2 of Table 6-44 =10.45 (median fracture intensity is identical to the 81th percentile, see Figure 6-28) combined with column 6 of Table 6-25 that gives proportion of 5, 4 and 1 yields for the different sets 10.45x5/10=5.2~5, 10.45x4/10=4.2~4 and 10.45x1/10=1.05~1. All fractures have an aperture of 0.74 mm. There are no lithophysae. The total porosity is 0.8% [10.45x(0.74x10^{-3} m^3) over 1 m^3 = 0.8%].

A summary table (Table 7-1) is given in the Conclusions Section.

6.10 FRACTURE CONNECTIVITY

Fracture connectivity is an important parameter because it suggests how many fractures actinide-laden water can reach. This section will support the assumption of good fracture connectivity (Assumption 5.10). This concept must be clearly separated from the concept of number of active fractures in natural conditions. There are several ways of estimating connectivity. The simplest way is to compare average fracture length to average spacing. If the former is significantly larger than the latter, there are good chances that the network is well connected and that all the fractures can potentially accept actinide minerals. When active fractures are progressively sealed, if it happens at all, the flow switches to a nearby fracture and keeps doing so until the whole network is plugged.

Several pieces of information have already suggested that the connectivity of the network is good even at the meter scale (Bodvarsson et al. 1997, p. 7-26). Numerical simulations by Anna and data from two boreholes (Anna 1998, Table 4) suggest that only 30% to 35% of the fractures longer than 1.5 m are not connected to the network. Using geometric arguments, especially comparison of fracture spacing and fracture length, Sonnenthal et al. in Bodvarsson et al. 1997 (p. 7-25) claim that the network is well above its percolation threshold in the TSw34 unit of the ESF and likely to form a well-connected network geometrically (Table 6-53). More generally, Sweetkind and Williams-Stroud (1996 - p. 64) establish that the connectivity is high in welded units such as TSw34 to TSw36. On the other hand, computer simulations suggest that only 18% to 27% (Liu et al. 1998) of these connected fractures are active under ambient conditions. As such, it is legitimate to think that at the beginning of the flow domain of concern for criticality issues (bottom of the drift) either that all the fractures are contacted by dripping water are active or that the flow switches from fracture to fracture as they are progressively plugged.

Table 6-53. Connectivity of Fractures (station 27+20 to 34+93 - ESF)

Size Range (m)	Fraction of Total	Spacing (m)
0.3 - 1.0	0.534	0.473
1.0 - 3.0	0.353	0.714
3.0 - 5.0	0.074	3.388
5.0 - 10.0	0.036	7.055
10.0 - 34.0	0.012	20.86

Source: Bodvarsson et al. (1997, Table 7.17)

Table 6-54 also suggests that fractures longer than 1 m form a well-connected system in the ECRB.

Table 6-54. Connectivity of Fractures > 1m (ECRB - all units)

Unit	Average Fracture Length (m) (Table 6-29)	Average Fracture Spacing (m) (Table 6-37)
TSw33	2.40	1.30
TSw34	2.0 - 2. 4	0.23 - 0.30
TSw35	2.4 (3.28)[a]	1.36 - 1.73
TSw36	2.81	0.51

Source: Table 6-29 and Table 6-37.
NOTE: [a] ESF results done on a very short distance.

Table 6-55 to Table 6-57 establish that the whole fracture system is well-connected at any fracture size as the fracture spacing is always smaller than the average fracture length. Because the connectivity of the fracture system is good, every fracture is potentially available for mineral accumulation. Hence the fracture intensity results given in Section 6.9.7 do represent a realistic upper bound.

Table 6-55. Mean Spacing by Length Intervals for the TSw34 Unit (for a total of two SSS intervals)

Length Interval (m)	Number of Discontinuities	Average Length (arithmetic) (m)	Geometric Mean Spacing (m)	Range (±2) of spacing (m)	Source in File
0.0 - 0.1	48	0.074	0.066	0 - 1.0	Cells M5 to T5
0.1 - 0.2	54	0.15	0.10	0 - 0.9	Cells M54 toT54
0.2 - 0.3	24	0.24	0.23	0 - 2.6	Cells M109 toT109
0.3 - 0.4	15	0.35	0.36	0 - 3.9	Cells M134 toT134
0.4 - 0.5[d]	5	0.45	0.18	0 - 3.0	Cells M150 toT150
0.5 - 1.0[d]	12	0.72	0.29	0 - 3.4	Cells M156 toT156
> 1 m[a]	34		0.12	0 - 1.9	Cells M169 toT169
> 1 m[b]	28.6	2.16 (geometric)	0.30	0.03 - 3.05	
> 1 m[c]	31.3	2.23 (geometric)	0.27	0.03 - 2.94	

Sources: DTN: GS990908314224.009
FILE (Att. IV CD-ROM): **ECRB_smallfract_spacing.xls**; worksheet: mn all by size range
NOTES: [a] Over the same interval stationing.
[b] Averaged over the whole TSw34 exposure and scaled to 10 m (848 fractures > 1 m (over 427.24 m). TSw34 is visible for 4 meters and 6 meters in the SSS (only for fractures > 1 m & dip > 65).
[c] Averaged over the whole TSw34 exposure and scaled to 10 m (931 fractures > 1 m over 427.24 m). TSw34 is visible for 4 meters and 6 meters in the SSS (for all discontinuities > 1 m).
[d] Results subject to caution because of the limited number of fractures in this range

Table 6-56. Mean Spacing by Length Intervals for the TSw35 Unit (for a total of three 6-m intervals)

Length Interval (m)	Number of Discontinuities	Average Length (arithmetic) (m)	Geometric Mean Spacing (m)	Range (±2) of spacing (m)	Source in File
0.0 - 0.1	92	0.073	0.065	0 - 1	Cells M5 to T5
0.1 - 0.2	127	0.15	0.08	0 - 0.8	Cells M98 toT98
0.2 - 0.3	73	0.25	0.13	0 - 1.4	Cells M226 toT226
0.3 - 0.4	44	0.36	0.19	0 - 1.9	Cells M300 toT300
0.4 - 0.5	19	0.44	0.26	0 - 11.0	Cells M345 toT345
0.5 - 1.0[d]	9	0.61	0.87	0 - 13.6	Cells M365 toT365
> 1 m[a]	5				
> 1 m[b]	5.5	2.35 (geometric)	1.36	0.46 - 12	
> 1 m[c]	6.2	2.51 (geometric)	1.29	0.07 - 23.79	

Sources: DTN: GS990908314224.009
FILES (Att. IV CD-ROM): **ECRB_smallfract_spacing.xls**; worksheet: II all by size range

NOTES: [a] Over the same interval stationing - average was not computed because only two of the discontinuities are tectonic fractures.
[b] Averaged over the whole TSw35 exposure and scaled to 18 m (267 fractures > 1 m over 879.29 m) (only for fractures > 1 m & dip > 65).
[c] Averaged over the whole TSw35 exposure and scaled to 18 m (301 fractures > 1 m over 879.29 m) (for all discontinuities > 1 m).
[d] Results subject to caution because of the limited number of fractures in this range.

Table 6-57. Mean Spacing by Length Intervals for the TSw36 Unit (for a total of one 6-m interval)

Length Interval (m)	Number of Discontinuities	Average Length (arithmetic) (m)	Geometric Mean Spacing (m)	Range (±2) of spacing (m)	Source in File
0.0 - 0.1	17	0.076	0.16	0. - 2.0	Cells M5 to T5
0.1 - 0.2	33	0.15	0.09	0. - 1.2	Cells M23 toT23
0.2 - 0.3	30	0.25	0.11	0. - 1.0	Cells M57 toT57
0.3 - 0.4	12	0.35	0.17	0. - 6.6	Cells M88 toT88
0.4 - 0.5[c]	4	0.47	0.42	0. - 5.0	Cells M101 toT101
0.5 - 1.0	17	0.68	0.19	0. - 1.5	Cells M106 toT106
> 1 m	7		0.50	0.2 - 1.5	Cells M124 toT124
> 1 m[a]	5.1	2.81 (geometric)	0.51	0.03 - 9.13	
> 1 m[b]	5.6	2.63 (geometric)	0.46	0.02 - 8.16	

Sources: DTN: GS990908314224.009
FILE (Att. IV CD-ROM): **ECRB_smallfract_spacing.xls**; worksheet: In all by size range

NOTES: [a] Averaged over the whole TSw36 exposure and scaled to 6 m (178 fractures > 1 m over 210.75 m) (only for fractures > 1 m & dip > 65).
[b] Averaged over the whole TSw36 exposure and scaled to 6 m (198 fractures > 1 over 210.75 m) (for all discontinuities > 1 m).
[c] Results subject to caution because of the limited number of fractures in this range.

6.11 REPRESENTATION FOR ACTINIDE ACCUMULATION IN LITHOPHYSAE

The preceding sections described the geometry of the lithophysae and fracture system in a static fashion. This section will provide elements to understand how much actinide or other mineral can actually accumulate within the open spaces of the rock. It is assumed that all the fractures are susceptible to complete plugging (see Section 6.10). The conceptual representation of accumulation in the lithophysae assumes that accumulation can proceed as long as some of the feeding fractures are open. The mineral accumulation thickness in the lithophysal cavities can be less than, equal to, or more than in the adjacent fractures. The maximum accumulation in a lithophysal cavity is also a function of the number of fractures connected to it. This representation assumes that calcite and opal are surrogates for actinide precipitation. This is probably true for calcic uranium minerals such as uranophane, boltwoodite and haiweeite, but much less for plutonium minerals that are oxides.

6.11.1 Comparison of Calcite Accumulation in Fractures and Lithophysae

There are some systematic quantitative measurements of secondary mineral infilling thickness (DTNs: GS980308315215.008 by the United States Geological Survey and GS990408314224.001/.002 by the United States Bureau of Reclamation). There are no available data on the secondary mineral thickness in the ECRB lithophysae. Most of the information comes from the ESF, in particular the upper lithophysal unit (TSw33), which has a higher lithophysal porosity than the TSw35 unit. It is assumed valid for this study (Assumption 5.11). Figure 6-31 and Figure 6-32 show that calcite is more abundant in this unit. Both figures also show that the secondary mineral thickness is similar in the ECRB and the ESF. Figure 6-32 suggests that lithophysae have on average a larger secondary mineral thickness than fractures.

In general, the calcite thickness increases with the lithophysal size as displayed in Figure 6-33. The correlation coefficient between lithophysal size and calcite thickness is about 0.4. Some large lithophysae have little calcite, but there are no small lithophysae with thick calcite accumulation. This observation supports the representation of relating accumulation thickness and number of fractures connected to the lithophysal cavity.

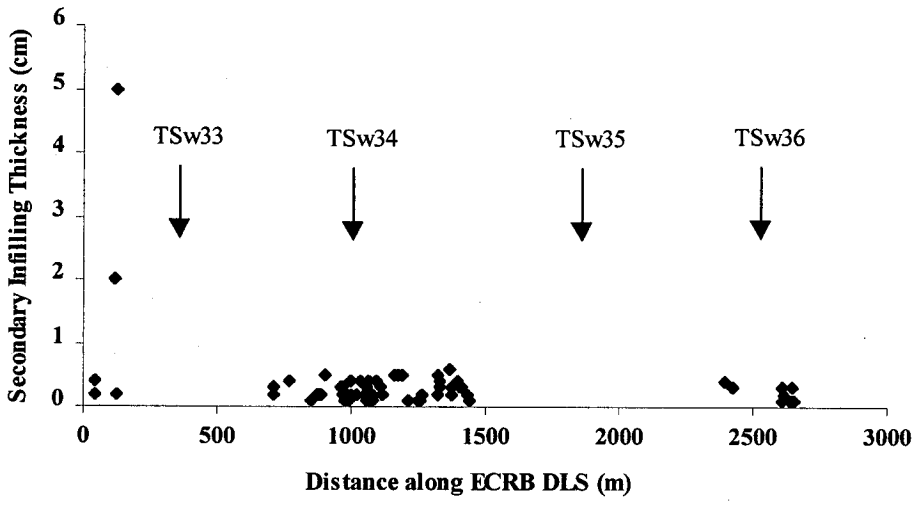

Sources: DTN: GS990408314224.001, GS990408314224.002
FILE (Att. IV CD-ROM): **FractureMineral_ECRB.xls;** worksheet "sheet1"

Figure 6-31. Secondary Mineral Thickness in Fractures of the ECRB

Figure 6-34) tries to relate accumulation thickness in a lithophysal cavity and in a fracture nearby and reveals that a reasonable bounding value for the thickness ratio is 10. We thus conservatively assume that a fracture can feed about 10 times its aperture to the total accumulation thickness of a lithophysal cavity. An alternative representation would be to assume a loguniform distribution between 1 and 10 as suggested by Figure 6-34. However, data are still too sketchy to support this less conservative representation. In any case, this observation supports that the representation should include the fact that accumulation thickness in the cavities is larger than in the fractures.

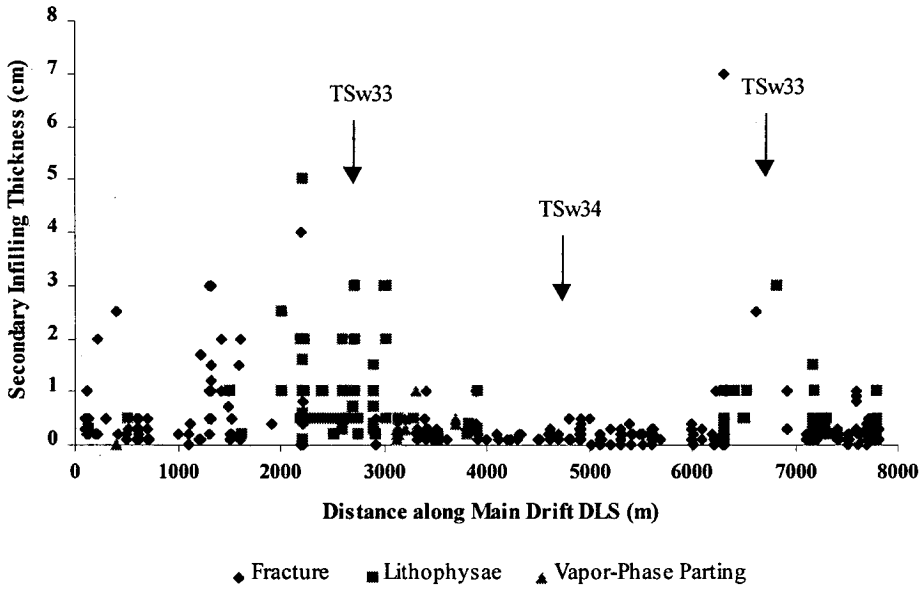

Sources: DTN: GS980308315215.008
FILE (Att. IV CD-ROM): **FractureMineral_ESF.xls**; worksheet "plot all"

Figure 6-32. Secondary Mineral Thickness in Openings of the ESF

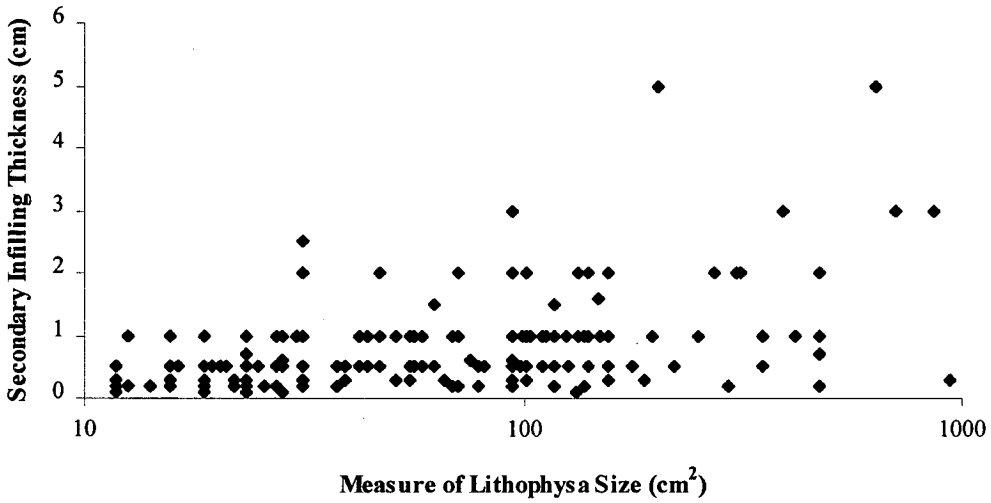

Sources: DTN: GS980308315215.008
FILE (Att. IV CD-ROM): **FractureMineral_ESF.xls**; worksheet "all L."
NOTE: The data points include all the lithophysal units from TSw34 up to the top of the North Ramp.

Figure 6-33. Secondary Infilling Thickness vs. Lithophysae Size

Another result supporting the same ratio of 10 is that only $1/10^{th}$ of the number of fractures with calcite in the TSw34 non-lithophysal unit has calcite in the lower lithophysal unit. Assuming that the precipitation mechanism is the same in both units, most of the calcite is precipitated in the lithophysae of the lithophysal unit. Figure 6-35 suggests that the feeding fractures are mainly vertical but also that horizontal fractures weight more than their fraction of the total number of fractures.

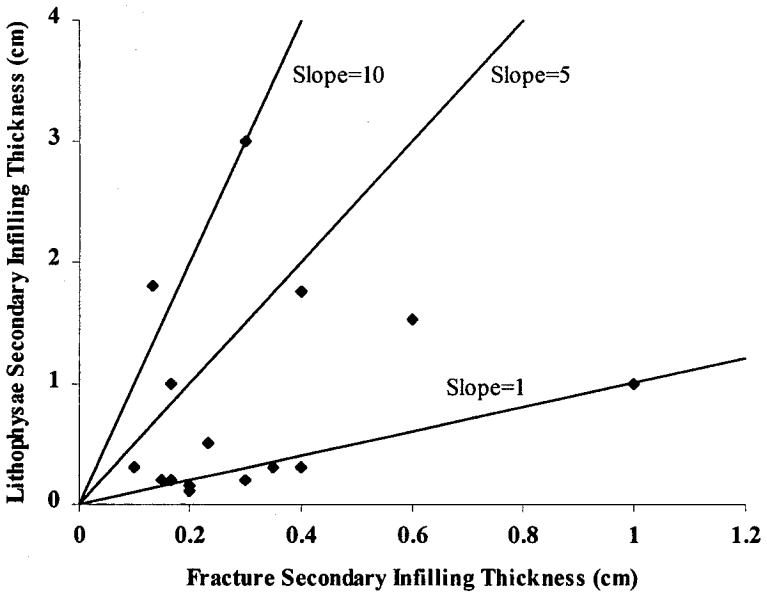

Sources: DTN: GS980308315215.008
FILE (Att. IV CD-ROM): **FractureMineral_ESF.xls**; worksheet "comp fract L."
NOTE: The data points include all the lithophysal units from TSw34 up to top of the the North Ramp.

Figure 6-34. Comparison between Secondary Mineral Infilling Thickness of a Lithophysae and of a Nearby Fracture

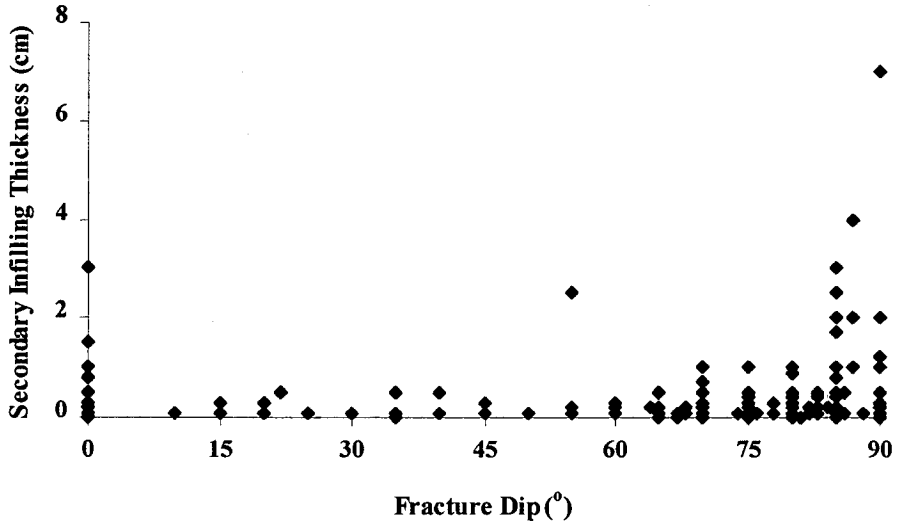

Sources: DTN: GS980308315215.008
FILE (Att. IV CD-ROM): **FractureMineral_ESF.xls**; worksheet "all fracture"
NOTE: The data points include all the lithophysal units from TSw34 up to the top of the North Ramp

Figure 6-35. Secondary Mineral Infilling Thickness as a Function of the Fracture Dip

6.11.2 Accumulation Mechanism in the Lithophysae

The type of flow through lithophysae can be estimated from observations from exposed lithophysae. Speleothems, such as dripstones, stalagmites, or stalactites, have never been observed in the ESF (Marshall et al. 1999, p. 2). It can be concluded that the flow through the lithophysae is always along the lithophysae walls and that there is no dripping. This means that a lithophysae is unlikely to become plugged at the bottom before it is plugged at the top. Marshall et al. 2000, pp. 4 and 5 suggest several chemical mechanisms for calcite and opal precipitation, but little is known to that respect.

6.11.3 Results of the Lithophysae Representation

Table 6-58 presents results for a range of lithophysae diameters. It is assumed that the number of fractures connected to the lithophysal cavity is given by the fracture spacing given by the CDF at this location. The average fracture aperture is given by Table 6-13. The average accumulation thickness is 10 times the product of the number of fractures to the average fracture aperture. These numbers do not take into account a possible limited supply of actinides in the waste packages. If the case of only one waste package is considered, only the amount physically available should be allowed to accumulate.

Table 6-58. Accumulation Thickness on the Lithophysal Cavity Walls

Lithophysal Cavity Diameter (m)		Worst Case	95th Percentile	Median
1	# of fractures[a]	18.1 (row 8, column 3)	12.12 (row 4, column 3)	12.12 (row 3, column 3)
	Average Fracture Aperture (mm)[b]	1.12 (row 8, columns 3 and 4)	0.95 (row 5, columns 3 and 4)	0.74 (median aperture)
	Average Accumulation Thickness (cm)[c]	*21.3*	*11.7*	*8.3*
0.5	# of fractures[a]	8.5	6	6
	Average Fracture Aperture (mm)[b]	1.37 (row 8, columns 2 and 3)	1.15 (row 5, columns 2 and 3)	0.74 (median aperture)
	Average Accumulation Thickness (cm)[c]	*11.4*	*6.9*	*5.0*
0.25	# of fractures[a]	4.25	3	3
	Average Fracture Aperture (mm)[b]	1.96 (row 8, columns 1 and 2)	1.65 (row 5, columns 1 and 2)	0.74 (median aperture)
	Average Accumulation Thickness (cm)[c]	*8.9*	*4.5*	*2.2*

NOTES: [a] Row and line given in Table 6-44. For 0.5-m and 0.25-m diameter cases, the 1-m diameter case is divided by 2 and 4, respectively.

[b] interpolated from Table 6-13. The highest value of the 2 runs is retained. Worst case interpolation for 1-m diameter lithophysal cavity is detailed below. Row 8, column 3 shows that the average aperture at 99.5% confidence is 1.30 mm for 10 fractures. Similarly, row 8, column 4 yields 1.08 mm for 20 fractures. Linear interpolation for 18.1 fractures between the couples (10, 1.30) and (20,1.08) yields (18.1, 1.12).

[c] average accumulation thickness is 10 times the product of the number of fractures and the average fracture aperture

7. CONCLUSIONS

This document may be affected by technical product input infomation that requires confirmation. Any changes to the document that may occur as a result of completing the confirmation activities will be reflected in subsequent revisions. The status of the technical product input information quality may be confirmed by review of the DIRS database.

7.1 SUMMARY OF RESULTS ON FRACTURE AND LITHOPHYSAL POROSITY

7.1.1 Fracture Aperture

Pneumatic and tracer tests give two different types of fracture apertures. The mean hydraulic fracture aperture given by pneumatic tests is the range of 0.1 to 0.2 mm (Table 6-6) while the mean solute transport aperture given by tracer test is 0.75 mm (Table 6-11). The solute transport aperture follows a lognormal distribution and is approximately at 2 mm at two standard deviations. The appropriate aperture to use for external accumulation is the solute transport aperture.

7.1.2 Lithophysae

The main repository unit (TSw35) contains numerous approximately spherical cavities of variable size (mm to m). They create an additional porosity to the rock. The average lithophysae porosity is 8.5% (Table 6-15) but it can be locally in the order of 30%. The size of the lithophysal cavities is only weakly correlated to their total porosity. The size geometric average is 18.5 cm (Table 6-15) but there is approximately an average of one lithophysae larger than 1 m in diameter in a WP length. A simple representation for accumulation in lithophysae was developed. The accumulation thickness can be as high as 20 cm in a 1m-diameter lithophysae (Table 6-58).

7.1.3 Fracture Frequency and Intensity

DLSs along drift walls record many parameters including fracture orientation, length and spacing. Most of the DLS record information only for fractures longer than 1 meter. However, small fractures cannot be neglected when the total volume open to accumulation is of interest because the connectivity of the network is good (Section 6.10) and because small fractures are abundant (Section 6.9.6). Scaling factors that take into account small fractures and correction factors that take into account measurement biases were derived. The end result is distribution functions for the fracture intensity of the different units. Fracture intensity is more relevant than fracture frequency for accumulation because it provides the fracture volume in a unit rock volume.

Table 7-1 provides the results directly applicable to criticality calculations with the assumption of either vertical or horizontal fractures (Assumption 5.2). Those results are not intended for direct use in flow computer codes. Flow code fracture parameters are fitted to field results at the different scales considered in the project. On the other hand, the results of this AMR rely mainly on static observations in tunnels. They do represent an upper bound of space open to actinide accumulation.

Table 7-1. Review of Scaled Field Results

Case	Parameter	TSw34	TSw35(1)	TSw35(2)	TSw36
Worst	Fracture Intensity (Set1 - Set2 - Hor.)	18 - 9- 1	13 - 4 -1	31 - 9 - 3	37 - 29 - 7
	Average Fracture Aperture (mm)	0.99	1.12	0.94	0.89
	Fracture Porosity (%)	2.7	2.0	4.1	6.5
	Lithophysae Porosity (%)	N/A	27	N/A	N/A
95th perc.	Fracture Intensity (Set1 - Set2 - Hor.)	8 - 4 - 1	8 - 3 - 1	N/A	16 - 13 - 3
	Average Fracture Aperture (mm)	0.92	1.02	N/A	0.88
	Fracture Porosity (%)	1.2	1.2	N/A	2.8
	Lithophysae Porosity (%)	N/A	18	N/A	N/A
Median	Fracture Intensity (Set1 - Set2 - Hor.)	3 - 2 - 0	8 - 3 - 1	N/A	5 - 4 - 1
	Average Fracture Aperture (mm)	0.74	0.74	N/A	0.74
	Fracture Porosity (%)	0.4	0.9	N/A	0.8
	Lithophysae Porosity (%)	N/A	7.1	N/A	N/A

NOTE: from Section 6.9.10
DEVELOPED DTN: MO0109SPAFIE10.006

Because typical fracture intensities, even at the 99.5th percentile, do not typically generate high enough fracture volume to reach nuclear criticality, CDFs for high fracture intensity were developed (Section 6.9.8). Table 7-2 displays an example for fractures >1 m.

Table 7-2. CCDF of the Average Number of Fracture (>1 m) / m

Fracture Frequency for Fracture >1 m	Unit TSw34	Unit TSw35	Unit TSw36
1	5.781E-01	2.344E-01	1.874E-01
2	3.324E-01	4.807E-02	9.490E-02
3	1.469E-01	1.650E-02	4.982E-02
4	4.623E-02	3.697E-03	1.305E-02
5	1.638E-02	1.138E-03	7.117E-03
6	4.096E-03	*2.649E-04*	1.186E-03
7	2.320E-03	*6.837E-05*	*9.040E-04*
8	*1.014E-03*	*1.764E-05*	*3.485E-04*
9	*4.436E-04*	*4.553E-06*	*1.343E-04*
10	*1.940E-04*	*1.175E-06*	*5.178E-05*
11	*8.482E-05*	*3.032E-07*	*1.996E-05*

NOTE: Copied from Table 6-46
DEVELOPED DTN: MO0109SPAFIE10.006

Another important result is that fracture spacing is not spatially correlated (Section 6.9.3) and that high fracture intensity cannot be sustained for long.

It should be noted that there are some inconsistencies that cannot be resolved at this point. The fracture aperture is calculated using only fracture > 0.3 m while the fracture intensity uses all fractures.

7.2 UNCERTAINTY ASSESSMENT

There are two main sources of uncertainty in this document: fracture porosity and scaling of the small-scale survey. The fracture space open to accumulation is directly related to the fracture porosity. Tracer tests give the most accurate results for porosity but they have been performed in limited locations in the TSw34 unit that makes only ~10% of the repository. A more extensive

tracer test campaign in the TSw35 unit is likely to modify the results. The Small Scale Survey in the TSw35 unit results have also an important impact on the final results because they are used to scale the extensive results for fractures > 1 m to the fracture intensity that includes all fractures. The Small Scale Survey has been performed on a limited drift length. Any additional measurement campaign is likely to change the results of this AMR. Although lithophysae characteristics are better known qualitatively rather than quantitatively, any additional data is unlikely to change the results of this document. Similarly a change in the fracture hydraulic parameters will impact flow results but not the space open to accumulation.

7.3 OUPUT DTNS

The following DTNs have been developed in this document:

MO0102SPAFRA01.002: Fracture intensity for external actinide accumulation (superseded).

MO0109SPAFIE10.006: Fracture intensity for external actinide accumulation.

MO0102SPALIT10.001: Lithophysae porosity and diameter distributions.

8. INPUTS AND REFERENCES

8.1 DOCUMENTS CITED

Albin, A.L.; Singleton, W.L.; Moyer, T.C.; Lee, A.C.; Lung, R.C.; Eatman, G.L.W.; and Barr, D.L. 1997. *Geology of the Main Drift - Station 28+00 to 55+00, Exploratory Studies Facility, Yucca Mountain Project, Yucca Mountain, Nevada.* Milestone SPG42AM3. Denver, Colorado: Bureau of Reclamation and U.S. Geological Survey. ACC: MOL.19970625.0096.

Anna, L.O. 1998. *Preliminary Three-Dimensional Discrete Fracture Model of the Topopah Spring Tuff in the Exploratory Studies Facility, Yucca Mountain Area, Nye County, Nevada.* Open-File Report 97-834. Denver, Colorado: U.S. Geological Survey. TIC: 236829.

Barr, D.L.; Moyer, T.C.; Singleton, W.L.; Albin, A.L.; Lung, R.C.; Lee, A.C.; Beason, S.C.; and Eatman, G.L.W. 1996. *Geology of the North Ramp — Stations 4+00 to 28+00, Exploratory Studies Facility, Yucca Mountain Project, Yucca Mountain, Nevada.* Denver, Colorado: U.S. Geological Survey. ACC: MOL.19970106.0496.

Bear, J. 1988. *Dynamics of Fluids in Porous Media.* New York, New York: Dover Publications. TIC: 217568.

Bear, J.; Tsang, C.F.; and de Marsily, G., eds. 1993. *Flow and Contaminant Transport in Fractured Rock.* San Diego, California: Academic Press. TIC: 235461.

Bodvarsson, G.S.; Bandurraga, T.M.; and Wu, Y.S., eds. 1997. *The Site-Scale Unsaturated Zone Model of Yucca Mountain, Nevada, for the Viability Assessment.* LBNL-40376. Berkeley, California: Lawrence Berkeley National Laboratory. ACC: MOL.19971014.0232.

BSC (Bechtel SAIC Company) 2001a. *Software Code: Add_Fracture.* V1.0. PC Windows98. 10498-1.0-00.

BSC 2001b. *Technical Work Plan for: Waste Package Design Description for LA.* TWP-EBS-MD-000004 REV01. Las Vegas, Nevada: Bechtel SAIC Company. ACC: MOL.20010702.0152.

BSC 2001c. *Site Recommendation Subsurface Layout.* ANL-SFS-MG-000001 REV 00 ICN 02. Las Vegas, Nevada: Bechtel SAIC Company. ACC: MOL.20010411.0131.

BSC 2001d. *Drift-Scale Coupled Processes (DST and THC Seepage) Models.* MDL-NBS-HS-000001 REV 01 ICN 01. Las Vegas, Nevada: Bechtel SAIC Company. ACC: MOL.20010418.0010.

Carlos, B.A.; Chipera, S.J.; and Bish, D.L. 1995. *Distribution and Chemistry of Fracture-Lining Minerals at Yucca Mountain, Nevada.* LA-12977-MS. Los Alamos, New Mexico: Los Alamos National Laboratory. ACC: MOL.19960306.0564.

CRWMS M&O 1998. "Unsaturated Zone Hydrology Model." Chapter 2 of *Total System Performance Assessment-Viability Assessment (TSPA-VA) Analyses Technical Basis Document.* B00000000-01717-4301-00002 REV 01. Las Vegas, Nevada: CRWMS M&O. ACC: MOL.19981008.0002.

CRWMS M&O 2000a. *Calculation of Permeability Change Due to Coupled Thermal-Hydrological-Mechanical Effects*. CAL-NBS-MD-000002 REV 00. Las Vegas, Nevada: CRWMS M&O. ACC: MOL.20000711.0192.

CRWMS M&O 2000b. *Drift Degradation Analysis.* ANL-EBS-MD-000027 REV 01. Las Vegas, Nevada: CRWMS M&O. ACC: MOL.20001206.0006.

CRWMS M&O 2000c. *Fault Displacement Effects on Transport in the Unsaturated Zone.* ANL-NBS-HS-000020 REV 01. Las Vegas, Nevada: CRWMS M&O. ACC: MOL.20001002.0154.

CRWMS M&O 2000d. *Particle Tracking Model and Abstraction of Transport Processes*. ANL-NBS-HS-000026 REV 00. Las Vegas, Nevada: CRWMS M&O. ACC: MOL.20000502.0237.

CRWMS M&O 2000e. *Rock Properties Model Analysis Model Report.* MDL-NBS-GS-000004 REV 00 ICN 02. Las Vegas, Nevada: CRWMS M&O. ACC: MOL.20010216.0001.

Curry, P.M. 2001. *Monitored Geologic Repository Project Description Document.* TDR-MGR-SE-000004 REV 02 ICN 02. Las Vegas, Nevada: Bechtel SAIC Company. ACC: MOL.20010628.0224.

Dershowitz, W.S. and Herda, H.H. 1992. "Interpretation of Fracture Spacing and Intensity." *Rock Mechanics, Proceedings of the 33rd U.S. Symposium, Santa Fe, New Mexico, 3-5 June, 1992*. Tillerson, J.R. and Wawersik, W.R., eds. 757-766. Rotterdam, The Netherlands: A.A. Balkema. TIC: 245647.

DOE (U.S. Department of Energy) 2000. *Quality Assurance Requirements and Description.* DOE/RW-0333P, Rev. 10. Washington, D.C.: U.S. Department of Energy, Office of Civilian Radioactive Waste Management. ACC: MOL.20000427.0422.

Domenico, P.A. and Schwartz, F.W. 1990. *Physical and Chemical Hydrogeology*. New York, New York: John Wiley & Sons. TIC: 234782.

Eatman, G.L.W.; Singleton, W.L.; Moyer, T.C.; Barr, D.L.; Albin, A.L.; Lung, R.C.; and Beason, S.C. 1997. *Geology of the South Ramp - Station 55+00 to 78+77, Exploratory Studies Facility, Yucca Mountain Project, Yucca Mountain, Nevada*. Milestone SPG42CM3. Denver, Colorado: U.S. Geological Survey. ACC: MOL.19980216.0328.

Gelhar, L.W. 1993. *Stochastic Subsurface Hydrology*. Englewood Cliffs, New Jersey: Prentice-Hall. TIC: 240652.

Lawrence Berkeley National Laboratory 1999. *Software Code: GSLIB V1.0 MGAMV2V1.201*. V1.0. Sun. 10087-1.0MGAMV2V1.201-00.

Liu, H.H.; Doughty, C.; and Bodvarsson, G.S. 1998. "An Active Fracture Model for Unsaturated Flow and Transport in Fractured Rocks." *Water Resources Research, 34*, (10), 2633-2646. Washington, D.C.: American Geophysical Union. TIC: 243012.

Maidment, D.R., ed. 1993. *Handbook of Hydrology.* New York, New York: McGraw-Hill. TIC: 236568.

Marshall, B.D.; Neymark, L.A.; Paces, J.B.; Peterman Z.E.; and Whelan, J.F. 1999. "Seepage Flux Conceptualized from Secondary Calcite in Lithophysal Cavities in the Topopah Spring Tuff, Yucca Mountain, Nevada." *Eos, Transactions (Supplement), 80*, (17), [S5]. Washington, D.C.: American Geophysical Union. TIC: 246466.

Marshall, B.D.; Neymark, L.A.; Paces, J.B.; Peterman, Z.E.; and Whelan, J.F. 2000. "Seepage Flux Conceptualized from Secondary Calcite in Lithophysal Cavities in the Topopah Spring Tuff, Yucca Mountain, Nevada." *SME Annual Meeting, February 28-March 1, 2000, Salt Lake City, Utah.* Preprint 00-12. [Littleton, Colorado]: Society for Mining, Metallurgy, and Exploration. TIC: 248608.

Mongano, G.S.; Singleton, W.L.; Moyer, T.C.; Beason, S.C.; Eatman, G.L.W.; Albin, A.L.; and Lung, R.C. 1999. *Geology of the ECRB Cross Drift - Exploratory Studies Facility, Yucca Mountain Project, Yucca Mountain, Nevada.* [Deliverable SPG42GM3]. Denver, Colorado: U.S. Geological Survey. ACC: MOL.20000324.0614.

Moscati, R.J. and Whelan, J.F. 1996. *Origins of Secondary Silica Within Yucca Mountain, Nye County, Southwestern Nevada.* Open-File Report 95-289. Denver, Colorado: U.S. Geological Survey. TIC: 225888.

Sweetkind, D.S. and Williams-Stroud, S.C. 1996. *Characteristics of Fractures at Yucca Mountain, Nevada: Synthesis Report.* Administrative Report. Denver, Colorado: U.S. Geological Survey. ACC: MOL.19961213.0181.

Sweetkind, D.S.; Barr, D.L.; Polacsek, D.K.; and Anna, L.O. 1997. *Administrative Report: Integrated Fracture Data in Support of Process Models, Yucca Mountain, Nevada.* Milestone SPG32M3. [Las Vegas, Nevada]: U.S. Geological Survey. ACC: MOL.19971017.0726.

Tsang, Y.W. 1992. "Usage of "Equivalent Apertures" for Rock Fractures as Derived from Hydraulic and Tracer Tests." *Water Resources Research, 28*, (5), 1451-1455. Washington, D.C.: American Geophysical Union. TIC: 245891.

8.2 INPUT DATA LISTED BY DATA TRACKING NUMBER

GS000608314224.004. Provisional Results: Geotechnical Data for Station 35+00 to Station 40+00, Main Drift of the ESF. Submittal date: 06/20/2000.

GS960708314224.008. Provisional Results: Geotechnical Data for Station 30 + 00 to Station 35 + 00, Main Drift of the ESF. Submittal date: 08/05/1996.

GS960708314224.010. Provisional Results: Geotechnical Data for Station 40+00 to Station 45+00, Main Drift of the ESF. Submittal date: 08/05/1996.

GS960808314224.011. Provisional Results: Geotechnical Data for Station 35+00 to Station 40+00, Main Drift of the ESF. Submittal date: 08/29/1996.

GS960908314224.014. Provisional Results - ESF Main Drift, Station 50+00 to Station 55+00. Submittal date: 09/09/1996.

GS971108314224.024. Revision 1 of Detailed Line Survey Data, Station 18+00 to Station 26+00, North Ramp, Exploratory Studies Facility. Submittal date: 12/03/1997.

GS971108314224.025. Revision 1 of Detailed Line Survey Data, Station 26+00 to Station 30+00, North Ramp and Main Drift, Exploratory Studies Facility. Submittal date: 12/03/1997.

GS971108314224.026. Revision 1 of Detailed Line Survey Data, Station 45+00 to Station 50+00, Main Drift, Exploratory Studies Facility. Submittal date: 12/03/1997.

GS971108314224.028. Revision 1 of Detailed Line Survey Data, Station 55+00 to Station 60+00, Main Drift and South Ramp, Exploratory Studies Facility. Submittal date: 12/03/1997.

GS980308315215.008. Line Survey Information from the Exploratory Studies Facility Obtained to Estimate Secondary Mineral Abundance. Submittal date: 03/24/1998.

GS990408314224.001. Detailed Line Survey Data for Stations 00+00.89 to 14+95.18, ECRB Cross Drift. Submittal date: 09/09/1999.

GS990408314224.002. Detailed Line Survey Data for Stations 15+00.85 to 26+63.85, ECRB Cross Drift. Submittal date: 09/09/1999.

GS990408314224.003. Full-Periphery Geologic Maps for Station -0+10 to 10+00, ECRB Cross Drift. Submittal date: 09/09/1999.

GS990408314224.004. Full-Periphery Geologic Maps for Station 10+00 to 15+00, ECRB Cross Drift. Submittal date: 09/09/1999.

GS990408314224.005. Full-Periphery Geologic Maps for Station 15+00 to 20+00, ECRB Cross Drift. Submittal date: 09/09/1999.

GS990408314224.006. Full-Periphery Geologic Maps for Station 20+00 to 26+81, ECRB Cross Drift. Submittal date: 09/09/1999.

GS990908314224.009. Detailed Line Survey Data for Horizontal and Vertical Traverses, ECRB. Submittal date: 09/16/1999.

GS991108314224.015. Geology of the ECRB Cross Drift: Tabular Data. Submittal date: 11/05/1999.

LB971212001254.001. DKM Basecase Parameter Set for UZ Model with Mean Fracture Alpha, Present Day Infiltration, and Estimated Welded, Non-Welded and Zeolitic FMX. Submittal date: 12/12/1997.

LB980912332245.002. Gas Tracer Data from Niche 3107 of the ESF. Submittal date: 09/30/1998.

LB990501233129.001. Fracture Properties for the UZ Model Grids and Uncalibrated Fracture and Matrix Properties for the UZ Model Layers for AMR U0090, "Analysis of Hydrologic Properties Data". Submittal date: 08/25/1999.

LB997141233129.001. Calibrated Basecase Infiltration 1-D Parameter Set for the UZ Flow and Transport Model, FY99. Submittal date: 07/21/1999.

8.3 OUTPUT DATA LISTED BY DATA TRACKING NUMBER

MO0102SPAFRA01.002. Fracture intensity for external actinide accumulation. Submittal date: 02/20/2001.

MO0109SPAFIE10.006. Fracture intensity for external actinide accumulation. Submittal date: 09/17/2001.

MO0102SPALIT10.001. Lithophysae porosity and diameter distributions. Submittal date: 02/20/201.

8.4 CODES, STANDARDS, REGULATIONS, AND PROCEDURES

AP-2.21Q, Rev. 1, BSCN 1, *Quality Determinations and Planning for Scientific, Engineering, and Regulatory Compliance Activities*. Washington, D.C.: U.S. Department of Energy, Office of Civilian Radioactive Waste Management. ACC: MOL.20010212.0018.

AP-3.10Q, Rev. 2, ICN 4, ECN 1. *Analyses and Models*. Washington, D.C.: U.S. Department of Energy, Office of Civilian Radioactive Waste Management. ACC: MOL.20010827.0114.

AP-3.15Q, Rev. 3. *Managing Technical Product Inputs*. Washington, D.C.: U.S. Department of Energy, Office of Civilian Radioactive Waste Management. ACC: MOL.20010801.0318.

AP-SI.1Q, Rev. 3, ICN 1, ECN 1. *Software Management.* Washington, D.C.: U.S. Department of Energy, Office of Civilian Radioactive Waste Management. ACC: MOL.20010705.0239.

AP-SIII.3.Q Rev. 1, *Submittal and Incorporation of Data to the Technical Data Management System.* Washington, D.C.: U.S. Department of Energy, Office of Civilian Radioactive Waste Management. ACC: MOL.20010801.0314.

ATTACHMENT I

COMPARISON OF SUPERSEDED DTN: MO0102SPAFRA01.002 AND DTN: MO0109SPAFIE10.006

(1 page)

In the course of the final review of the document, several minor mistakes and typos were revealed. This attchment details the differences between the initial superseded DTN and the final DTN. Boths DTNs are presented in 10 Microsoft Excel worksheets in Table I - 1.

Table I - 1. Comparison of DTNs

Worksheet	Comments
Transport Aperture	No difference
ECRB-ESF Fracture Orientation	No difference
ECRB Fracture > 1m spacing	No difference
Fracture > 1m spacing PLOT	No difference
ECRB SSS Fracture spacing	No difference
ECRB SSS Fracture spacing PLOT	No difference
ECRB SSS fracture intensity	Minor differences encountered (< 1.5%)
ECRB SSS fracture intensity PLO	Minor differences encountered (< 1.5%)
Extrapolation	No difference
Porosity	Some differences encountered

SOURCE: File (Att. IV CD-ROM): DTN_Comparison.xls

The worksheet "Porosity" contains slightly different values for fracture aperture and fracture porosity. Those values are not directly used in criticality calculations because they do not lead to the high density of accumulation needed for criticality. Extrapolations to very high values (see Section 6.9.8) are needed for criticality. They are presented in the worksheet "Extrapolation".

ATTACHMENT II

ACRONYMS

(1 page)

AMR	Analysis and Model Report
ATDT	Automated Technical Data Tracking System
BSC	BECHTEL SAIC Company
CCDF	Complementary Cumulative Distribution Function
CDF	Cumulative Distribution Function
CD-ROM	Compact Disc - Read-Only Memory
CRWMS	Civilian Radioactive Waste Management System
DIRS	Document Input Reference System
DLS	Detailed Line Survey
DTN	Data Tracking Number
ECRB	Enhanced Characterization of the Repository Block
ESF	Exploratory Studies Facility
EW	East West
FPGM	Full Periphery Geology Maps
FSU	Fracture SubUnit
IFZ	Intensely Fractured Zone
M&O	Management and Operating Contractor
N/A	Not Applicable
NS	North South
OCRWM	Office of Civilian Radioactive Waste Management
QA	Quality Assurance
SSS	Small-Scale Survey
VPM	Vapor Phase Minerals

ATTACHMENT III

FILES ON ELECTRONIC MEDIA (CD-ROM)

(3 pages)

All the input, output, and pre- and post-processing files relative to this calculation have been copied to a CD-ROM. Details about the organization of the CD-ROM and a list of files follow.

The files are organized into five sections:

File Name	Size (Bytes)	Date	Time
Complement_to_ECRB_smallfract_spacing.xls	380,928	8/28/01	5:27p
Complement_to_ESF26-60.xls	6,370,816	8/28/01	5:10p
DTN_Comparison.xls	5,016,576	8/28/01	10:36a
FractureIntensityNew.xls	126,464	8/29/01	11:38a
fractureMineral_ECRB.xls	211,456	8/29/01	11:08a
fractureMineral_ESF.xls	457,216	8/29/01	11:06a
Lithophysae.xls	204,800	8/29/01	10:04a
Niche3107_Alcove5_forporosity.xls	56,832	8/28/01	12:10p
Percentage_SSS.xls	52,224	8/29/01	9:57a
Directory of ECRB_Fracture _Spacing			
allHorVert.xls	753,152	4/12/01	9:29a
allHorVert_unchanged.xls	767,488	4/12/01	9:28a
CDF_Fracturespacing&intensity.xls	696,832	7/27/01	11:26p
ECRB_study_TSw36.xls	1,576,960	4/11/01	2:27p
ECRB_study_TSw35.xls	4,307,968	4/11/01	3:45p
ECRB.xls	1,141,248	4/11/01	12:57p
ECRB_smallfract_spacing.xls	2,351,104	8/29/01	9:52a
ECRB_spacing.xls	664,064	4/11/01	4:53p
ECRB_study_TSw33.xls	1,637,888	4/11/01	4:34p
ECRB_study_TSw34.xls	3,883,008	4/11/01	3:50p
Directory of ESF_Fracture_Spacing			
ESF26-60.xls	5,881,856	4/11/01	3:50p
ESF26-60_all.xls	3,641,856	4/11/01	11:43a
ESF27.20-42.00.xls	1,113,600	4/11/01	12:00p
ESF42.00-51.50.xls	1,865,728	4/11/01	11:57a
ESF51.50-57.29.xls	596,992	4/11/01	12:00p
ESF_study_TSw35.xls	339,456	4/11/01	12:46p
Directory of Fracture_Aperture			
Aperture_dist_tsw34.xls	24,576	4/11/01	10:48a
Aperture_distribution_TSw34_run1.xls	3,119,616	4/11/01	11:02a
Aperture_distribution_TSw34_run2.xls	2,451,456	4/11/01	11:04a
Aperture_distribution_TSw35-36_run1.xls	4,116,480	4/11/01	11:09a
Aperture_distribution_TSw35-36_run2.xls	3,316,736	4/11/01	11:08a
Directory of MC_for_Multiple_Fracture_Spacing			
FractSp_stat_00a_sp_summary.xls	30,208	4/19/01	10:22a
FractSp_stat_00a_sp=2_2.xls	1,675,264	4/18/01	4:29p

FractSp_stat_00a_sp=1_3.xls	1,266,176	4/18/01 4:21p
FractSp_stat_00a_sp=5_1.xls	2,814,976	4/18/01 4:37p
FractSp_stat_00a_sp=5_5.xls	2,820,096	4/18/01 9:59p
FractSp_stat_00a_sp=2_3.xls	1,672,704	4/18/01 4:30p
FractSp_stat_00a_sp=1_4.xls	1,265,664	4/18/01 4:22p
FractSp_stat_00a_sp=5_2.xls	2,810,880	4/18/01 9:32p
FractSp_stat_00a_sp=2_4.xls	1,675,776	4/18/01 5:13p
FractSp_stat_00a_sp=1_5.xls	1,270,272	4/18/01 4:23p
FractSp_stat_00a_sp=5_3.xls	2,812,416	4/18/01 9:35p
FractSp_stat_00a_sp=1_1.xls	1,272,832	4/18/01 4:20p
FractSp_stat_00a_sp=2_5.xls	1,681,920	4/18/01 5:33p
FractSp_stat_00a_sp=2_1.xls	1,670,656	4/18/01 4:29p
FractSp_stat_00a_sp=5_4.xls	2,818,048	4/18/01 9:33p
FractSp_stat_00a_sp=1_2.xls	1,273,856	4/18/01 4:21p
FractSp_stat_00a_sp=10_1.xls	4,666,880	4/18/01 4:24p
FractSp_stat_00a_sp=10_2.xls	4,664,320	4/18/01 4:25p
FractSp_stat_00a_sp=10_3.xls	4,695,552	4/18/01 4:26p
FractSp_stat_00a_sp=10_4.xls	4,683,264	4/18/01 4:27p
FractSp_stat_00a_sp=50_2.xls	19,315,200	4/18/01 4:41p
FractSp_stat_00a_sp=50_1.xls	19,367,424	4/18/01 10:08p
FractSp_stat_00a_sp=20_2.xls	8,345,088	4/18/01 4:32p
FractSp_stat_00a_sp=20_1.xls	8,382,464	4/18/01 4:31p
FractSp_stat_00a_sp=20_3.xls	8,341,504	4/18/01 4:33p
FractSp_stat_00a_sp=10_5.xls	4,676,096	4/18/01 4:28p
FractSp_stat_00a_sp=20_5.xls	8,334,848	4/18/01 4:36p
FractSp_stat_00a_sp=20_4.xls	8,340,480	4/18/01 4:35p

Directory of variograms

Subdirectory of TSw34_ns+ew

ewbis.dat	12,121	4/14/00 6:02p
ewbis_lag=0.05_tol=0.01.out	142,218	7/26/00 10:57a
ewbis_lag=0.05_tol=0.01.xls	418,816	7/26/00 11:00a
ewbis_lag=0.05_tol=0.025.out	142,218	7/26/00 10:57a
ewbis_lag=0.05_tol=0.025.xls	418,816	7/26/00 11:00a
ewbis_lag=0.2_tol=0.1.out	142,218	7/26/00 10:58a
ewbis_lag=0.2_tol=0.1.xls	399,360	7/26/00 11:00a
ewbis_lag=0.5_tol=0.25.out	142,218	7/26/00 10:58a
ewbis_lag=0.5_tol=0.25.xls	393,728	7/26/00 11:00a
gamv3.par	1,162	7/26/00 10:56a
nsbis_lag=1_tol=0.7.xls	50,176	7/26/00 10:52a
nsbis_lag=1_tol=0.7.out	142,218	7/26/00 10:50a
nsbis.dat	7,047	4/14/00 5:51p
nsbis_lag=0.05_tol=0.025.out	142,218	7/26/00 10:50a
nsbis_lag=0.05_tol=0.025.xls	466,432	7/26/00 10:53a
nsbis_lag=0.1_tol=0.05.out	142,218	7/26/00 10:50a
nsbis_lag=0.1_tol=0.05.xls	406,016	7/26/00 10:52a
nsbis_lag=0.5_tol=0.25.out	142,218	7/26/00 10:50a
nsbis_lag=0.5_tol=0.25.xls	393,728	7/26/00 10:52a
nsbis_lag=1.0_tol=0.1.out	142,218	7/26/00 10:50a
nsbis_lag=1.0_tol=0.1.xls	50,176	7/26/00 10:52a

Subdirectory of TSw35_ns+ew

ew35.dat	6,192	4/15/00 7:16a
ew35-1.dat	1,964	4/15/00 7:39a
ew35-1_lag=0.5_tol=0.25.out	355,218	7/26/00 11:23a

ew35-1_lag=0.5_tol=0.25.xls	392,704	7/26/00 11:29a
ew35-1_lag=1.0_tol=0.5.out	355,218	7/26/00 11:23a
ew35-1_lag=1.0_tol=0.5.xls	443,392	7/26/00 11:29a
ew35-1_lag=2.0_tol=1.0.out	355,218	7/26/00 11:24a
ew35-1_lag=2.0_tol=1.0.xls	391,680	7/26/00 11:29a
ew35-2.dat	5,441	4/15/00 7:46a
ew35-2_lag=0.1_tol=0.05.out	355,218	7/26/00 11:24a
ew35-2_lag=0.1_tol=0.05.xls	404,480	7/26/00 11:29a
ew35-2_lag=0.2_tol=0.1.out	355,218	7/26/00 11:24a
ew35-2_lag=0.2_tol=0.1.xls	452,096	7/26/00 11:29a
ew35-2_lag=0.5_tol=0.25.out	355,218	7/26/00 11:25a
ew35-2_lag=0.5_tol=0.25.xls	444,928	7/26/00 11:29a
ew35-2_lag=2.0_tol=1.0.out	355,218	7/26/00 11:25a
ew35-2_lag=2.0_tol=1.0.xls	391,680	7/26/00 11:29a
ew35_lag=0.1_tol=0.05.out	355,218	7/26/00 11:25a
ew35_lag=0.1_tol=0.05.xls	406,016	7/26/00 11:30a
ew35_lag=0.5_tol=0.25.out	355,218	7/26/00 11:26a
ew35_lag=0.5_tol=0.25.xls	448,000	7/26/00 11:30a
ew35_lag=1.0_tol=0.5.out	355,218	7/26/00 11:26a
ew35_lag=1.0_tol=0.5.xls	392,192	7/26/00 11:30a
gamv3.par	1,157	7/26/00 11:13a
ns35.dat	1,396	4/15/00 7:15a
ns35_lag=0.5_tol=0.25.out	355,218	7/26/00 11:26a
ns35_lag=0.5_tol=0.25.xls	393,216	7/26/00 11:29a
ns35_lag=1.0_tol=0.5.out	355,218	7/26/00 11:26a
ns35_lag=1.0_tol=0.5.xls	443,392	7/26/00 11:28a
ns35_lag=1.5_tol=0.75.out	355,218	7/26/00 11:27a
ns35_lag=1.5_tol=0.75.xls	391,680	7/26/00 11:30a
Subdirectory of TSw36_allatonce		
ewns36-2_lag=1.0_tol=0.5.xls	392,192	7/26/00 11:35a
ewns36-2_lag=1.0_tol=0.5.out	355,218	7/26/00 11:35a
ewns36.dat	4,380	4/15/00 9:06a
ewns36-1.dat	3,303	4/15/00 9:05a
ewns36-2.dat	1,122	4/15/00 9:06a
ewns36-1_lag=0.1_tol=0.05.out	355,218	7/26/00 11:34a
ewns36-1_lag=0.1_tol=0.05.xls	404,480	7/26/00 11:36a
ewns36-1_lag=0.5_tol=0.25.out	355,218	7/26/00 11:34a
ewns36-1_lag=0.5_tol=0.25.xls	444,928	7/26/00 11:36a
ewns36-2_lag=0.1_tol=0.05.out	355,218	7/26/00 11:34a
ewns36-2_lag=0.1_tol=0.05.xls	399,872	7/26/00 11:36a
ewns36-2_lag=0.5_tol=0.25.out	355,218	7/26/00 11:35a
ewns36-2_lag=0.5_tol=0.25.xls	444,416	7/26/00 11:35a
gamv3.par	1,165	7/26/00 11:35a

OFFICE OF CIVILIAN RADIOACTIVE WASTE MANAGEMENT

1. QA: QA

SPECIAL INSTRUCTION SHEET

file list 10-1-01 MK

Complete Only Applicable Items

This is a placeholder page for records that cannot be scanned.

2. Record Date	3. Accession Number
09/21/2001	ATT-TO MOL.20010925.0197
4. Author Name(s)	**5. Author Organization**
JEAN-PHILIPPE NICOT	N/A

6. Title/Description
DESCRIPTION OF FRACTURE SYSTEMS FOR EXTERNAL CRITICALITY REPORTS

7. Document Number(s)	8. Version Designator
ANL-NBS-GS-000010	REV. 00
9. Document Type	**10. Medium**
DATA	CD-ROM / DISK

11. Access Control Code
PUB

12. Traceability Designator
DC# 26199

(AB) 10-02-01

13. Comments
THIS IS A SPECIAL PROCESS CD-ROM AS PART OF ATTACHMENT IV THIS DATA SUBMITTAL TO THE RECORDS PROCESSING CENTER IS FOR ARCHIVE PURPOSES ONLY, AND IS NOT AVAILABLE FOR VIEWING OR REPRODUCTION ~~RPC~~

OFFICE OF CIVILIAN RADIOACTIVE WASTE MANAGEMENT
ELECTRONIC FILE CERTIFICATION

QA: N/A

1. DOCUMENT TITLE:

Description of Fracture Systems for External Criticality Reports

2. IDENTIFIER (e.g., DI OR PI):	3. REVISION DESIGNATOR:
ANL-NBS-GS-000010	Rev. 00

ATTACHED SOFTWARE FILE INFORMATION

4. PDF FILE SUBMITTED: ☐ YES ☑ NO

5. FILE NAMES(S) WITH FILE EXTENSION(S) PROVIDED BY THE SOFTWARE:

SEE ATTACHED

6. DATE LAST MODIFIED:	7. NATIVE APPLICATION: (i.e., EXCEL, WORD, CORELDRAW)	8. FILE SIZE IN KILOBYTES:
SEE ATTACHED	Excel & Word	SEE ATTACHED

9. FILE LINKAGE INSTRUCTIONS/INFORMATION:

STANDARD

10. PRINTER SPECIFICATION (I.E., HP4SI) INCLUDING POSTSCRIPT INFORMATION (i.e., PRINTER DRIVER) AND PRINTING PAGE SETUP: (i.e., LANDSCAPE, 11 X 17 PAPER)

8 x 1/2(portrait)=HP Laserjet 5si

11. COMPUTING PLATFORM USED: (i.e., PC, SUN, WIN 95, NT, HP)	12. OPERATING SYSTEM AND VERSION: (i.e., WINDOWS UNIX, SOLARIS)
PC #115815	Windows

13. ADDITIONAL HARDWARE/SOFTWARE REQUIREMENT USED TO CREATE FILE(S):	14. ACCESS RESTRICTIONS: (COPYRIGHT OR LICENSE ISSUES)
NONE	NONE

COMMENTS/SPECIAL INSTRUCTIONS

15. IS SOFTWARE AVAILABLE FROM SOFTWARE CONFIGURATION MANAGEMENT? ☑ YES ☐ NO
SOFTWARE MEDIA TRACKING NUMBER N/A.

NOTE: The software product(s) to develop this document are Commercial-Off-The-Shelf (COTS) software products which require no Software Media Number (SMN). The COTS software products are under Software Configuration Management (SCM) control.

CERTIFICATION

16. DOCUMENT OWNER (Print and Sign):			17. DATE:
Susan LeStrange for Jean-Philippe Nicot Susan LeStrange			09/24/2001
18. ORGANIZATION:	19. DEPARTMENT:	20. LOCATION/MAIL STOP:	21. PHONE:
BSC	WP	MS423/1026F	295-4580
22. SUBMITTED BY (Print and Sign): Daynett D. Vasecky			23. DATE: 9-25-01

DC USE ONLY

24. DATE RECEIVED:	25. DATE FILES TRANSFERRED:	26. DC NO.:
9/26/01	n/a	26199
27. NAME (Print and Sign): n/a		28. DATE: 9/26/01

ATTACHMENT III

FILES ON ELECTRONIC MEDIA (CD-ROM)

(3 pages)

All the input, output, and pre- and post-processing files relative to this calculation have been copied to a CD-ROM. Details about the organization of the CD-ROM and a list of files follow.

The files are organized into five sections:

File Name	Size (Bytes)	Date	Time
Complement_to_ECRB_smallfract_spacing.xls	380,928	8/28/01	5:27p
Complement_to_ESF26-60.xls	6,370,816	8/28/01	5:10p
DTN_Comparison.xls	5,016,576	8/28/01	10:36a
FractureIntensityNew.xls	126,464	8/29/01	11:38a
fractureMineral_ECRB.xls	211,456	8/29/01	11:08a
fractureMineral_ESF.xls	457,216	8/29/01	11:06a
Lithophysae.xls	204,800	8/29/01	10:04a
Niche3107_Alcove5_forporosity.xls	56,832	8/28/01	12:10p
Percentage_SSS.xls	52,224	8/29/01	9:57a
Directory of ECRB_Fracture _Spacing			
allHorVert.xls	753,152	4/12/01	9:29a
allHorVert_unchanged.xls	767,488	4/12/01	9:28a
CDF_Fracturespacing&intensity.xls	696,832	7/27/01	11:26p
ECRB_study_TSw36.xls	1,576,960	4/11/01	2:27p
ECRB_study_TSw35.xls	4,307,968	4/11/01	3:45p
ECRB.xls	1,141,248	4/11/01	12:57p
ECRB_smallfract_spacing.xls	2,351,104	8/29/01	9:52a
ECRB_spacing.xls	664,064	4/11/01	4:53p
ECRB_study_TSw33.xls	1,637,888	4/11/01	4:34p
ECRB_study_TSw34.xls	3,883,008	4/11/01	3:50p
Directory of ESF_Fracture_Spacing			
ESF26-60.xls	5,881,856	4/11/01	3:50p
ESF26-60_all.xls	3,641,856	4/11/01	11:43a
ESF27.20-42.00.xls	1,113,600	4/11/01	12:00p
ESF42.00-51.50.xls	1,865,728	4/11/01	11:57a
ESF51.50-57.29.xls	596,992	4/11/01	12:00p
ESF_study_TSw35.xls	339,456	4/11/01	12:46p
Directory of Fracture_Aperture			
Aperture_dist_tsw34.xls	24,576	4/11/01	10:48a
Aperture_distribution_TSw34_run1.xls	3,119,616	4/11/01	11:02a
Aperture_distribution_TSw34_run2.xls	2,451,456	4/11/01	11:04a
Aperture_distribution_TSw35-36_run1.xls	4,116,480	4/11/01	11:09a
Aperture_distribution_TSw35-36_run2.xls	3,316,736	4/11/01	11:08a
Directory of MC_for_Multiple_Fracture_Spacing			
FractSp_stat_00a_sp_summary.xls	30,208	4/19/01	10:22a
FractSp_stat_00a_sp=2_2.xls	1,675,264	4/18/01	4:29p

FractSp_stat_00a_sp=1_3.xls	1,266,176	4/18/01 4:21p
FractSp_stat_00a_sp=5_1.xls	2,814,976	4/18/01 4:37p
FractSp_stat_00a_sp=5_5.xls	2,820,096	4/18/01 9:59p
FractSp_stat_00a_sp=2_3.xls	1,672,704	4/18/01 4:30p
FractSp_stat_00a_sp=1_4.xls	1,265,664	4/18/01 4:22p
FractSp_stat_00a_sp=5_2.xls	2,810,880	4/18/01 9:32p
FractSp_stat_00a_sp=2_4.xls	1,675,776	4/18/01 5:13p
FractSp_stat_00a_sp=1_5.xls	1,270,272	4/18/01 4:23p
FractSp_stat_00a_sp=5_3.xls	2,812,416	4/18/01 9:35p
FractSp_stat_00a_sp=1_1.xls	1,272,832	4/18/01 4:20p
FractSp_stat_00a_sp=2_5.xls	1,681,920	4/18/01 5:33p
FractSp_stat_00a_sp=2_1.xls	1,670,656	4/18/01 4:29p
FractSp_stat_00a_sp=5_4.xls	2,818,048	4/18/01 9:33p
FractSp_stat_00a_sp=1_2.xls	1,273,856	4/18/01 4:21p
FractSp_stat_00a_sp=10_1.xls	4,666,880	4/18/01 4:24p
FractSp_stat_00a_sp=10_2.xls	4,664,320	4/18/01 4:25p
FractSp_stat_00a_sp=10_3.xls	4,695,552	4/18/01 4:26p
FractSp_stat_00a_sp=10_4.xls	4,683,264	4/18/01 4:27p
FractSp_stat_00a_sp=50_2.xls	19,315,200	4/18/01 4:41p
FractSp_stat_00a_sp=50_1.xls	19,367,424	4/18/01 10:08p
FractSp_stat_00a_sp=20_2.xls	8,345,088	4/18/01 4:32p
FractSp_stat_00a_sp=20_1.xls	8,382,464	4/18/01 4:31p
FractSp_stat_00a_sp=20_3.xls	8,341,504	4/18/01 4:33p
FractSp_stat_00a_sp=10_5.xls	4,676,096	4/18/01 4:28p
FractSp_stat_00a_sp=20_5.xls	8,334,848	4/18/01 4:36p
FractSp_stat_00a_sp=20_4.xls	8,340,480	4/18/01 4:35p

Directory of variograms

Subdirectory of TSw34_ns+ew

ewbis.dat	12,121	4/14/00 6:02p
ewbis_lag=0.05_tol=0.01.out	142,218	7/26/00 10:57a
ewbis_lag=0.05_tol=0.01.xls	418,816	7/26/00 11:00a
ewbis_lag=0.05_tol=0.025.out	142,218	7/26/00 10:57a
ewbis_lag=0.05_tol=0.025.xls	418,816	7/26/00 11:00a
ewbis_lag=0.2_tol=0.1.out	142,218	7/26/00 10:58a
ewbis_lag=0.2_tol=0.1.xls	399,360	7/26/00 11:00a
ewbis_lag=0.5_tol=0.25.out	142,218	7/26/00 10:58a
ewbis_lag=0.5_tol=0.25.xls	393,728	7/26/00 11:00a
gamv3.par	1,162	7/26/00 10:56a
nsbis_lag=1_tol=0.7.xls	50,176	7/26/00 10:52a
nsbis_lag=1_tol=0.7.out	142,218	7/26/00 10:50a
nsbis.dat	7,047	4/14/00 5:51p
nsbis_lag=0.05_tol=0.025.out	142,218	7/26/00 10:50a
nsbis_lag=0.05_tol=0.025.xls	466,432	7/26/00 10:53a
nsbis_lag=0.1_tol=0.05.out	142,218	7/26/00 10:50a
nsbis_lag=0.1_tol=0.05.xls	406,016	7/26/00 10:52a
nsbis_lag=0.5_tol=0.25.out	142,218	7/26/00 10:50a
nsbis_lag=0.5_tol=0.25.xls	393,728	7/26/00 10:52a
nsbis_lag=1.0_tol=0.1.out	142,218	7/26/00 10:50a
nsbis_lag=1.0_tol=0.1.xls	50,176	7/26/00 10:52a

Subdirectory of TSw35_ns+ew

ew35.dat	6,192	4/15/00 7:16a
ew35-1.dat	1,964	4/15/00 7:39a
ew35-1_lag=0.5_tol=0.25.out	355,218	7/26/00 11:23a

ew35-1_lag=0.5_tol=0.25.xls	392,704	7/26/00 11:29a
ew35-1_lag=1.0_tol=0.5.out	355,218	7/26/00 11:23a
ew35-1_lag=1.0_tol=0.5.xls	443,392	7/26/00 11:29a
ew35-1_lag=2.0_tol=1.0.out	355,218	7/26/00 11:24a
ew35-1_lag=2.0_tol=1.0.xls	391,680	7/26/00 11:29a
ew35-2.dat	5,441	4/15/00 7:46a
ew35-2_lag=0.1_tol=0.05.out	355,218	7/26/00 11:24a
ew35-2_lag=0.1_tol=0.05.xls	404,480	7/26/00 11:29a
ew35-2_lag=0.2_tol=0.1.out	355,218	7/26/00 11:24a
ew35-2_lag=0.2_tol=0.1.xls	452,096	7/26/00 11:29a
ew35-2_lag=0.5_tol=0.25.out	355,218	7/26/00 11:25a
ew35-2_lag=0.5_tol=0.25.xls	444,928	7/26/00 11:29a
ew35-2_lag=2.0_tol=1.0.out	355,218	7/26/00 11:25a
ew35-2_lag=2.0_tol=1.0.xls	391,680	7/26/00 11:29a
ew35_lag=0.1_tol=0.05.out	355,218	7/26/00 11:25a
ew35_lag=0.1_tol=0.05.xls	406,016	7/26/00 11:30a
ew35_lag=0.5_tol=0.25.out	355,218	7/26/00 11:26a
ew35_lag=0.5_tol=0.25.xls	448,000	7/26/00 11:30a
ew35_lag=1.0_tol=0.5.out	355,218	7/26/00 11:26a
ew35_lag=1.0_tol=0.5.xls	392,192	7/26/00 11:30a
gamv3.par	1,157	7/26/00 11:13a
ns35.dat	1,396	4/15/00 7:15a
ns35_lag=0.5_tol=0.25.out	355,218	7/26/00 11:26a
ns35_lag=0.5_tol=0.25.xls	393,216	7/26/00 11:29a
ns35_lag=1.0_tol=0.5.out	355,218	7/26/00 11:26a
ns35_lag=1.0_tol=0.5.xls	443,392	7/26/00 11:28a
ns35_lag=1.5_tol=0.75.out	355,218	7/26/00 11:27a
ns35_lag=1.5_tol=0.75.xls	391,680	7/26/00 11:30a
Subdirectory of TSw36_allatonce		
ewns36-2_lag=1.0_tol=0.5.xls	392,192	7/26/00 11:35a
ewns36-2_lag=1.0_tol=0.5.out	355,218	7/26/00 11:35a
ewns36.dat	4,380	4/15/00 9:06a
ewns36-1.dat	3,303	4/15/00 9:05a
ewns36-2.dat	1,122	4/15/00 9:06a
ewns36-1_lag=0.1_tol=0.05.out	355,218	7/26/00 11:34a
ewns36-1_lag=0.1_tol=0.05.xls	404,480	7/26/00 11:36a
ewns36-1_lag=0.5_tol=0.25.out	355,218	7/26/00 11:34a
ewns36-1_lag=0.5_tol=0.25.xls	444,928	7/26/00 11:36a
ewns36-2_lag=0.1_tol=0.05.out	355,218	7/26/00 11:34a
ewns36-2_lag=0.1_tol=0.05.xls	399,872	7/26/00 11:36a
ewns36-2_lag=0.5_tol=0.25.out	355,218	7/26/00 11:35a
ewns36-2_lag=0.5_tol=0.25.xls	444,416	7/26/00 11:35a
gamv3.par	1,165	7/26/00 11:35a